Towards *in vivo* imaging of early *Rhizobium* Nod factor responses

Gerard van der Krogt

Promotor: Prof. dr. A.H.J. Bisseling
Hoogleraar in de Moleculaire Biologie
Wageningen Universiteit

Samenstelling promotiecommissie:
Prof. dr. H.P. Spaink, Universiteit Leiden
Prof. dr. A.M.C. Emons, Wageningen Universiteit
Dr. ir. M.A. Hink, Wageningen Universiteit
Dr. Ir. A.R. van der Krol, Wageningen Universiteit

Dit onderzoek is uitgevoerd binnen de onderzoekschool voor Experimentele Plantwetenschappen.

Towards *in vivo* imaging of early *Rhizobium* Nod factor responses

Gerard N.M. van der Krogt

Proefschrift
ter verkrijging van de graad van doctor
op gezag van de rector magnificus
van Wageningen Universiteit
Prof. dr. M.J. Kropff
in het openbaar te verdedigen
op vrijdag 24 februari 2006
des namiddags te halftwee in de aula

Towards *in vivo* imaging of early *Rhizobium* Nod factor responses
Krogt, van der Gerard

Thesis Wageningen University, The Netherlands
With references - with summary in Dutch

ISBN 90-8504-371-9

The research described in this thesis was carried out at the Laboratory of Molecular Biology, Wageningen University, The Netherlands.

Dwazen verwerpen wat ze zien,
niet wat ze denken.
Wijzen verwerpen wat ze denken,
niet wat ze zien.

Huang Po (- 850)

Abbreviations

aa:	amino acid
ABA:	ABscisic Acid
ABD:	Actin Binding Domain
ADF:	Actin Depolymerizing Factor
ABP:	Actin Binding Protein
ABRE:	ABA-Responsive promoter Element
BFP:	Blue Fluorescent Protein
CAT:	Chloramphenicol Acetyl Transferase
CFP:	Cyan Fluorescent Protein
CLSM:	Confocal Laser Scanning Microscopy
DRE:	Dehydration Responsive Elements
F-actin:	Filamentous actin
FLIM:	Fluorescence Lifetime Imaging Microscopy
FP:	Fluorescent Protein
FRET:	Fluorescence Resonance Energy Transfer
FSPIM:	Fluorescence Spectral Imaging Microscopy
G-actin:	Globular actin
GFP:	Green Fluorescent Protein
GUS:	β-Glucuronidase
IT:	Infection Thread
LCOs:	Lipochitooligosaccharides
LysM-RLKs:	LysM domains containing Receptor-Like serine/threonine Kinases
MCS:	Multiple Cloning Site
PA-FP	Photo Activatable Fluorescent Protein
PKA:	Protein Kinase A
PTFE:	Polytetrafluorethylene
RFP:	Red FP
RNAi:	RNA interference
wtGFP:	wild-type Green Fluorescent Protein
YFP:	Yellow Fluorescent Protein
Ycam2:	Yellow-cameleon-2

Contents

Outline

The goal in this thesis is to explore the possibility of live imaging of cellular events using fluorescence microscopy in combination with Green Fluorescent Protein (GFP) based reporter constructs in root hairs during the *Rhizobium*-legume interaction. Legumes have the ability to establish an endosymbiotic relationship with soil bacteria of different genera, collectively named rhizobia, that results in nitrogen-fixing root nodules. The formation of root nodules begins when bacteria colonize the root surface and start secreting signal molecules, named Nod factor. These molecules induce responses in root epidermal cells; e.g. [Ca2+] spiking, actin skeleton rearrangement (Mirabella *et al.* 2002). Ultimately, specific infection structures are formed in root hairs, which guide the bacteria through the epidermis and outer cortical cells towards the newly formed nodule primoridum (Mylona 1995; Long 1996; Bladergroen *et al.* 1998; Hadri 1998; Schultze *et al.* 1998).
The known [Ca^{2+}]–responses and actin skeleton alterations in root hairs were used as parameters to explore whether these can be monitored in living root hairs. However imaging approaches using FP based reporter constructs require the availability of efficient transformation procedures. Therefore *Agrobacterium rhiogenes* based transformation of *Medicago truncatula* (Medicago) and *Lotus japonicus* (Lotus), was optimised (**Chapter 2**).
Several pilot experiments indicted that transgenes did have negative effects on plant/root development. This is in our system of importance since we use an *A. rhizogenes* root transformation procedure to obtain root hairs expressing the FP reporter constructs. If the negative influence on root growth is too high no transgenic roots will be obtained from the shoot. Therefore it was decided to test which tissue specific and inducible promoters could be used to create a set of promoters to facilitate future imaging studies. Thus several root epidermis specific promoters were analyzed for their suitability (**Chapter 2**). In **Chapter 3,4,5** inducible promoters have been studied that can be activated by a specific treatment by which the level, place and timing of expression can be controlled.
To study the dynamics of actin in living cells a vital actin probe had to be developed. Therefore fusions of FPs with actin, actin binding proteins (ABPs), and actin binding protein domains (ABDs), respectively, were made. Their usefulness was tested in *Vigna* mesophyll protoplasts (**Chapter 6**). In addition some attempts were made to express the most promising construct in root hairs. *In vivo* [Ca^{2+}] imaging was tested using use the FP based sensor Ycam, enabling [Ca^{2+}] imaging (Miyawaki *et al.* 1997). Ycam was expressed and tested in root hairs (**Chapter 7**) by using one of the previously tested root epidermis specific promoters (Chapter 2). Finally the potential of the tested approaches is discussed (**Chapter 8)**.

Chapter 1

Introduction

A major challenge in experimental biology is to obtain insight in behavior of molecules (proteins) in living cells. The predominant strategy to achieve this is by labeling the molecules with fluorescent tags, followed by inspection with an epifluorescence microscope. Traditionally, fluorescent labeling was done by chemical modification of purified molecules, followed by loading into the cells. During the last decade especially fluorescent proteins like Green Fluorescent Protein (GFP) have markedly extended the possibilities to obtain cells with fluorescently tagged proteins that have maintained their biological activity. This GFP development was paired with a major progress in fluorescence microscopy based techniques, which boosted the imaging of these fluorescent tagged proteins even further.
In this chapter first synthetic fluorescent probes and GFP and derivatives, respectively, are described. This is followed by a short description of the early steps of the *Rhizobium*-legume symbiosis. In this description the focus lies on *Rhizobium* root hair responses, as this is the area in which we will apply *in vivo* imaging. At the end of this introduction the potential of fluorescent proteins in studies on this plant microbe interaction is described.

Fluorescent synthetic probes
Fluorescent probes can be used in several ways. First, fluorescent probes can be used to label a protein of interest, enabling tracking of this protein in the cell. Second, these probes can be used as a synthetic fluorescent reporter molecule, to detect changes in cellular ion concentrations, voltage etc. (Haugland 2002).

Tagged proteins:
To study the behavior of proteins in living cells they need to be tagged with a fluorescent molecule. Initially this was done *in vitro* with a synthetic fluorescent group and such labeled molecules had to be introduced in cells by microinjection. These experiments provided insight in the dynamics of these molecules and even protein-protein interaction studies using FRET were possible (see below). However, such a labeled protein has several major disadvantages like; its usage is labor intensive, the injected protein might miss essential modifications and it is difficult to introduce such concentrations that are biologically relevant. Currently, protein labeling and introduction into cells is mostly done using recombinant DNA technology. Hereby fusions with a fluorescent protein, GFP, are made and expressed inside the cell (see below).

Sensors:

Synthetic based sensors can be used in living cells to detect changes in cellular ion concentrations, voltage, pH, [Ca^{2+}] et cetera (Haugland 2002). Spectral properties of such a reporter depend on the concentration of another molecule and therefore can be used to monitor changes in parameters of these molecules. One example is the calcium sensitive ratiometric emission reporter Indo-1. This reporter (excitation 340nm) has a fluorescence emission maximum at 398nm when calcium is bound

whereas in the calcium free form the maximum is shifted to 482nm. The ratio of the 2 emission maxima indicates the calcium concentration. These values are independent of local probe concentration, optical path length or spatial excitation light distribution. So by a pixel-by-pixel quantification of the ratio an image of the Ca^{2+} distribution can be obtained. In plant root hairs such ratiometric probes provided a good insight in the dynamics and the subcellular differences in [Ca^{2+}] and pH (Ruijter 1998; Goedhart 2001). Most living cells can be loaded very efficiently with these fluorescent reporter molecules due to the presence of a chemical group, facilitating transport of the reporter over the cell membrane (Haugland 2002; Fricker *et al.* 1999). However, not all these probes can be loaded into plant cells, especially due to the presence of the cell wall (Goedhart 2001). In part these limitations can be circumvented by microinjections, but in general it is technically difficult to inject plant cells and this is especially the case for vulnerable cells such as root hairs. These problems are overcome by using GFP based sensors. But even more important, using GFP, sensors for other more complex in structure molecules can be made (see below).

Fluorescent GFP and derivatives

GFP a green fluorescent protein was discovered in 1955 (Davenport *et al.* 1955), but till it was cloned in 1992 it had hardly been studied (Figure 1a) (Prasher *et al.* 1992; Chalfie *et al.* 1994). After the cloning of Wild-type GFP (wtGFP) gene from the jellyfish *Aequorea victoria*, the great potential of GFP in cell biological research was widely recognized. Predominantly because in numerous cases fusions could be made between GFP and a protein of interest, this without loosing the biological function of the protein of interest. Such fusions facilitated tracking of proteins in time and space, in the living cell (Tsien 1998). But also the GFP characteristics make it very suited to be used as a fluorescent protein tag. It is a rather small protein (21 kDa) and does not require cofactors to become fluorescent (Cody *et al.* 1993; Ormö *et al.* 1996; Yang *et al.* 1996). It has a cylindrical ß-can structure (Figure 1b). Eleven strands of a ß-sheet form an anti-parallel barrel with short helices forming lids on each end of this can. The chromophore is positioned inside the can, as part of a distorted α-helix, which runs along the axis of the can.

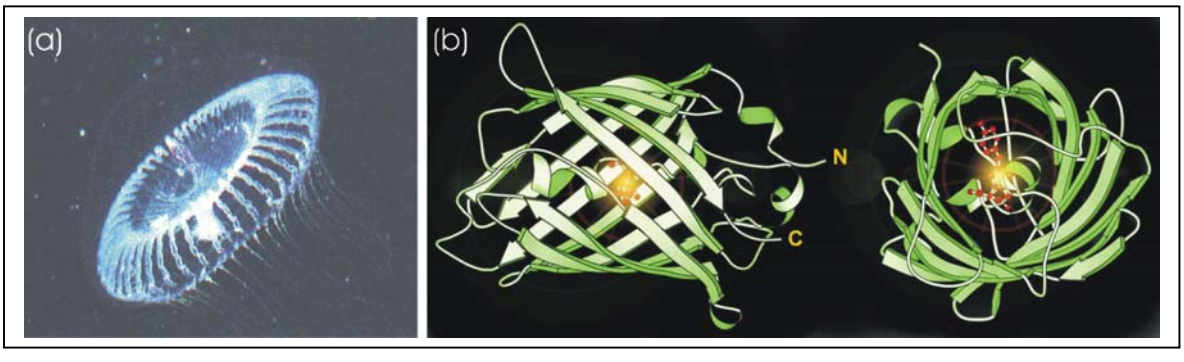

Figure 1. (**a**) The jellyfish *Aequorea victoria* containing wtGFP (Maniatis *et al.* 2000) (**b**) Schematic representation of green fluorescent protein, tripeptide fluorophore in red (Varian Australia Pty Ltd; Maniatis *et al.* 2000).

This barrel structure protects the fluorescent chromophore from loosing its fluorescent properties by solvents or detergents (González *et al.* 1997). It also makes it temperature insensitive up to 65ºC (Bokman *et al.* 1981), protease insensitive (Roth

et al. 1983) and active between pH values of 5.5-12.0 (Bokman *et al.* 1981; Patterson *et al.* 1997). So in short, GFP is a rather robust fluorescent probe.
GFP also can be used to make fusion proteins by means of recombinant DNA technology, it has a great potential to be used as fluorescent tag to study the behavior of proteins in living cells. By doing so the mentioned disadvantages of *in vitro* labeling with a synthetic fluorescent group can be eliminated.
The impact GFP made in research is illustrated by the 15000 studies published last decade, in which GFP itself is studied or used as reporter (www.NCBI.nlm.nih.gov). Nowadays GFP expands now from basic science to more industrial applications: For example GFP is used to track meat-fermenting lactobacilli in Japanese sausages (Gory *et al.* 2001), the spread of bacteria that consume diesel oil in soil (Dandie *et al.* 2001) and GFP is even used to make fluorescent plants or fish for decorative purposes (Gong *et al.* 2003; Choi *et al.* 2004). So GFP went from “zero to hero”.

GFP mutants for heterologous biological systems:
To obtain efficient translation in heterologous biological systems some alterations in codon usage and amino acids (aa) of GFP were needed. Such GFPs mutation optimization procedures allowed expression in many organisms like dictostelium, yeast, and animals. Also to facilitate the use of GFP also in plant cells several additional mutations were needed. Haseloff *et al.* showed that plants recognize a cryptic splice site within the coding sequence of wtGFP mRNA, yielding a non-fluorescent protein, therefore mutations were required to circumvent this splicing (Siemering *et al.* 1996; Haseloff *et al.* 1997). Also mutations causing changes in spectral properties were needed, to allow detection in cells with high auto-fluorescence, such as caused by chloroplasts and cell wall components (Govers *et al.* 1998; Gadella 1999).

Spectral GFP mutants:
Spectral GFP mutants would allow tracking of several fusion proteins in one cell simultaneous. So in addition to species related optimization also GFPs with markedly modified fluorescence properties have been made (Heim *et al.* 1995; Haseloff *et al.* 1997; Davis *et al.* 1998). This resulted in GFPs with shifted emission spectra, Blue FPs, Cyan FPs, Yellow FPs and Red FPs. Beside these GFP derivatives new FPs with different spectral properties were discovered for example *Discosoma sp*. DsRED and *Heteractis crispa* HcRED, All together this resulted in a good collection of FPs with different excitation and emission spectra (Figure 2).

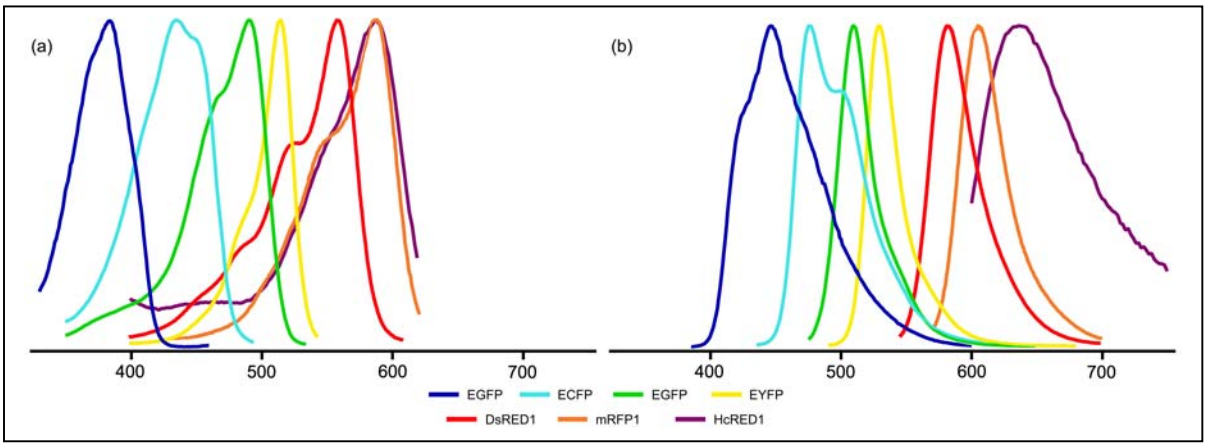

Figure 2. Normalized excitation (**a**) and emission (**b**) spectra of several fluorescent proteins. Enhanced Blue FP(EBFP), Cyan FP (ECFP), Green FP (EGFP), Yellow FP (EYFP), Red FPs (DsRed from *Discosoma sp*. and it monomeric RFP (mRFP1) derivative and HcRed1 from *Heteractis crispa*) (Tsien 1998; Matz *et al.* 1999; Baird *et al.* 2000; Campbell *et al.* 2002; Nagai *et al.* 2002; Rizzo *et al.* 2004; Shanner *et al.* 2004) (graphs are adapted from Miyawaki *et al.* (Miyawaki *et al.* 2003)).

As shown (Figure 2) the excitation and emission spectra of the FPs are sufficiently different to select FP couples that can be tracked simultaneously. It turned out even to be possible to follow 4 FPs simultaneously (Kato *et al.* 2002; Hutter 2004).

GFP based sensors:

Mutations in GFP not only resulted in spectral variants, but also in some cases the spectral properties of mutated GFPs became depended on environmental parameters like intracellular ion concentrations or redox potentials. Such mutated forms can be used as sensors and provide subcellular information about such parameters (Miesenbock *et al.* 1998; Baird *et al.* 1999; Jayaraman *et al.* 2000; Sujatha *et al.* 2000; Nagai *et al.* 2001; Hanson *et al.* 2004).

In addition to these more or less coincidently obtained sensor GFPs, sensors also can be tailor made by inserting a specific protein domain into the cylindrical ß-can structure of GFP (Nagai *et al.* 2000; Nagai *et al.* 2001). An example of such a domain is the calmoduline domain, which can bind the cellular compound, calcium (Ca^{2+}). Upon calcium binding the calmoduline-GFP barrel structure is distorted upon which also the fluorescence emission is altered. However, a more [Ca^{2+}] sensitive sensor (referred to as Cameleon) was made with [Ca^{2+}] detection based on FRET (Figure 4c). Cameleon (see also Chapter 7) was one of the first GFP based FRET sensors.

FRET (Fluorescence Resonance Energy Transfer) is a photophysical phenomenon by which energy is transferred in a non-radiative manner from a donor fluorophore to an acceptor fluorophore (Figure 3a,c) (Förster 1948; Herman 1989; Clegg 1996). When such a fluorophore donor/acceptor couple (for example CFP/YFP) is in close proximity (R≈10 nm) and appropriate angle, excitation of the donor fluorphore (CFP) can lead then to quenching of donor emission and an increased, sensitized acceptor fluorphore (YFP) emission (Figure 3c) (Gordon *et al.* 1998; van Rheenen *et al.* 2004). The R_0 value is the distance between donor and acceptor at which the FRET efficiency is 50% (i.e. 50% of the excitation energy absorbed by the donor is transferred to the acceptor). When donor and acceptor are separated by >1.5 x R_0

the FRET efficiency is dropped to < 8%. When donor and acceptor are separated by <0.5 x R_0, the FRET efficiency is 98%. So FRET only occurs in a very short range of *R* (Figure 3b) and therefore provides an excellent means to study whether molecules are very close or even directly interacts such as in protein–protein interactions (Figure 4a) (Tsien 1998; Bader *et al.* 2004). By fusing now CFP respectively YFP to proteins of interest CFP/YFP FRET can be used to determine if these proteins interact. But in a similar way fusions (sensors) can be designed which can provide intracellular information (see below) by means of FRET changes.

FRET changes can be determined by measuring the ratio of acceptor/donor fluorescence. The ratio is a good measure because upon FRET the acceptor fluorescence is decreased and the donor fluorescence is increased. This approach has high temporal and spatial resolution but is not quantitative. An attractive way to measure ratio changes in a rapid manner but with a low spatial resolution in root hairs is by means of Fluorescence SPectral IMaging (FSPIM). FSPIM combines low spatial resolution with a high spectral resolution. FSPIM is very suited to measure FRET changes in root hairs due to their elongated shape, making them very suited to align them with the detection slit of the spectrograph. Consequently for every position across the slit, and thus the root hair, a complete emission spectrum of CFP/YFP can be obtained (Gadella *et al.* 1997; Gadella *et al.* 1999). However, FSPIM is not suited to measure FRET in a very quantitative manner. Other approaches are more appropriate, for example sensitized emission (van Rheenen *et al.* 2004). With sensitized emission measurements, the acceptor fluorescence upon donor excitation is measured and the ratio is calculated quantitatively. So FRET can be followed quantitatively over time with a high spatial resolution. However this approach is less suitable for very rapid ratio changes and needs a lot of labor since many corrections must be made. FRET also can be quantified very accuratly by using fluorescence lifetime (τ) measurements of the donor fluorphore. If the donor is quenched by an acceptor fluorphore the average time the donor stays in its excited state (lifetime) is reduced (Figure 3c). Unlike fluorescence intensity-based FRET measurments, fluorescence lifetime (τ) imaging (FLIM) is not dependening on local chromophore concentration, direct absorption of donor fluorescence (e.g. by chlorophyll) or on photobleaching, and consequently provides quantitative information about the FRET efficiency. Altough FLIM started as an expensive technique requiring specialized knowledge recent developements circumvented this shortcoming (Verveer *et al.* 2000; van Rheenen *et al.* 2005).

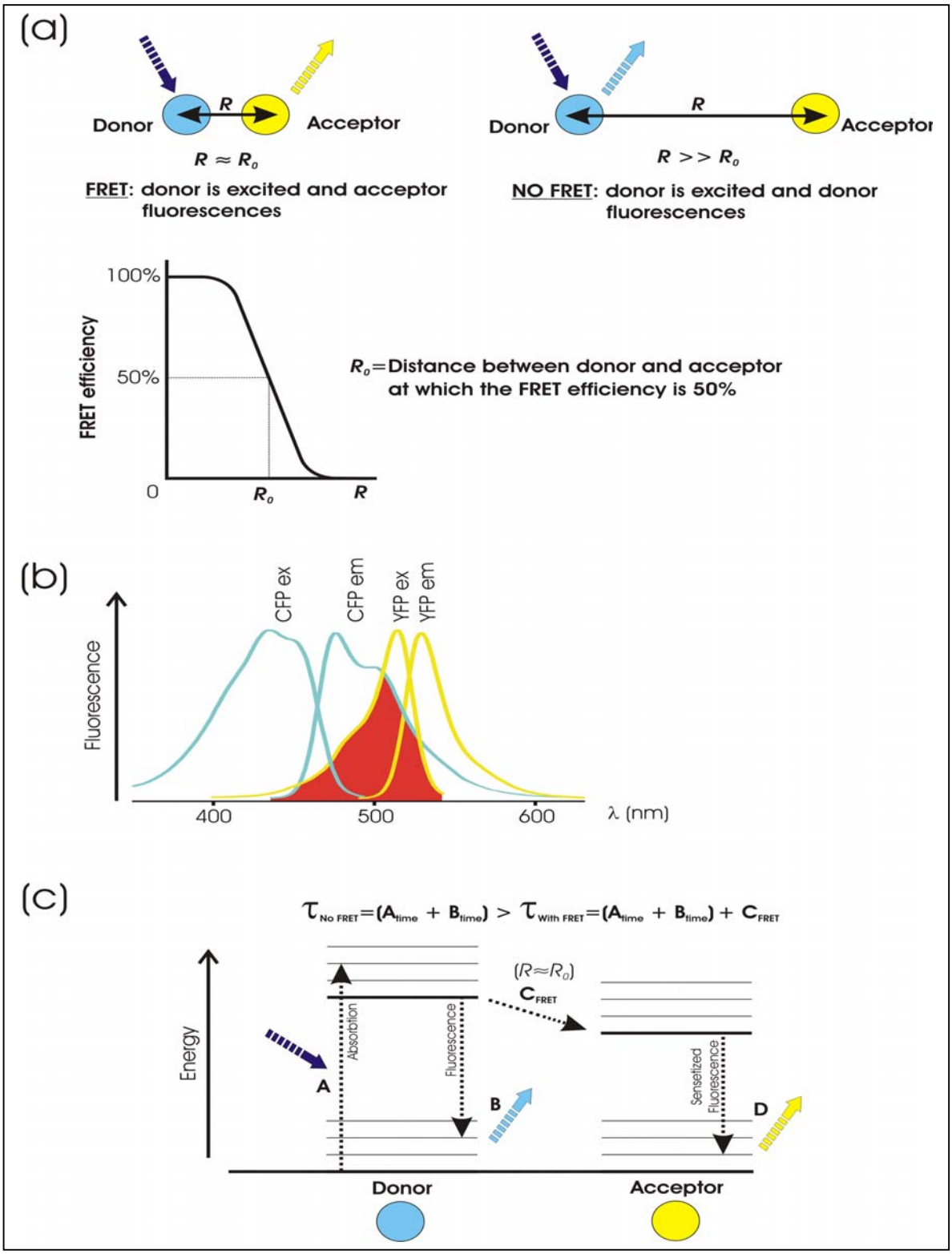

Figure 3. (**a**) FRET occurs when CFP (donor) and YFP (acceptor) are in close proximity, R≈ R_0. The R_0, (Förster radius) is the distance between donor and acceptor at which the FRET efficiency is 50%. When donor and acceptor are separated by 1.5 x R_0, the FRET efficiency is dropped to <8%. When donor and acceptor are separated by <0.5 x R_0, the FRET efficiency is >98%. (**b**) Spectral overlap between donor fluorescence and acceptor absorbance that enable CFP/YFP FRET. The spectral overlap for the cyan fluorescent protein (CFP) and the yellow fluorescent protein (YFP) is indicated in red. (**c**) The Jablonski energy level diagram visualizes the CFP and YFP excitation, emission and

FRET process. (A) The CFP becomes excited by excitation light. (B) CFP falls back to its ground state and emits light of a lower energy, longer wavelength, then the excitation light. (C) CFP transfers its energy in a non-radiative manner to the YFP acceptor fluorphore, and the acceptor emits light (sensitized emission). So FRET causes a reduction of donor emission and an increased acceptor emission. If the donor is quenched by an acceptor fluorphore the average time the donor stays in its excited state, lifetime (τ), is reduced.

The FRET based Cameleon sensor is based on a calmoduline protein. In Cameleon calmoduline is fused to an M13 calmoduline-binding domain and all flanked by a donor and acceptor FP (Figure 4c) (Miyawaki *et al.* 1997; Miyawaki *et al.* 1999; Griesbeck *et al.* 2001; Mizuno *et al.* 2001; Truong *et al.* 2001; Nagai *et al.* 2002; Nagai *et al.* 2004). The calmoduline domain can bind Ca^{2+} upon which it conformation changes and it can bind the M13 region. Since the distance of the FPs in the cameleon Ca^{2+} sensor depend on the [Ca^{2+}], FRET efficiency can be used to quantify the [Ca^{2+}].
Using a Cameleon-like design, also probes for other more complex in structure second messengers (cAMP or phospholipids) can be made (Zaccolo *et al.* 2000; van der Wal *et al.* 2001; Ponsioen *et al.* 2004). For example for cAMP several of such FRET sensors were constructed. One such sensor is based on Protein Kinase A (PKA). PKA is composed of, two regulatory and two catalytic subunits, and upon binding cAMP, this complex falls apart in its subunits. The sensor is based on this property . By linking a donor, or acceptor FP, respectively to these subunits [cAMP] can be measured (Figure 4a) (Zaccolo *et al.* 2000). A second [cAMP] sensor was made by using the cAMP binding protein, Epac1. Therefore Epac1 flanked by a donor and an acceptor FP respectively. In absence of cAMP FRET occurs, however upon binding of cAMP to Epac1, the protein undergoes a conformational changes and FRET is lost (Figure 4b) (Ponsioen *et al.* 2004).

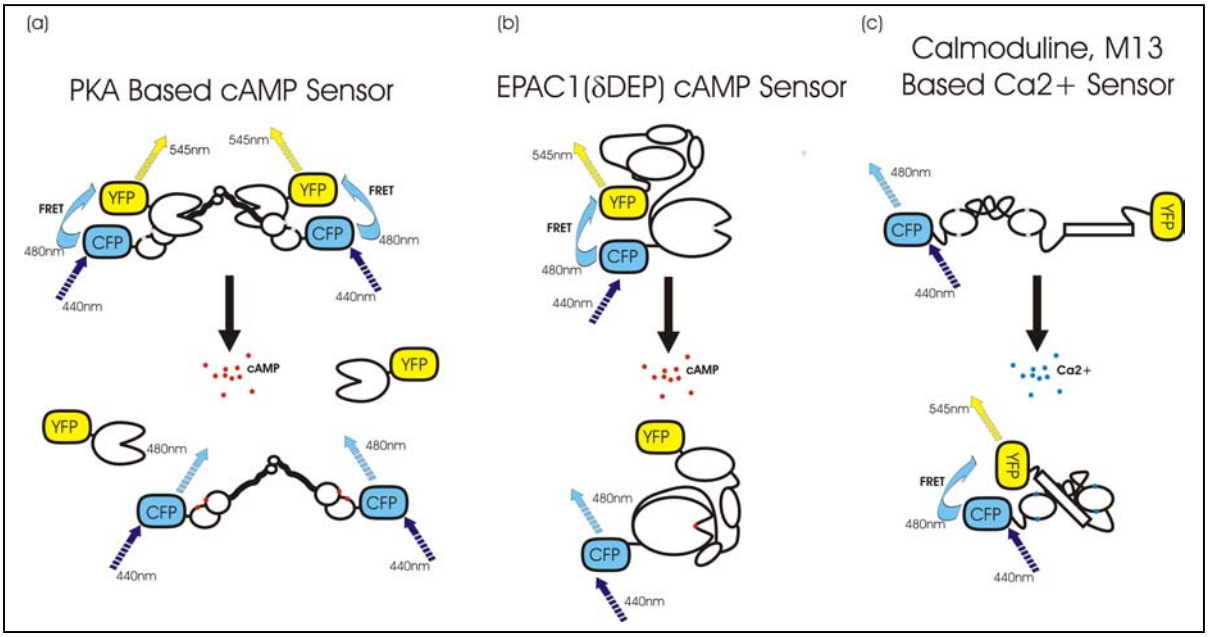

Figure 4. FRET based biosensors. (**a**) The PKA based cAMP sensor, CFP fused to the regulatory and YFP to the catalytic subunits. In the presence of cAMP, regulatory and catalytic subunits form a complex, resulting in FRET, which is lost upon cAMP binding (Adams *et al.* 1991; Zaccolo *et al.* 2000). (**b**) A cAMP sensor based on YFP/CFP fused to Epac1(δDEP), resulting in FRET. Upon binding of cAMP, the protein undergoes a conformational changes and FRET is lost (Ponsioen *et al.* 2004). (**c**)

The Ca2+ sensor, Yellow-cameleon-2 (Ycam2), based on a fusion of YFP and CFP to a calmoduline and a M13 domain. Upon binding of Ca^{2+} to the calmodulin this domain associates with the M13 region and FRET is induced (Nagai *et al.* 2004),

Such ‘’tailor made’’ biosensors will enable live imaging of cellular events with high (sub-cellular) resolution and high sensitivity. FRET is a powerful technique that can be used for FP based sensors. It is to be expected that more vital imaging probes based on FPs will be designed.

So GFP technology in combination with fluorescence microscopy created several new possibilities for *in vivo* imaging of cellular events. The *Rhizobium*-legume symbiosis (see below) involves various physiological and cell biological changes in the root epidermis. Therefore this is an attractive system to apply such *in vivo* imaging techniques.

The *Rhizobium*-legume symbiosis

Legumes like Medicago, Lotus, soybean, pea, and peanut et cetera. have the unique ability to establish an endosymbiosis with bacterial species that are collectively called rhizobia. This *Rhizobium*-legume symbiosis takes place in nodules that are formed on the roots of the plant (Figure 5). Within these nodules rhizobia are hosted in an intracellular manner and there they find the physiological conditions that allow them to reduce atmospheric nitrogen into ammonia.

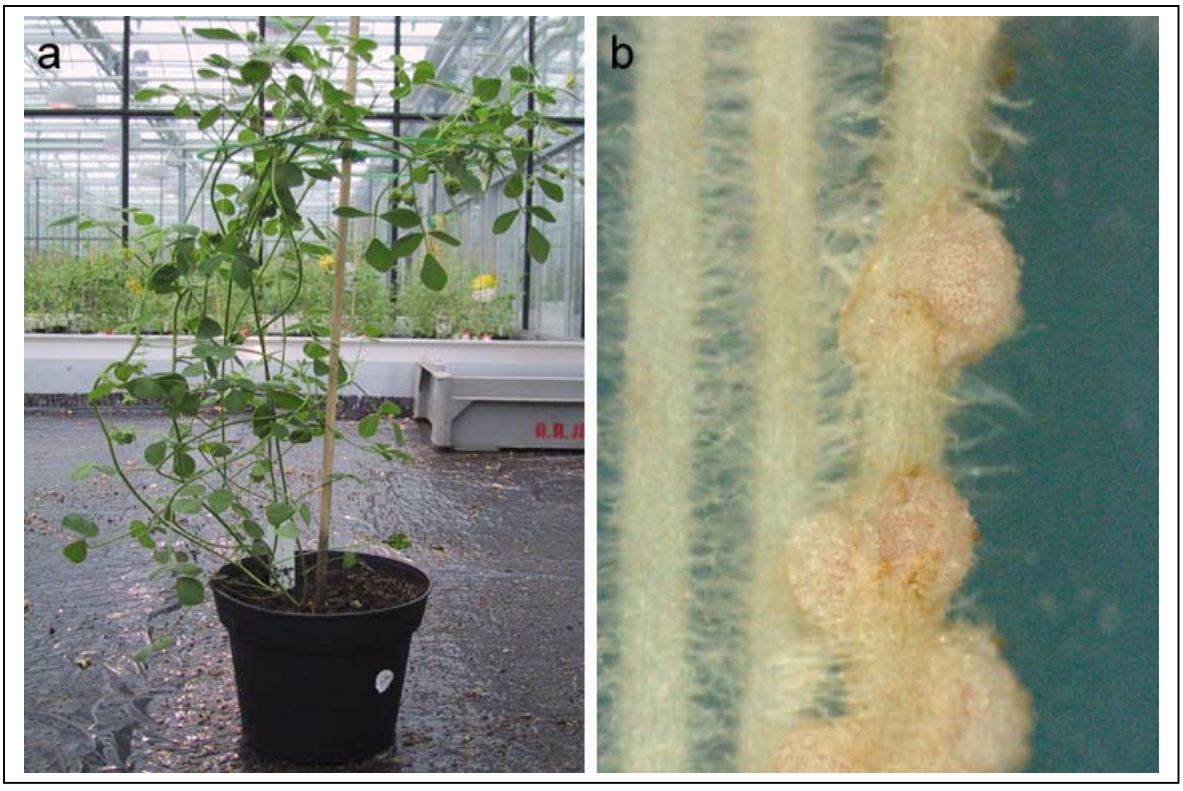

Figure 5. (**a**) *Medicago truncatula* plant with (**b**) root nodules.

Nodule formation is set in motion by Nod factors secreted by rhizobia. These Nod factors are lipochitooligosaccharides (LCOs), (Figure 6) and their production is initiated by the legume host. Legumes can secrete compound e.g., flavonoids which can induce the expression of rhizobial genes essential for the synthesis and secretion of Nod factors.

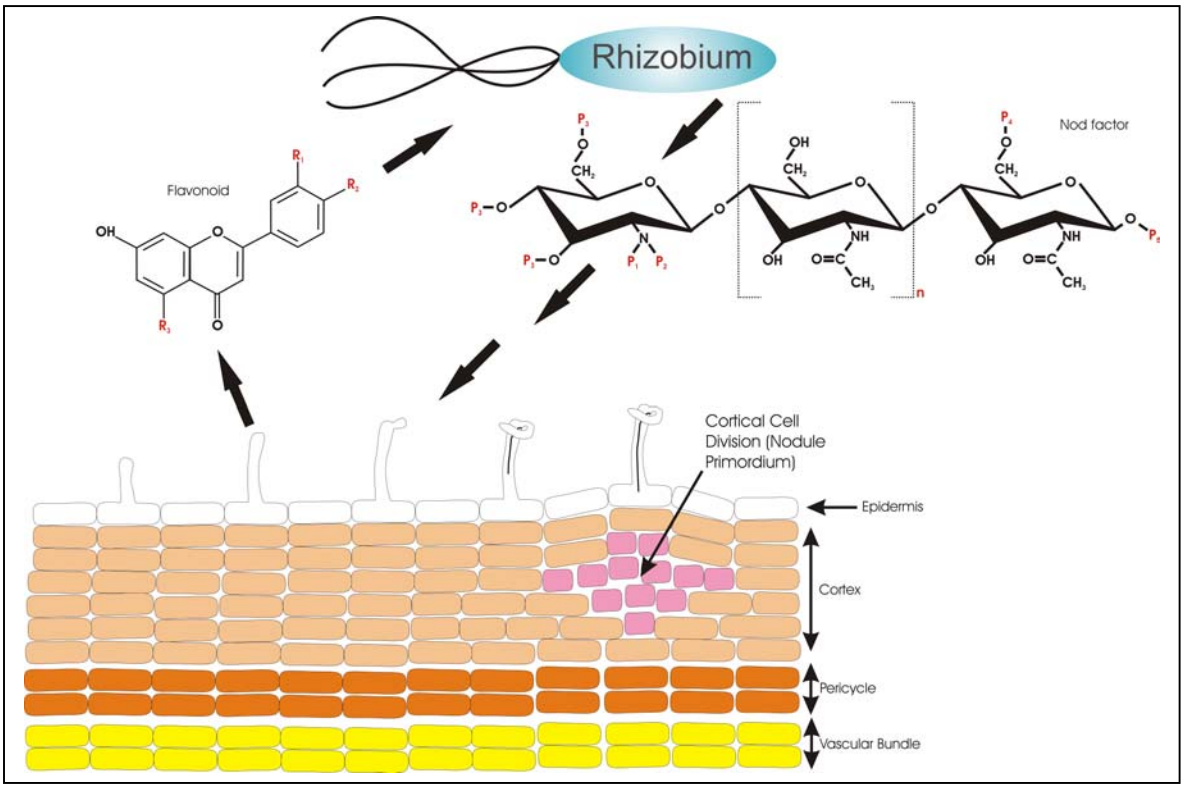

Figure 6. A schematic representation of the early events of the *Rhizobium*-legume interaction. Flavonoids produced and secreted by the legume root are sensed by the rhizobia upon which lipochitooligosaccharides (LCOs), so-called Nod factors are secreted by the rhizobia. Upon recognition of the Nod factors rhizobia become entrapment in the root hair curls. Further, cortical cell division, gene expression and infection thread (IT) formation are induced. Species specific side groups of Nod factors and flavonoids are indicated by $P_{1\text{-}5}$ / n(=1 to 5) and $R_{1\text{-}3}$ (for details see Heidstra and Bisseling, 1996 (Heidstra *et al.* 1996))

Upon Nod factor perception by the root hairs several physiological and cell biological processes are induced within minutes. Membrane depolarization within 1 minute (Ehrhardt *et al.* 1992; Felle 1995; Kurkdjian 1995), calcium spiking within 6 to 10 minutes. (Ehrhardt *et al.* 1996; Cárdenas *et al.* 1999; Wais *et al.* 2000; Walker *et al.* 2000) and an increase of fine actin filaments in the subapical area of the root hair within 3-15 minutes (Ruijter *et al.* 1999). Such responses in root hairs probably contribute to the start of the infection but also to the induction of cortical cell division (Limpens *et al.* 2004). These events occur upon LCO treatment in all growing or growth terminating root hairs, making it relatively simple to image these early responses or behavior of specific molecules before morphological changes take place. In contrast the responses in pericycle and cortex are very local and therefore it will be very hard to image behavior of specific molecules preceding a morphological responses like cell division. Therefore molecular behavior in relation to early LCO responses can more efficiently be imaged in root hairs.

At a later stage (1-3hrs) all root hairs in the susceptible zone do deform and also the expression of the first early nodulin genes (for example ENOD11 and ENOD12) is induced, within several hours (Pichon *et al.* 1992; Journet *et al.* 1994; Journet *et al.* 2001; Esseling *et al.* 2003). In root hairs the Nod factor secreting rhizobia induce root hair curling. In this way some rhizobia become entrapped in the cavity of such a curl and induce the formation of an infection thread (IT) (Figure 6,7).

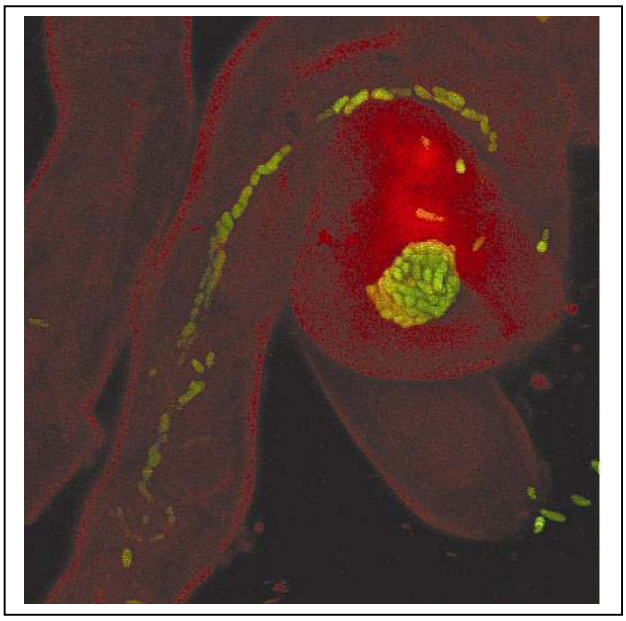

Figure 7. *M. truncatula* root hair with in the root hair curl entrapped rhizobia expressing GFP, The root hair cell wall is stained red with propidium iodine and an infection thread (IT) is visible. The curl, containing a rhizobial colony, is the starting point of the IT which grows down to the base of the root hair. In the curl and IT individual GFP expressing rhizobia can be seen (Kindly provided by Carolien Franken)

This IT is a tubular structure containing rhizobia that grows to the base of the root hair and subsequently traverses cortical cells (Figure 6) (Newcomb 1976; Callaham *et al.* 1981). By using GFP expressing rhizobia insight was obtained concerning IT formation and growth (Gage *et al.* 1996; Cheng *et al.* 1998). GFP expressing rhizobia are instrumental to detect a rare event like initiation of IT formation. Concomitantly with the infection process, the Nod factors induce cell division in some cortical cells by which a nodule primordium is formed. The IT grows to and enters the primordium, were it ramifies, and releases the bacteria in primordium cells. The released bacteria and surrounding root tissues now differentiate in such a way that an effective nitrogen fixing root nodule is formed (Figure 5b) (Goodchild *et al.* 1966; Newcomb 1976; Roth *et al.* 1989).

All early steps of nodule formation are induced by the Nod factors. These signaling molecules are most likely perceived by transmembrane receptor kinases (RLKs) whose extra-cellular regions contain LysM domains (LysM-RLKs) (Limpens *et al.* 2003; Madsen *et al.* 2003; Radutoiu *et al.* 2003). In addition to these receptors several additional Nod factor signaling genes were identified in Medicago and Lotus

(Geurts *et al.* 2005). These are essential for most early responses (Catoira *et al.* 2000; Wais *et al.* 2000; Caitoira *et al.* 2001). *DmI-1, DmI-2* are essential for Ca^{2+} spiking whereas *DmI3* is not. All three are essential for e.g., *MtENOD11* induction. These *DmI* genes as well as *Hcl* and *Nsp 1* and *Nsp2* are all essential for root hair curling, infection thread formation and induction of cortical cell division (Sagan *et al.* 1995; Caitoira *et al.* 2000; Caitoira *et al.* 2001; Oldroyd *et al.* 2003). It is probable that the proteins encoded by the Nod factor signaling genes will be the focus of research during the coming years. It will be a challenge to integrate studies on Nod factor signaling proteins and those focused on more common but also by Nod factor activated steps.

FP and its future role in elucidating Nod factor signaling in the *Rhizobium*-legume symbiosis

Three root cell types are involved in the legume-*Rhizobium* interaction. These are epidermis cells, especially those containing a root hair, cortical and pericycle cells. Ultimately, it will be important to image processes in all these cell types. However, for technical as well as scientific reasons it is attractive to start the use of innovative light microscopy studies with root hairs, where the initial steps of the symbiosis take place.

The legume-*Rhizobium* interaction is set in motion by signal molecules from the bacteria that induce responses in the root epidermis, the outermost cell layer and therefore accessible for microscopy. This is especially the case for the epidermal cells carrying a root hair. The initial responses induced by rhizobial Nod factors in root hairs occur in the fast majority of the hairs. Examples are the changes in the actin configuration in the apex of the hairs, the spiking of Ca^{2+} around nuclei or the influx of Ca^{2+} at the apex. All these responses have in common that they occur at a subcellular level and so the spatial information combined with molecular behaviour will be very useful.

Moreover, the epidermal response that is biologically most significant is root hair curling followed by infection thread formation. These responses are only induced in a very small subset of hairs and therefore microscopy will be essential to study mechanisms controlling these responses. Further, it is probable that infection thread formation will involve 2 subsequent Nod factor signalling events occurring at different positions in hairs (Geurts *et al.* 2005). Therefore full insight in the molecular mechanism controlling the start of infection can only be obtained when microscopy is used. The need for microscopy is further underlined by the first localization studies of legume proteins that play a key role in early Nod factor signalling, since these studies show that they locate at plasma membrane, plastids, nuclear envelope and nuclei, respectively (Limpens *et al.* 2003; Imaizumi-Anraku *et al.* 2005; Kalo *et al.* 2005; Smit *et al.* 2005).

Chapter 2

Root epidermis specific expression in *Medicago truncatula* roots

Abstract

In order to facilitate the study of rhizobia induced responses in root hairs of the legume *Medicago truncatula* (Medicago), 3 putative root epidermis specific promoters were tested. To be able to test these promoters we optimized the *Agrobacterium rhizogenes* root transformation procedure for Medicago. This transformation method results in compound plants that have primary transformed roots on a non-transgenic shoot. Transformation efficiencies were determined using a *CaMV35S::GUS* (β-glucuronidase) reporter construct. On average 10 roots emerged from the callus initially formed at the site of *A. rhizogenes* inoculation. GUS analysis showed that about 80% of the plants have at least one transgenic root, whereas on average 6 transgenic roots were formed. Subsequently, putative root epidermis specific promoters were tested using this transformation procedure. Therefore the pea *PsLYK3*, *PsRH2* and tomato *LeEXT1* promoter were fused to the GUS reporter gene and used for *A. rhizogenes* root transformation. *LeEXT1* and *PsRH2* showed to be root epidermis specific in Medicago and resulted in a high expression level. *LeEXT1* is specifically expressed in root hairs (trichoblasts) whereas *PsRH2* is active in all root epidermal cells spanning form the elongation zone up to the zone containing mature root hairs.

Keywords *Agrobacterium rhizogenes*, *Medicago truncatula*, Promoter analysis, Root epidermis specific promoter, *PsRH2*, *PsLYK3*, *LeEXT1, CaMV35S.*

Gerard N.M. van der Krogt, Carolien Franken, René Geurts and Ton Bisseling

Introduction

Legumes have the ability to establish an endosymbiotic relationship with soil bacteria of different genera, collectively named rhizobia, that results in nitrogen-fixing root nodules. The formation of root nodules begins when bacteria colonize the root surface and start secreting signal molecules -named Nod factor-. These molecules induce responses in root epidermal cells; e.g. membrane depolarization, [Ca2+] spiking, actin skeleton rearrangement and activation of certain early nodulin genes (Mirabella *et al.* 2002). Ultimately, specific infection structures are formed in root hairs, which guide the bacteria through the epidermis and outer cortical cells towards the newly formed nodule primoridum (Mylona 1995; Long 1996; Bladergroen *et al.* 1998; Hadri 1998; Schultze *et al.* 1998).
Medicago truncatula (Medicago) is a legume model plant (Cook 1999; Oldroyd *et al.* 2001), able to establish such a symbiosis with *Sinorhizobium meliloti* (Mylona 1995; Long 1996; Bladergroen *et al.* 1998; Hadri 1998; Schultze *et al.* 1998). To express trans-genes in Medicago, transformation procedures have been developed. Stable transformed Medicago lines can be obtained using *Agrobacterium tumefaciens* within about 9 months, (Chabaud 1996; Trinh *et al.* 1998; Trieu *et al.* 2000). However significantly faster, transgenic roots can be obtained using *Agrobacterium rhizogenes*. This latter transformation method results in compound plants that have transformed roots on a non-transgenic shoot, which can be obtained within 6-8 weeks (Trinh *et al.* 1998; Boisson-Dernier *et al.* 2001).
In order to study rhizobia induced responses in root hairs, transformation procedures can be used for example to; (a) modulate processes in root hairs by reverse genetics (lally *et al.* 2001; Potter *et al.* 2001; Limpens *et al.* 2004); (b) to introduce Fluorescent Protein (FP) based vital reporters to monitor (1) promoter activity, (2) responses like local changes in [Ca2+] and pH (Miesenbock *et al.* 1998; Gadella *et al.* 1999), (3) to image *in vivo* changes in a cytoskeletal configuration or organelle movement (Kost *et al.* 1998; Marc *et al.* 1998; Hanson *et al.* 2001) or (4) to localize tagged proteins (Schneider *et al.* 1998; Lazarowitz *et al.* 1999; Kim *et al.* 2000). Constitutive expression of such trans-genes could affect regeneration of transgenic tissue resulting in suppression of the trans-gene. A more restricted expression of the trans-gene only in target cells could greatly facilitate such studies.
We selected putative root epidermis specific promoters namely, *PsRH2* and *PsLYK3* of pea (*Pisum sativum*), and *LeEXT1* of tomato (*Lycopersicom esculentum*) and tested their expression pattern in Medicago roots obtained by *A. rhizogenes* mediated transformation (Mylona *et al.* 1994; Geurts 1998; Bucher *et al.* 2002). The transcriptional activity of these promoters was compared to that of the *CaMV35S* promoter, which is most frequently used for over-expression studies in plants (Odell *et al.* 1985).

PsRH2 (*P. sativum* ROOT HAIR2) was identified by 2D gel electrophoresis of root and root hair protein preparations of pea, and subsequently the cDNA as well as genomic clones were isolated (Mylona *et al.* 1994). By *in situ* hybridizations it was shown that in pea *PsRH2* is specifically expressed in the root epidermis and is activated at the stage of epidermis formation where its expression precedes root hair formation.

The tomato *LeEXT1(L. esculentum EXTENSIN1*) gene encodes an extensin-like cell wall protein. *In situ* hybridisation and promoter-GUS analysis showed that it is specifically expressed in the epidermis of tomato roots, but unlike *PsRH2* it is only active in root hairs (trichoblasts) (Bucher *et al.* 2002). This gene is first activated when the root hairs are formed and remains active in older hairs. Trichoblast specific expression was further demonstrated by regulating root hair development. Also it was shown that the *LeEXT1* promoter maintains its root hair specific expression pattern in other Solanacea's plant species, namely, potato and tobacco. In contrast, in Arabidopsis the root hair specificity of *LeEXT1* is not maintained and expression could be observed in rhizodermal cells, in the cortex including the endodermis and in the stele of the root (Baumberger *et al.* 2001). Therefore it has to be tested whether *LeEXT1* has a root hair specific expression in Medicago.

PsLYK3 (*P. sativum* LysM domain containing receptor kinase) encodes a putative membrane bound LysM domain containing receptor kinase, highly homologous to Medicago *LYK3*. RT-PCR experiments showed also that this gene in pea is active in root hairs and nodules but not in leaves, flowers and pods. *PsLYK3* was isolated from a pea genomic phage library (Geurts 1998; Gualtieri *et al.* 2002) and here we tested whether the 2kb upstream region of *PsLYK3* could be used to express a transgene in the root epidermis of Medicago.

The cauliflower mosaic virus promoter,*CaMV35S*, is a promoter often used to drive the expression of a transgene. This promoter is active in various plant organs, including roots (Fromm *et al.* 1985; Odell *et al.* 1985; Jefferson *et al.* 1987; Rhodes *et al.* 1988; Benfey *et al.* 1989; Lyznik *et al.* 1989; Terrada *et al.* 1990; Quaedvlieg *et al.* 1998).In this study the *CaMV35S* promoter is used as a reference for activity to (semi) quantify the activity of the promoters tested. Therefore the *PsRH2*, *LeEXT1*, *PsLYK3* and *CaMV35S* promoters were fused to the *ß-glucuronidase (GUS)* reporter gene, expression patterns were analyzed and the expression levels were compared to that of *CaMV35S*.
In addition the *CaMV35S::GUS* construct was used to test the *A. rhizogenes* hairy root transformation system efficiency.

Materials and methods

Bacterial strains and plant material

Agrobacterium strain MSU 440 containing the Ri plasmid pRiA4 of A. rhiz. strain A4 (Sonti *et al.* 1992) was used to transform *Medicago truncatula* Jemalong A17.

Hairy root transformation

Root transformation was performed, with a few modifications, according to Stiller *et al.* (Stiller *et al.* 1997). Sterilized seeds (10 min in conc. H_2SO_4, five rinses with sterile water,10min commercial bleach, seven rinses with sterile water) were germinated in the dark on a wet filter paper on top of solid Fahråeus (0.9% Daishin agar (Brunswig)) at 4°C overnight. Subsequently, they were incubated upside down at 24°C for 1 day. The seed coats of the germinated seeds were removed and the seeds were transferred to filter paper, placed on top of agar plates, with the same medium and sealed for about two third with Parafilm. The dishes were incubated in a growth chamber in a vertical position with a 16/8 hour day/night cycle at 21°C. Five days later the plantlets, have unfolded cotyledons, root and a shoot. A fresh plate of *A. rhizogenes* is used and streaked on the hypocotyl with a sterile curled

glass pipette. Subsequently the root is removed by cutting the hypocotyl with a scalpel in the area were the *A. rhizogenes* was streaked. By doing so the freshly cut surface will be infected by *A. rhizogenes*. The hypocotyls are covered by an additional filter paper and cultivated for five days. Then filters plus plants were transferred to emergence medium plates (1x SH-A salts (major elements; minor elements; Iron compounds) (Schenk *et al.* 1972), 1x UM-C vitamins(100mg/l Myoinositol; 5mg/l Nicotinic acid; 10mg/l Pyriodoxine-HCl; 10mg/ml Thiamine-HCl; 2 mg/l Glycine (Clara L. Diaz pers. comm. (Diaz *et al.* 1989))), 1% sucrose, 3mM MES, pH 5.8, 0.9% agar (Daishin), 300 µg/ml Cefotaxime). After 6 to 18 days after infection with *A. rhizogenes* the newly formed roots can be analyzed.

Constructs

All cloning work was carried out according to standard procedures (Maniatis *et al.* 2000), and all constructs made by PCR were sequenced.

pCAMBIA 1304 *CaMV35S*::*GUS* was obtained from CAMBIA, Canberra, Australia, www.cambia.org.

pBIN19 *PsRH2::GUS* was made by isolating the upstream promoter region of 1.1 kb (HindIII/Xba) from pDC49C-GUS (provided by Chiang and Hadwiger) (Chiang *et al.* 1990), This HindIII/Xba fragment was cloned into pBIN 101.1.

pBIN19 *LeExt1(∆gen1.1)::GUS* construct is described by Bucher *et al.* (Bucher *et al.* 2002).

pBIN(+)*PsLYK3::*GUS-*eCaMV35S::DsRED* is made in the following way.
To insert *PsLYK::GUS*, the pBIN-basis *e35S::DsRED* (see Chapter 4) was digested (XbAI/HindIII) to insert *GUS*. Subsequently the *PsLYK3* promoter (3,46 kb) was PCR amplified from a genomic phage library using the following oligonucleotides containing the extra restriction sites EcoRI/NcoI; respectively 5'TGGTGAATTCTATCGAGTATCTT3' (underlined EcoRI) and 5'TGAGTTCCATGGAATCAATAAGGG3' (underlind NcoI). This *PsLYK3* fragment was cloned (EcoRI/NcoI) into the intermediate vector pCAMBIA1304 (GFP-GUS) and from this clone isolated (EcoRI/XbaI) and cloned into the pBIN-basis GUS-*eCaMV35S::DsRED*.

Histochemical GUS analysis

GUS staining was performed according to Jefferson *et al.* (Jefferson *et al.* 1987) with a few alterations. Plant material was incubated in 0.05% (w/v) X-Gluc (Duchefa) in 0.1M sodium phosphate buffer with 3% sucrose, 5µM ferrocyanide, 5µM ferricyanide (pH 7). Vacuum infiltration was applied for 30 minutes and the sample was incubated at 37°C.

Sectioning

Samples were embedded in Technovit 7100 as described in the protocol from Kulzer. 10µm sections were made using a Leica microtome and mounted in Euparal (Agar Scientific LTD.).

Microscopy

For imaging a Nikon SMZ-U stereomicroscope and a Nikon optiphot-2 bright field microscope were used to analyze the GUS experiment. Photographs were made using a Nikon coolpix990 digital camera. For fluorescence imaging a Leica MZFLII stereomicroscope fitted with DsRED excitation/emission filters and equipped with a digital Leica DC300F camera was used. Images were processed using Photoshop 5.5 and illustrator 8.0.

Results

Efficiency of *Agrobacterium rhizogenes* root transformation system.
Medicago was transformed using the *A. rhizogenes* root transformation procedure. *A. rhizogenes* containing a Ri-plasmid and also a binary plasmid with a transgene of interest is streaked on the hypocotyl. Subsequently, the root is removed by cutting the hypocotyl in the *A. rhizogenes* treated region. By doing so the freshly cut surface is infected with *A. rhizogenes,* resulting in callus formation, and subsequently new roots are formed. Most roots developing from the callus have in general the T-DNA originating form the Ri-plasmid inserted. Often, T-DNA insertion is accompanied by co-insertion of the transgene originating from the binary plasmid. Roots containing detectable expression levels of the transgene of interest will be called transgenic. To determine the transformation efficiency the percentage of plants having at least one transgenic root showing GUS activity will be calculated. Since in this case "transformation efficiency" is determined by detecting the protein encoded by the transgene it is well possible that the percentage of roots co-transformed with the transgene is higher, because in some transgenic roots the transgene did not resulted in detectable expression levels.

To determine the transformation efficiency initially the *CaMV35S::GUS* transgene was used. On average 10 roots are formed from a callus (3 weeks post inoculation with *A. rhizogenes*) and GUS analysis showed that about 80% of the plants contained one or more transgenic roots (n= 90 plants). Plants that do contain transgenic roots have on average 6 transgenic roots. Similar experiment where conducted using the putative epidermis specific promoters. In all cases GUS activity could be detected, and similar transformation efficiencies where obtained by using the same criteria as described above, although expression levels can vary form root to root (Figure 1).

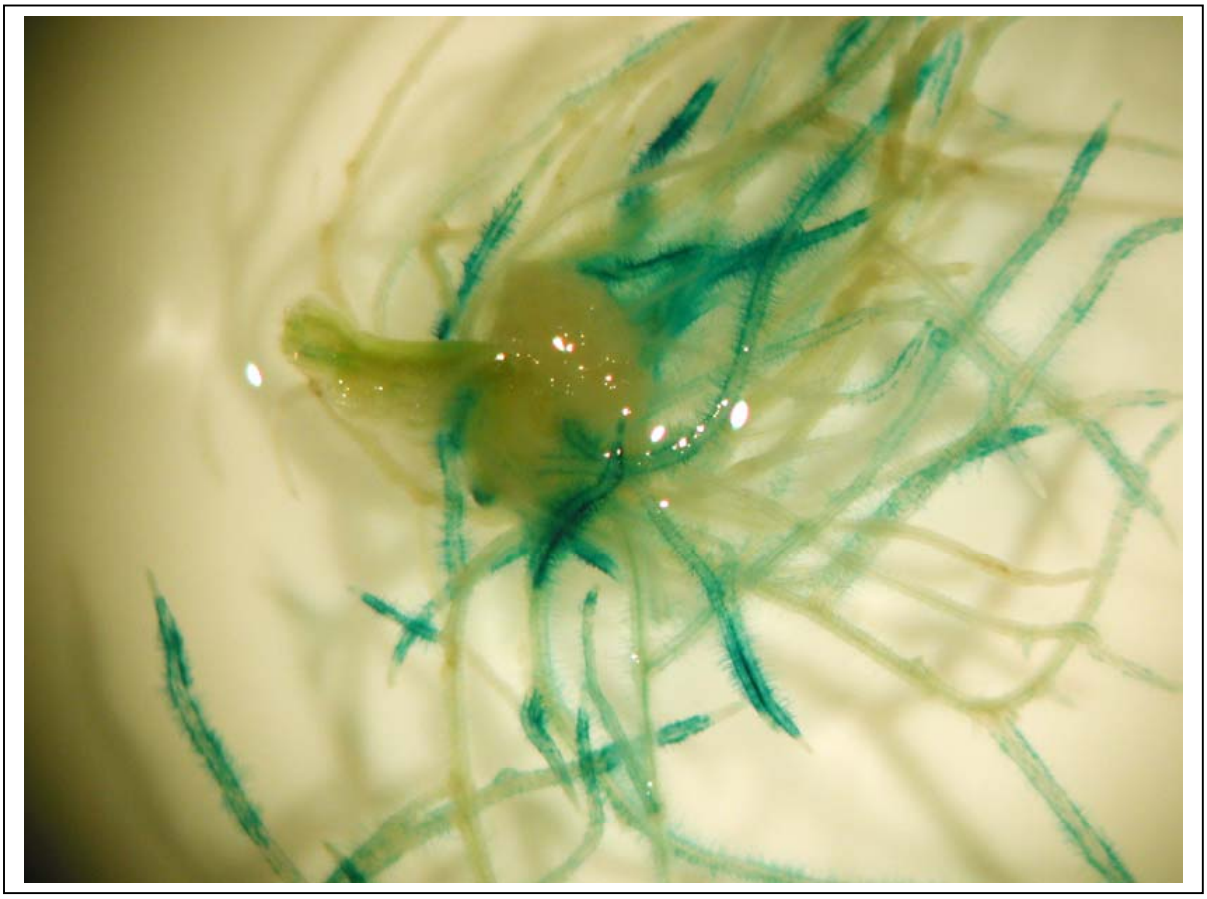

Figure 1. Medicago callus with newly formed transgenic roots .The roots express *LeEXT1::GUS*. Callus and roots were stained for GUS activity for 6 hours in appropriate buffer.

Also chimeric roots are formed suggesting that roots can be formed from two or more cells of which not all where co-transformed with the transgene. About 20% of all co-transformed hairy roots are chimeric (Figure 2).

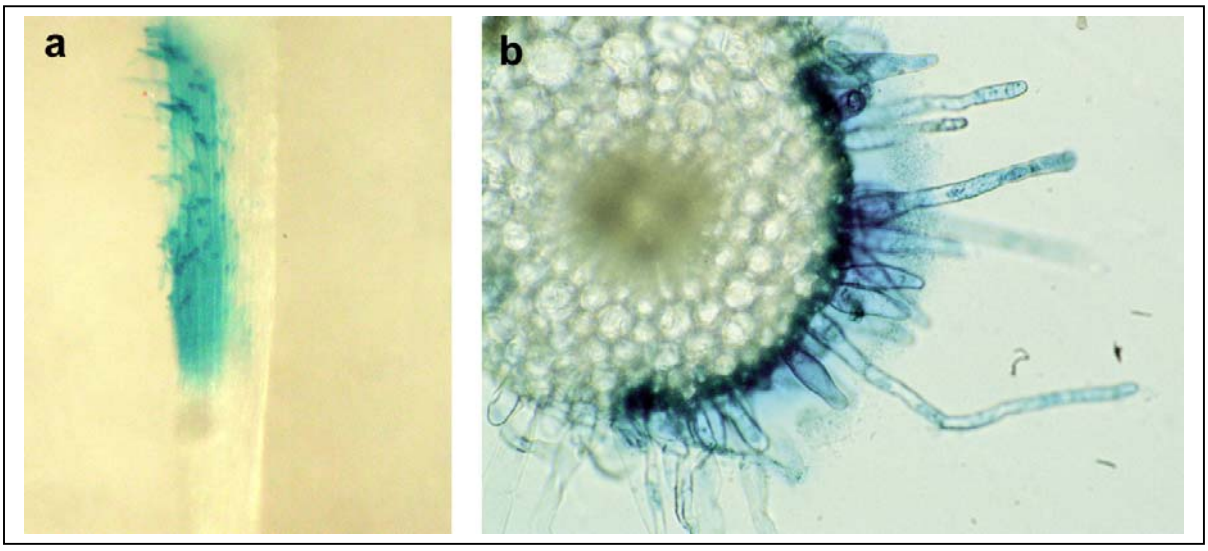

Figure 2. Histochemical localization of GUS activity in a Medicago root expressing *PsRH2::GUS*. (**a**) A chimeric root in which only a part of the epidermis shows GUS activity. (**b**) A cross section of a chimeric root.

In conclusion, *A. rhizogenes* root transformation is a fast and reliable procedure, therefore very suited for testing efficiently many DNA constructs. Therefore we used this system to determine whether the *PsLYK3*, *PsRH2* or *LeEXT1* promoters have an epidermis specific expression pattern. To test which promoters have a root epidermal specific expression the following constructs were used for transformation; *CaMV35S::GUS*, *PsLYK3::GUS*, *PsRH2::GUS* and *LeEXT1::GUS*. Calli with roots of about 30 plants are harvested 3 weeks after transformation and stained for GUS activity for 6 or, if needed 21 hours.

***CaMV35S::GUS* expression pattern**
Roots transformed with *CaMV35S*::*GUS* were stained for 6 hours for GUS activity. The strong blue staining (Figure 3a,b) preferentially occurred in the root tip and vascular tissue whereas GUS activity in the root epidermis is low or not even detectable. Longer staining (up to 21 hours) allowed detection of expression in the epidermis and root hairs (Figure 3b).

***PsLYK3::GUS* expression pattern**
Roots transformed with *PsLYK3::GUS* stained for GUS activity for 6 hours did not result in detectable GUS activity. After staining for 21 hours 5% of the plants showed GUS activity in one or two roots. However, in these cases GUS activity was found in all tissues (Figure 3c,d.) and the vascular tissue and the root tip region stain more intense than the rest of the root. This is a weak promoter (21 hours of staining) for all root cell types, including root hairs.

***PsRH2::GUS* expression pattern**
Roots transformed with *PsRH2::GUS* were stained for GUS activity for 6 hours after which 50% of the plants show GUS activity in one or more roots. This GUS activity was found in epidermal cells with as well as without root hairs (Figure e,f). The highest *GUS* expression level occurs in the zone that starts just above the root tip and remains active in the differentiation and elongation zones. So, this promoter seems active during all stages of root hair development To determine whether the *PsRH2* promoter is exclusively active in Medicago root epidermis, longitudinal sections were made (Figure 3f) showing that this is indeed the case. Further it can be concluded that the *PsRH2* promoter in Medicago has a similar expression pattern as in pea (Mylona *et al.* 1994). The GUS activity found in root hairs transformed with *PsRH2::GUS* is higher (6 hours) then *CaMV35S*::*GUS* (21 hours) and is root epidermis specific in Medicago.

***LeEXT1::GUS* expression pattern**
Roots transformed with *LeEXT1::GUS* were stained for GUS activity for 6 hours after which 80% of the plants show blue staining in one or more roots (Figure 3g,h). This GUS expression is epidermis specific and mainly restricted to trichoblasts. This trichoblast specific expression is similar as found in tomato and potato (Bucher *et al.* 2002). In Medicago the promoter has also a low activity in atrichoblast cells just above the root tip (Figure 3g). The GUS activity found in root hairs transformed with

LeEXT1::GUS (80% of the plants have a transgene expression detectable by staining for 6 hours) is higher than *PsRH2*::*GUS* (50% in 6 hours).

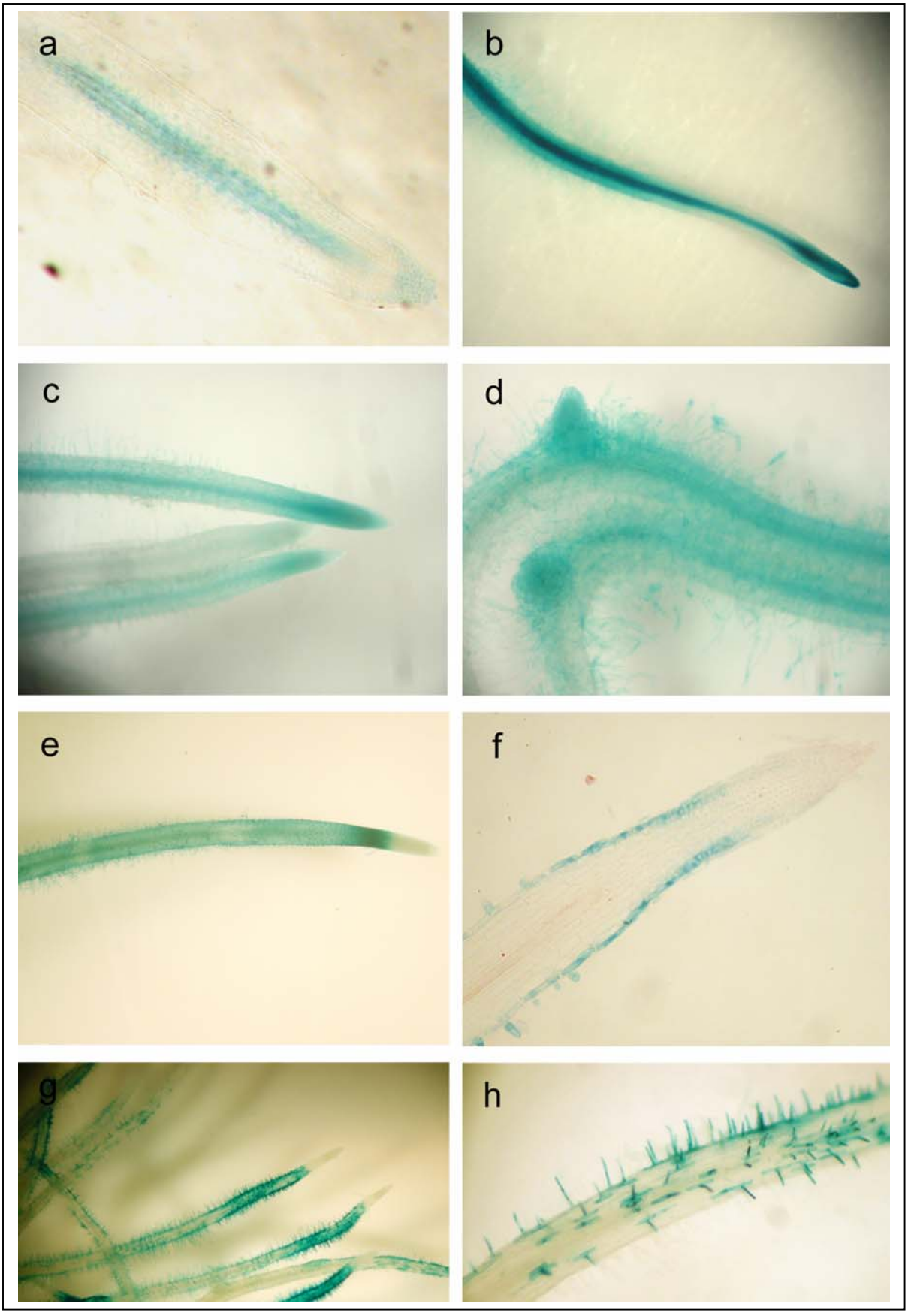

Figure 3. Histochemical localization of GUS activity in Medicago roots expressing; (**a-b**) *CaMV35S*::*GUS* , (**a**) a longitudinal section of a root stained for 6 hours, (**b**) a root stained for 21 hours. (**c,d**) *PsLYK3*::*GUS* expression in roots stained for 21 hours. (**e,f**) *PsRh2::GUS* expression in

,(**e**) a root stained for 21 hours, (**f**) a longitudinal section of such a root. (**g-,h**) *LeExt1::GUS* roots stained for 6 hours.

Discussion

In this chapter we first determined the efficiency of an *A. rhizogenes* based *M. truncatula* root transformation procedure. The frequency of transformed plants is 80%, with on average 60% (6 out of 10) of the roots co-transformed. Further, only 5% of the roots are chimaeric. So the procedure tested here is a very reliable and efficient method to produce transgenic roots. Using a similar protocol Boisson-Dernier *et al.* obtained Medicago plant transformation efficiencies of 60%, with on average 30% of the roots co-transformed (2 out of 6) (Boisson-Dernier *et al.* 2001). They were able to increase the transformation efficiency to at least 95% with on average 60% of the roots co-transformed (4 out of 6) by using kanamycin based selection. However, using an antibiotic selection step in our *A. rhizogenes* transformation procedure did not significantly improve the transformation efficiency (data not shown; Joop Vermeer pers. comm.). The size of the DNA fragment present between the T-DNA borders affects the transformation efficiency. By eliminating the *NPTII* kanamicin resistance gene (0.8 Kb), still present in the plant transformation vectors used (*LeExt(∆gen1.1)* and *PsRH2*), transformation efficiencies probably can be slightly increased.
Our aim was to test the suitability of heterologous promoters to drive the expression of a transgene of interest in the Medicago root epidermis. *PsLYK3* and *CaMV35S* show both a low activity in the epidermis. Based on RT-PCR experiments we expected *PsLYK3* to be active in the root epidermis (Gualtieri *et al.* 2002), however this appeared not to be the case. The used promoter region showed to be active in the root tip and root vascular tissue. The reason for this might be the lack of an upstream promoter regulatory domain missing in the region used. *LeEXT1* and *PsRH2* were shown to be root epidermis specific in Medicago, where *LeEXT1* is mainly restricted to trichoblasts. These two promoters give, compared to the *CaMV35S* promoter, higher expression levels in root hairs. Further, the *LeEXT1* promoter has the highest expression level in trichoblasts compared to the here tested promoters. The *PsRH2* and *LeEXT1* promoters will allow us now to manipulate and visualize rhizobia induced responses in root hairs and minimize effects of transgenes expressed on other root cell types.

Acknowledgements We like to thank Marcel Bucher for providing the pBIN*Ext1*(∆*gen1.1*)::GUS construct, Chiang and Hadwiger for the pDC49C-GUS plasmid, CAMBIA (Canberra, Australia) for providing us with the pCAMBIA 1304 *CaMV35S::*GUS, and Clara L. Diaz for her help with the hairy root transformation procedure.

Chapter 3

The Ethanol-inducible promoter system used in *Medicago truncatula* roots

Abstract

Inducible promoter systems are used to express on demand a transgene. Here we describe the ethanol inducible promoter system in *Medicago truncatula* (Medicago) roots, transformed using the *Agrobacterium rhizogenes* root transformation procedure. The ethanol inducible promoter system contains a transcription factor, AlcR, which is inactive in the absence of ethanol, whereas in the presence of ethanol, the AlcR transcription factor is activated and can by itself induce transcription of the *AlcA* promoter, driving a gene of interest, here the β-glucuronidase reporter gene (GUS). Roots expressing this construct can be obtained within several weeks using the *Agrobacterium rhizogenes* root transformation procedure. Plant transformations normally include growth in a sterile confined space e.g. petridishes. Further, to study the legume-*Rhizobium* interaction, the transgenic plants often need to be maintained at similar conditions. It was shown that under such conditions endogenous ethanol is made, restricting the use of the ethanol inducible promoter system. To circumvent such endogenous ethanol production we developed growth conditions by which plants can be transformed and maintained while the level of endogenously produced ethanol remains below the threshold level to activate AlcR. In addition after root drenching with a 2% ethanol solution GUS induction was successful in 50-75% of the plants. Further we showed that the induction of the transgene by ethanol can be restricted to the root epidermis by using a root epidermis specific promoter. This tissue specific promoter would minimize putative effects of an expressed transgene during root development due to endogenous ethanol production, since the gene would be only activated in the epidermis.
In short; the fast *A. rhizogenes* root transformation procedure for Medicago can be combined with an attractive inducible promoter, the ethanol inducible AlcR/AlcA system.

Keywords Ethanol inducible promoter, Agrobacterium rhizogenes transformation, *Lotus japonicus*, *Medicago truncatula*, Promoter analysis, Root epidermis

Gerard N.M. van der Krogt, Carolien Franken, Renze Heidstra and Ton Bisseling

Introduction

Several inducible promoter systems are used to express on demand a transgene. The most frequently used inducible systems are those regulated by the following inducers, tetracycline, Cu^{2+}, dexamethasone (Aoyama *et al.* 1997) and ethanol (Caddick *et al.* 1998). Inducible promoter systems have the advantage that the level and timing of expression can be controlled. Thus the transgene can be activated at a selected developmental stage, enabling studies on gene products interfering with e.g. regeneration, cell division or reproduction. Further, by controlling inducible promoters primary effects can be more easily distinguished from secondary effects (Caddick *et al.* 1998). An inducible system would be a very attractive option for expressing transgenes if it meets the following criteria: First, when the inducer is not applied the transgene should not be transcribed. Second, neither the inducing agent nor parts of the inducible system itself should influence the expression of endogenous genes or affect other cell functions. For example the glucocorticoid-inducible GVG system can cause severe growth defects in *Lotus japonicus* (Andersen *et al.* 2003).

An attractive inducible promoter is the ethanol (acetaldehyde) inducible system (Caddick *et al.* 1998; Salter *et al.* 1998; Roslan *et al.* 2001; Sweetman *et al.* 2002; Deveaux *et al.* 2003; Schaarschmidt *et al.* 2004). This system contains a transcription factor, AlcR, which is inactive in the absence of ethanol, whereas in the presence of ethanol, the AlcR transcription factor is activated and can by itself induce transcription of *AlcA* promoter containing genes. The ethanol inducible system has several advantages. First, both AlcR and AlcA originate from *Aspergillus nidulans*, and since higher plants and *A.nidulans* are phylogenetically not closely related it is unlikely that putative plant homologues of the AlcR protein would efficiently activate the *AlcA* promoter. Second, by locally applying ethanol (or acetaldehyde) the transgene can be induced more or less in an organ specific manner (Sweetman *et al.* 2002; Schaarschmidt *et al.* 2004), which can be further improved by putting the *AlcR* gene under control of an organ/tissue specific promoter. Third, *AlcR* is activated in a dose-dependent manner (Roslan *et al.* 2001; Sweetman *et al.* 2002; Chen *et al.* 2003; Deveaux *et al.* 2003). Fourth, ethanol has a low toxicity for plant and human and is inexpensive. A disadvantage of this system is that plants can produce some ethanol when grown under anaerobic conditions when they switch their energy metabolism from respiration to fermentation (Drew 1997; Caddick *et al.* 1998; Salter *et al.* 1998; Roslan *et al.* 2001). Fifth, the strength of the induced *AlcA* promoter containing genes is sufficient to enable abundant expression to allow gene induced phenotypes, gene silencing (RNAi), visualization of Green Fluorescent Protein (GFP) (fusions) etc. (Chen *et al.* 2003; Deveaux *et al.* 2003; Ketelaar *et al.* 2004).

Legumes, have the unique ability to establish an endosymbiosis with rhizobia. This interaction results in the formation of a new plant organ, a nitrogen fixing root nodule. Root hairs are the first target of rhizobial signals during the initial steps of nodule formation (Long 1996). Future studies on *Rhizobium* induced processes in root hairs would be facilitated if transgenes could be expressed in root hairs in a well-controlled manner. *Medicago truncatula (*Medicago) and *Lotus japonicus* (Lotus) are chosen as model legumes. They have a small diploid genome, autogamous genetics and further they can be efficiently transformed (Handberg *et al.* 1992; Oldroyd *et al.* 2001). Stable transformed plants can be obtained using *Agrobacterium tumefaciens*. Such transgenic plants can be made within 3 to 6 months. However, transgenic roots can already be obtained within several weeks, with an *Agrobacterium rhizogenes* root

transformation procedure (see Chapter 2). *A. tumefaciens* as well as *A. rhizogenes* based plant transformations can include a selection step during which plants are grown in a sterile confined space (e.g. petridishes) on medium containing antibiotics. Further, to study the legume-*Rhizobium* interaction the transgenic plants often need to be maintained at similar conditions. It was shown that under such conditions endogenous ethanol is made (Salter *et al.* 1998; Deveaux *et al.* 2003), restricting the use of the ethanol inducible promoter system. To circumvent such endogenous ethanol production we developed growth conditions by which plants can be maintained in a small sterile container while the level of endogenously produced ethanol remains below the threshold level to activate AlcR. Also we showed that the induction of the transgene by ethanol can be restricted to the root epidermis by using a root epidermis specific promoter. In this way the fast *A. rhizogenes* root transformation procedure for Lotus as well as Medicago can be combined with an attractive inducible promoter system.

Materials and methods

Bacterial strains and plant material

Agrobacterium strain MSU 440 containing the Ri plasmid pRiA4 of A. rhiz. strain A4 (Sonti *et al.* 1992) was used to transform *Medicago truncatula* Jemalong A17 and *Lotus japonicus* Gifu (accession No. B-129-S9 germ plasm reg. No. GP-158, PI 591056).

Hairy root transformation

Root transformation was performed, with a few modifications, according to Stiller et al. (1997)(Stiller *et al.* 1997). Sterilized seeds (10 min (Lotus 2 min) in conc. H_2SO_4, five rinses with sterile water, 10 min commercial bleach, seven rinses with sterile water) were germinated in the dark on a wet filter paper on top of solid Fahråeus medium (0.9% Daishin agar (Brunswig)) at 4°C overnight. Subsequently, they were incubated upside down at 24°C for 1 day. The seed coats of the germinated seeds were removed and the seeds were transferred to filter paper, placed on top of agar plates, with the same medium and sealed for about two third with Parafilm. The dishes were incubated in a growth chamber in a vertical position with a 16/8 hour day/night cycle at 21°C. Five days later the plantlets, have unfolded cotyledons, root and a shoot. A fresh plate of *A. rhizogenes* is used and bacteria from this plate were streaked on the hypocotyl using a sterile curled glass pipette. Subsequently, the root is removed by cutting the hypocotyl with a scalpel in the area were the *A. rhizogenes* was streaked. By doing so the freshly cut surface will be infected by *A. rhizogenes*. The hypocotyls are covered by an additional filter paper and cultivated for five days. Then filters plus plants were transferred to emergence medium plates (1x SH-A salts (major elements; minor elements; Iron compounds)(Schenk *et al.* 1972), 1x UM-C vitamins (100mg/l Myoinositol; 5mg/l Nicotinic acid; 10mg/l Pyriodoxine-HCl; 10mg/ml Thiamine-HCl; 2 mg/l Glycine (Clara L. Diaz pers. comm. (Diaz *et al.* 1989))), 1% sucrose, 3mM MES, pH 5.8, 0.9% agar (Daishin), 300 µg/ml Cefotaxime). In most cases each root originates from a single transformed cell (see Chapter 2). After 6 to 18 days after infection with *A. rhizogenes* the newly formed roots can be analyzed.

Constructs

All cloning work was carried out according to standard procedures and all DNA fragments made by PCR were sequenced.

pBIN*CaMV35S::AlcR-AlcA::GUS* (Figure 3a)

The ß-glucuronidase (GUS) gene (Jefferson *et al.* 1987) of pBIN101.1 (Clontech, USA) was isolated (BamHI/EcoRI) and cloned into pBluescriptSKII (Clontech, USA). From the new vector *GUS* was isolated (BamHI/ClaI) and used to replace the chloramphenicol acetyl transferase (*CAT*) reporter gene (Cullen 1987) of the pACN vector (Caddick *et al.* 1998; Salter *et al.* 1998), creating pAGN. The *alcA::GUS* was isolated (HindIII) from the pAGN vector and used to replace *alcA::CAT* of the pSRNACN vector (Caddick *et al.* 1998; Salter *et al.* 1998), creating pBIN*CaMV35S::AlcR-AlcA::GUS* (Figure 3a).

pBIN+*PsRh2::AlcR-AlcA::GUS* (Figure 3b)
The pBINPLUS vector (Engelen *et al.* 1995) contains a *NPTII* kanamicin resistance gene which was removed (Bsu36I/Bst98I), creating pBIN-basis. The multiple cloning site (MCS) was digested (SalI/EcoRI), blunded and ligated, creating pBIN+(7,8) with the following MCS; AscI/HindIII/(PstI, not usable)/SphI/PacI. This is the binairy vector used for introducing the two parts of the inducible promoter system, the *PsRh2::AlcR* and the *AlcA::GUS* cassette. The *PsRh2::AlcR* cassette was made by PCR (1.1kb *PsRh2* promoter including 5'UTR) using drrg495 as a template (pDC49C-GUS was kindly provided by Chiang and Hadwiger) in combination with the following oligonucleotides; 5'TTAATTAACATATGTAAACAGGTCGGTCT3' (underlined PacI), 5'GAATTCGGGTGCTTGCCTAGCTGT (underlined EcoRI) and inserted in pGEM-Teasy (Promega, USA). *AlcR* was isolated from binSRNACatN (Caddick *et al.* 1998; Salter *et al.* 1998) using EcoRI/HindIII and together with *PsRh2* cloned in pBIN+(7,8), creating pBIN+ *PsRh2::AlcR*.
The *AlcA::GUS* cassette was made by removing *CAT* from pACN (Caddick *et al.* 1998; Salter *et al.* 1998). *CAT* was removed (PstI). A new MCS was made by combining oligonucleotides;
5'GCTCGAGTCTAGAGCTAGCGCGGCCGCGGAAT3',
5'TCGGATCCGAGCTCGGTACCACTAGTCTGCA3',
5'GCGGCCGCGCTAGCTCTAGACTCGAGCTGCA3',
5'GACTAGTGGTACCGAGCTCGGATCCGAATTCC3'.
These were inserted in the PstI site, creating the MCS,
5'PstI/XhoI/XbaI/NheI/NotI/EcoRI/BamHI/SacI/KpnI/SpeI/PstI3'. This MCS is under control of the *AlcA* promoter, creating the pGMCV. Using PCR *AlcA::MCS* was amplified from pGMCV using oligonucleotides containing the HindIII/AscI sites; 5'GGGCGCGCCCGGGATAGTTCCGACCTA3' (underlines AscI) , 5'AAGCTTAGAGATCTAGTAACATAGATG3' (underlined HindIII) and inserted in pGEM-Teasy (Promega, USA), transferred to pBIN+(7,8) (HindIII/AscI), creating *pBIN+AlcA::MCS.*
The GUS gene was taken from pMON GUS (Bokhoven *et al.* 1993) (XbaI/BamHI) and inserted (NheI/BamHI) in the MCS of *pBIN+AlcA::MCS*, creating *pBIN+AlcA::GUS*.
The *PsRrh2::AlcR* fragment of pBIN+ *PsRh2::AlcR* was inserted in *pBIN+AlcA::GUS* (PacI/HindIII), creating pBIN+*PsRh2::AlcR-AlcA::GUS* (Figure 3b).

Ethanol treatment

The roots, 5 plants per petridish, were induced by pippetting 5 ml Fåhraeus medium containing 2% ethanol (v/v) on top of the roots for two times with an interval of 48 hours (Roslan *et al.* 2001).

Histochemical GUS staining

GUS staining was performed according to Jefferson et al. (Jefferson *et al.* 1987) with a few alterations. Plant material was incubated in 0.05% (w/v) X-Gluc (Duchefa) in 0.1M sodium phosphate buffer with 3% sucrose, 5µM ferrocyanide, 5µM ferricyanide (pH 7). Vacuum infiltration was applied for 30 minutes and the sample was incubated at 37°C.

Sectioning

Samples were embedded in Technovit 7100 as described in their protocol (Heraeus Kulzer, Germany) 10µm sections were made using a Leica microtome and mounted with Euparal (Agar Scientific LTD.).

Microscopy

For imaging a Nikon SMZ-U stereomicroscope and a Nikon optiphot-2 bright field microscope were used to analyze the GUS experiment. Photographs were made using a Nikon coolpix990 digital camera. Images were processed using Photoshop 5.5 and illustrator 8.0.

Results

The ethanol-inducible *AlcA* gene expression construct driving the *CAT* reporter gene was kindly provided by Zeneca Agrochemicals. Within this construct *GUS* was replaced by *CAT* (Figure 1a). Since the ethanol sensitive transcription regulator AlcR is under control of the *CaMV35S* promoter this construct can be used to test whether endogenous ethanol accumulation occurs in a root tissue and would lead to "constitutive" GUS expression.

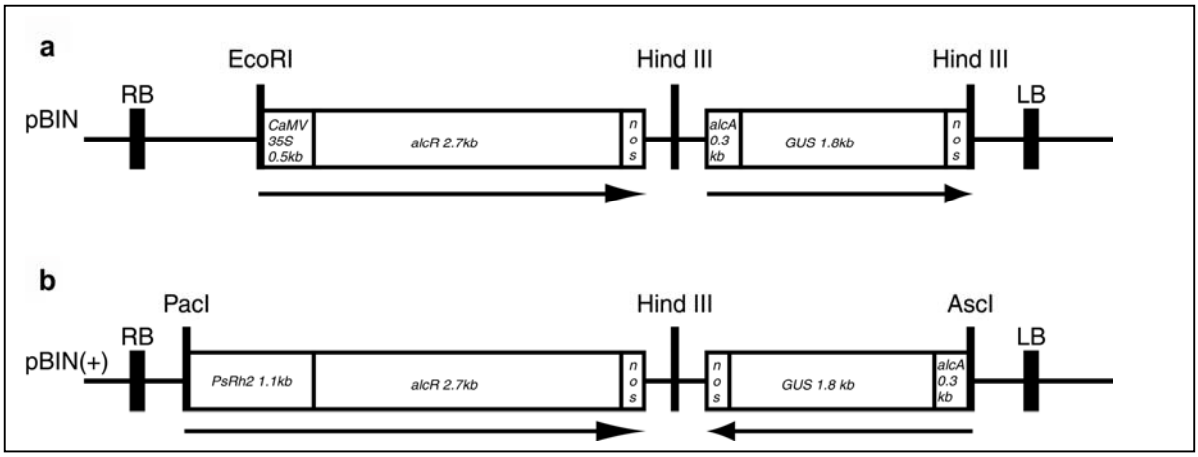

Figure 1. The *AlcA* and *AlcR* based ethanol inducible expression constructs.
(**a**) *CaMV35S* promoter is fused to *AlcR*. The GUS reporter gene (Jefferson *et al.* 1987) was placed under control of *pAlcA* (Caddick *et al.* 1998) and introduced into pBIN (Bevan 1984).
(**b**) This construct is similar to that shown in (a) except for three modifications. First, the *CaMV35S* promoter was replaced by the *PsRh2* root epidermis specific promoter (see Chapter 2). Second, the orientation of the p*AlcA-p35S*::*GUS* was reversed to minimize an effect of the *PsRh2* promoter on the expression of the *AlcA*. Third, this cassette was introduced into the high copy pBIN+ (Engelen *et al.* 1995) plant transformation vector.

Under microaerobic conditions plants can form ethanol (Caddick *et al.* 1998; Salter *et al.* 1998; Roslan *et al.* 2001). To test whether during the used growth conditions ethanol accumulates at a level at which it activates AlcR, several pilot experiments were performed and one typical experiment will be described. Lotus plants were transformed with the *CaMV35S::AlcR-AlcA::GUS* construct using the *A. rhizogenes* transformation procedure and grown for 2 weeks in sealed petridishes till an extended root system was formed (Figure 2).

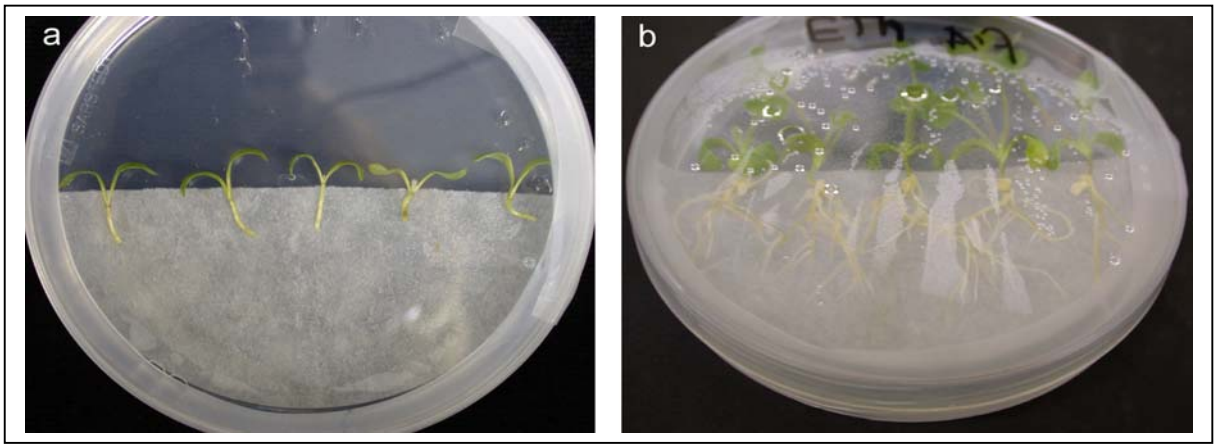

Figure 2. (**a**) Five plants after inoculation with A. rhizogenes. Note removed roots. The plants were grown on a filter paper that was placed on top of an agar-feeding layer. (**b**) After 3 weeks each non transgenic shoot contained several transgenic roots.

Subsequently, roots were screened for GUS activity, 57% of the plants showed some GUS activity. This GUS induction is probably due to production of ethanol caused by the micro anaerobic conditions in sealed petridishes. To determine whether the GUS activity is caused by ethanol and not by plant homologues of the AlcR protein, Medicago and Lotus plants were grown under aerobic conditions, in aeroponics (Figure 3) (similarly as described by (Bauchrowitz *et al.* 1996)).

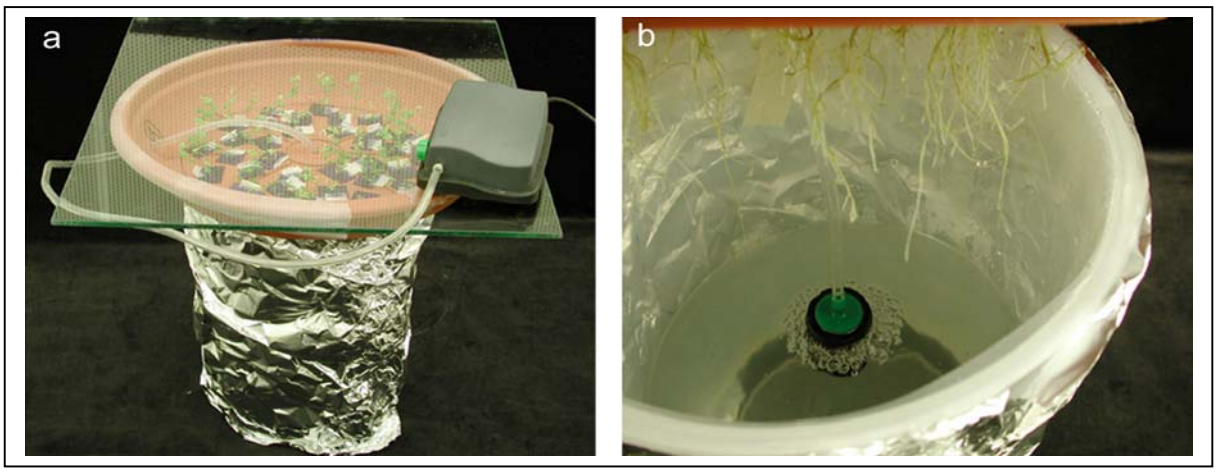

Figure 3. The aeroponic beaker system. (**a**) The shoots grown under a glass cover and separated from the aerosol by a plastic tray. (**b**) The roots hanging in the beaker containing an aerosol of Fåhraeus medium (Fåhreaeus 1957). An air stone coupled to a pump forms aerosols.

These plants showed no GUS induction, so induction of *AlcA* is not due to AlcR plant homologous.
To obtain a more aerobic growth condition in petridishes two modifications were introduced. First, dishes were partially sealed (~2/3). Second, an opening of ~1 cm^2 in the cover of the petridish was made on which a gas permeable (O_2) polytetrafluorethylene (PTFE) membrane (Milliwrap Adhesive Membrane, Millipore)

was placed. 45 Medicago plants were transformed with the same construct and were grown in partially sealed petridishes and divided in two groups. 14 plants were grown in petridishes with the PTFE filter covering the opening in the plate cover. The other 31 plants were grown in petridishes with the intact cover. Of these 31 plants 17 were induced with ethanol by drenching the roots two times with an interval of 48 hours with Fåhraeus medium containing 2% ethanol (v/v) (Roslan *et al.* 2001). All plants were analyzed for GUS activity, and the results are summarized in Table I.

Table I. GUS induction of *CaMV35S::AlcR* transformed Medicago roots grown in partially open plates. 14 transformed plants were grown in plates having in addition a PTFE filter covered opening in the lit. 31 plants were grown in petridishes with an intact lit, and of these, 17 plants were induced by two times root drenching with ethanol.

	Control		**2% Ethanol**
	With filter	**Without filter**	**Without filter**
	n = 14	n = 14	n = 17
Duration of GUS staining (hours)			
5	0 (0%)	0 (0%)	8 (47%)
24	0 (0%)	0 (0%)	13 (76%)

GUS activity was not detectable in the control plants from dishes with as well without a filter in the cover. So partially sealed plates are sufficient to create growth conditions for Medicago by which endogenously produced ethanol remains below the threshold level for AlcR activation.
Further 76% of the ethanol treated Medicago plants have GUS activity. So the ethanol inducible promoter system functions efficiently in Medicago roots.

To create an inducible system especially suited for expressing plant genes involved in the *Rhizobium*-legume interaction the root epidermis specific promoter *PsRh2* (see Chapter 2) was used to drive the *AlcR* gene (Figure 1b). The ethanol inducible system under control of *PsRh2* would minimize also a putative effect of an expressed transgene during root development since the gene would only be activated in the epidermis. The *PsRh2* gene has been cloned from pea where it is activated at an early stage of root epidermis formation and precedes root hair formation (Mylona *et al.* 1994). The *PsRh2* promoter is active in a similar manner in Medicago (Figure 4) (see Chapter 2).

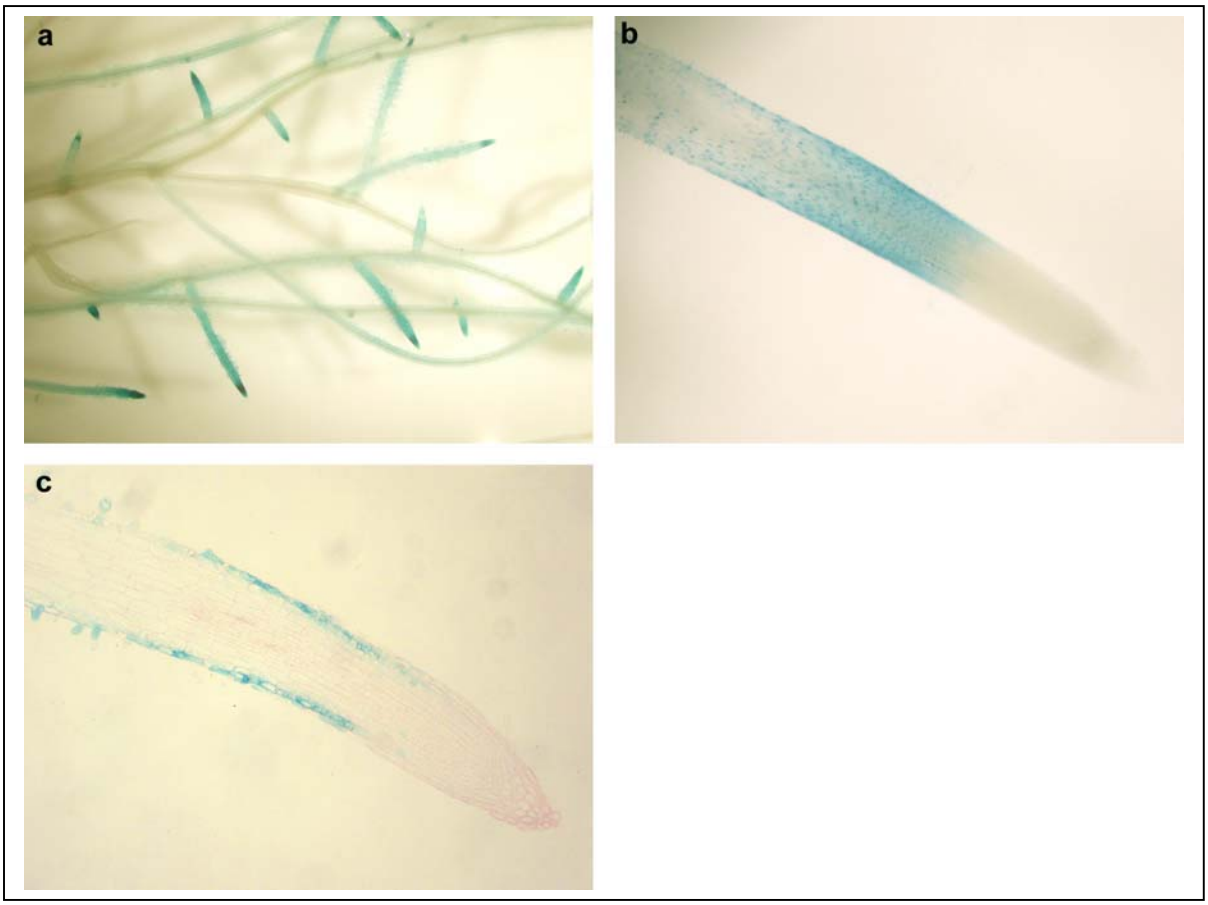

Figure 4. GUS activity in a Medicago root expressing *PsRh2::GUS*. (**a,b**) Medicago roots expressing *PsRh2::GUS.* (**c**) Median longitudinal section.

36 Medicago plants were transformed using the *PsRh2::AlcR* construct (Figure 1b), and grown in the partially sealed petridishes. The *GUS* expression data are summarized in Table II.

Table II. GUS induction of *PsRh2::AlcR* transformed Medicago roots grown in partially open plates. 40 plants, of which 25 were induced with ethanol, were analyzed for GUS activity.

	Control	**2% Ethanol**
	n = 15	n = 25
Duration of GUS staining (hours)		
24	0 (0 %)	14 (56 %)

The data presented in Table II show that in roots containing *PsRh2::AlcR* GUS activity is induced by ethanol, in more than 50% of the plants. Also the GUS activity is now restricted to the root epidermis of Medicago.

Discussion

Our studies for the first time show that the ethanol inducible promoter system can be used in a confined space, enabling plant transformations and legume-*Rhizobium* interaction studies. Additionally we showed that the promoter system could be used in combination with the tissue specific *PsRH2* promoter. By using a set of promoters that are active in the root epidermis or only in root hairs, putative toxic effects can be minimized.

Ethanol induction was successful in 50-75% of the plants. However it should be kept in mind that co-transformation efficiency is maximally 80% (see Chapter 2). This implies that ethanol induction occurs in the vast majority of the co-transformed roots. Therefore the combination of the inducible promoter that can be activated in a root tissue specific manner with the *A. rhizogenes* transformation procedure will be a very attractive experimental tool by which gene expression can be altered in the tissue that is the first target in the *Rhizobium*-legume interaction.

Acknowledgements We like to thank Jackie Paine from Zeneca Agrochemicals for providing us with the pSRNACN vector.

Chapter 4

The cold inducible *Arabidopsis thaliana RD29A* promoter

Abstract

Inducible promoter systems are used to express a transgene on demand. Here we tested whether the Arabidopsis promoter *AtRD29A(-694,1)* and the promoter construct *AtRD29A*/71bpX3(DREX3), which contains 3 DRE elements of the *AtRD29A* promoter, can be used as cold (4°C) inducible promoters in *Agrobacterium rhizogenes* transformed roots of *Medicago truncatula* (Medicago). The *AtRD29A(-694,1)* promoter can be induced in *Arabidopsis thaliana* by dehydration-, high-salt-, or low-temperature-which requires the DRE elements. It can also be induced by abscisic acid (ABA) involving the ABRE element. *AtRD29A*/71bpX3(DREX3) lacks the ABRE element, by which induction by ABA is eliminated. To test whether *AtRD29A*/71bpX3(DREX3) and *AtRD29A(-694,1)* can be used as cold inducible promoters, fusions were made with the *ß–glucuronidase* (*GUS*) reporter gene. *AtRD29A*/71bpX3(DREX3) was not active in Medicago roots, whereas *AtRD29A(-694,1)* is. However, *AtRD29A(-694,1)* is equally active in control and cold treated roots of Medicago. Since dehydration during growth was not the cause of the constitutive expression, we concluded that these promoters couldn't be used as cold inducible promoters in Medicago.

Keywords *Arabidopsis thaliana,* AtRD29A, Cold Inducible Promoter, *Medicago truncatula.*

Gerard N.M. van der Krogt, Carolien Franken, Vered Raz, Rossana Mirabella and Ton Bisseling

Introduction

As mentioned in chapter 3, inducible promoter systems have two main advantages. First, the level and timing of expression of a transgene can be controlled. Second, primary effects of the transgene can be more easily distinguished from secondary effects. An inducible system is very attractive if it meets 2 criteria: First, when the inducer is not applied the transgene should not be transcribed. Second, neither the inducing agent nor parts of the inducible system itself should influence the expression of endogenous genes or affect other cell functions (Gatz 1996; Gatz 1997; *Zuo *et al.* 2000).
Here we explore whether a new inducible promoter system could be developed from the *Arabidosis thaliana RD29A* (*AtRD29A*) promoter which can be induced by dehydration, high salt and low temperature, respectively (Yamaguchi-Shinozaki *et al.* 1993; Yamaguchi-Shinozaki *et al.* 1994). This promoter can be induced in all vegetative tissues of Arabidopsis plants, including roots. The root expression is determined by the *AtRD29A* promoter element as1 (Benfey *et al.* 1989; Lam *et al.* 1989; Yamaguchi-Shinozaki *et al.* 1994). The *AtRD29A* promoter can be activated by abscisic acid (ABA) through the ABA-dependent signaling pathway, which requires the ABA-responsive promoter element ABRE (Zeevaart *et al.* 1988; Yamaguchi-Shinozaki *et al.* 1994; Seo *et al.* 2002). Further, this promoter can also be activated through an ABA-independent pathway by dehydration, high salt-, and low temperature, which involves the 2 DRE elements (Yamaguchi-Shinozaki *et al.* 1994). A single DRE element (71bp) in combination with a minimal promoter is sufficient to be induced in Arabidopis by e.g. a cold treatment (Yamaguchi-Shinozaki *et al.* 1994). Such a single DRE element containing promoter as well as the *AtRD29A* promoter can be induced by exposing plants to 4°C, in Arabidopsis AtDR29A mRNA can already be detected 5 hours after the start of a cold treatment. Cold exposure would cause rather little stress to plants and also can be applied rather straightforward. We decided to test whether *AtRD29A* promoter derivatives controlling *ß–glucuronidase* (*GUS*) are suitable as cold treatment inducible promoter system. This was tested in Arabidopsis as well Medicago (*Medicago truncatula*) roots.

Arabidopsis and, Medicago roots can be transformed using the *Agrobacterium rhizogenes* co-transformation procedure (chapter 2). This transformation procedure creates composite plants; transformed roots on a non-transgenic shoot (Boisson-Dernier *et al.* 2001). About 80% of the Medicago plants have one or more transformed roots and on average 60% (6 roots out of 10) of the roots of these plants are transgenic. For the *A. rhizogenes* transformation of Arabidopsis similar results were obtained although the efficiency of transformation is more variable (Limpens *et al.* 2004). To be able to distinguish transformed - from non transformed roots, *DsRED* encoding a red fluorescent protein (Matz *et al.* 1999; Baird *et al.* 2000; Jach *et al.* 2001; Campbell *et al.* 2002; Limpens *et al.* 2004), was used as selectable marker (see also chapter 5).

Materials and Methods.

Bacterial strains and plant material

Agrobacterium strain MSU 440 containing the Ri plasmid pRiA4 of A. rhiz. strain A4 (Sonti *et al.* 1992) was used to transform *Medicago truncatula* Jemalong A17 and *Arabidopsis thaliana* Colombia.

Hairy root transformation

Root transformation was performed, with a few modifications, according to Stiller *et al.* (Stiller *et al.* 1997). Sterilized seeds (Medicago: 10 min in conc. H_2SO_4, five rinses with sterile water, 10 min commercial bleach, seven rinses with sterile water / Arabidopsis: 5 min in commercial bleach, five rinses with sterile water) were germinated in the dark on wet filter paper on top of solid Fahråeus (0.9% Daishin agar (Brunswig)) at 4°C overnight. Subsequently, the petri dishes were incubated upside down at 24°C for 1 day. The seed coats of the germinated seeds were removed and the seeds were transferred to filter paper, placed on top of agar plates, with the same medium and sealed for about two third with Parafilm. The dishes were incubated in a growth chamber in a vertical position with a 16/8 hour day/night cycle at 21°C. Five days later the plantlets have unfolded cotyledons, a root and a shoot. A fresh plate of *A. rhizogenes* is used and the bacteria are streaked on the hypocotyl with a sterile curled glass pipette. Subsequently, the root is removed by cutting the hypocotyl with a scalpel in the area were the *A. rhizogenes* was streaked. By doing so the freshly cut surface will be infected by *A. rhizogenes*. The hypocotyls are covered by an additional filter paper and cultivated for five days. Then filters plus plants were transferred to emergence medium plates (1x SH-A salts (major elements; minor elements; Iron compounds) (Schenk *et al.* 1972), 1x UM-C vitamins(100mg/l Myoinositol; 5mg/l Nicotinic acid; 10mg/l Pyriodoxine-HCl; 10mg/ml Thiamine-HCl; 2 mg/l Glycine (Clara L. Diaz pers. comm. (Diaz *et al.* 1989))), 1% sucrose, 3mM MES, pH 5.8, 0.9% agar (Daishin), 300 µg/ml Cefotaxime). 6 to 18 days after infection with *A. rhizogenes* the newly formed roots can be analyzed.

Constructs

All cloning work was carried out according to standard procedures (Maniatis *et al.* 2000), and all constructs made by PCR were sequenced.

pBIN(+)*DR29A::GUS-eCaMV35S::DsRED* (Figure 1a).
DsRED1-1 (Clontech Laboratories, Palo Alto, CA, U.S.A.) was amplified with the following oligonucleotides containing the extra restriction sites XbaI and BamHI;
5'GCTCTAGAACA**ATG**GCGCGCTCCTCCAAGAAC3' (underlind XbaI) containing the start codon (bold) and a plant kozak sequence (Lutcke *et al.* 1987), 5'CGGGATC*CTA*CAGGAACAGGTGGTG3' (underlined BamHI) containing a stop codon (Italic). The amplified fragment was cloned in pGEM-T and subsequently subcloned (XbaI/BamHI) in pMON999 (Bokhoven *et al.* 1993). The sites BglII/XbaI between *eCaMV35S* and the start of *DsRED* were cut, filled and ligated, similar for the BamHI site between the end of *DsRED* and *tnos*, creating pM999 *eCaMV35S::DsRED-tnos* with eliminated BglII/ClaI/BamHI sites. The *eCaMV35S::Dsred::tnos* fragment was amplified using the following oligonucleotides containing the extra restriction sites AscI/HindIII;
5'GGCGCGCCCCCGATCTAGTAACAT3' (underlined AscI) and 5'AAGCTTCTGCAGGTC3' (underlined HindIII).
Second, pBIN-basis was made by altering the pBINPLUS vector (Engelen *et al.* 1995). The *NPTII* kanamicin resistance gene was removed from pBINPLUS by digesting with Bsu36I and Bst98I, blund end formation and subsequently ligated, creating pBIN-basis. In this vector the *eCaMV35S::DsRED::tnos* PCR product was cloned using AscI/HindIII creating pBIN-basis *eCaMV35S::DsRED*.
Third, *DR29A(-694,1)* was PCR amplified from genomic DNA of *A. thaliana*, Columbia using the following oligonucleotides containing the extra restriction sites HindIII/XbaI;
5'AAGCTTTATTATAGAATTTTACTGGTTA3' (underlined HindIII),
5'TCTAGATTTCCAAAGATTTTTTTCTT3' (underlined XbaI), and cloned in pGEM-T and subcloned (HindIII/XbaI) in pBIN-basis *eCaMV35S::DsRED* creating pBIN-basis *DR29A-eCaMV35S::DsRED*.
Fourth, this construct was digested (PacI/XbaI) and ligated with the PacI-*tnos-GUS*-XbaI insert from pBIN*CaMV35S::AlcR-AlcA::GUS* (chapter 3), creating pBIN-basis *tnos:GUS::DR29A-eCaMV35S::DsRED*.
Fifth, the HindIII-*tnos:GUS:DR29A*-HindIII cassette was isolated using Hind III and re-inserted in reversed orientation, creating pBIN(+)*DR29A::GUS-eCaMV35S::*DsRED.

pBIN101 *DR29A(-694):GUS* (Figure 1c)
This construct was made by cloning *DR29A*(-694) (Hind III/XbaI) upstream of *GUS* of pBIN101 (Clontech, USA).

Cold induction

Arabidopsis was grown at 22°C and Medicago at 21°C. These plants were cold treated at 4°C under dim light for 12 hours and subsequently they were grown at normal conditions for 15 hours before GUS staining.

Histochemical GUS analysis

GUS staining was performed according to Jefferson *et al.* (Jefferson *et al.* 1987) with a few modifications. Plant material was incubated in 0.05% (w/v) X-Gluc (Duchefa) in 0.1M sodium phosphate buffer with 3% sucrose, 5µM ferrocyanide, 5µM ferricyanide (pH 7). Vacuum infiltration was applied for 30 minutes and the sample was incubated at 37°C.

Sectioning

Samples were embedded in Technovit 7100 as described in the protocol of Kulzer. 10µm sections were made using a Leica microtome and mounted in Euparal (Agar Scientific LTD.).

Microscopy

For imaging a Nikon SMZ-U stereomicroscope and a Nikon optiphot-2 bright field microscope were used to analyze the GUS experiment. Photographs were made using a Nikon coolpix990 digital camera. For fluorescence imaging a Leica MZFLII stereomicroscope fitted with DsRED excitation/emission filters and equipped with a digital Leica DC300F camera was used. Images were processed using Photoshop 5.5 and illustrator 8.0.

Results

An artificial promoter, 71bpX3 (DREX3), containing 3 *AtDR29A* DRE elements, fused to a *AtRD29A* minimal promoter, was made by Yamaguchi-Shinozaki *et al.* (Figure 1a). This promoter fused to GUS could be induced in Arabidopsis shoots by a cold treatment, 10h at 4°C (Yamaguchi-Shinozaki *et al.* 1994; Liu *et al.* 1998). In a parallel study we used the 71bpX3 (DREX3) promoter to control a cyclin CycD3 antisense construct. This construct inhibited expression of this gene in the apical part of Arabidopsis seedlings, but not in roots (unpublished results). This strongly suggested that this promoter couldn't be induced in roots.

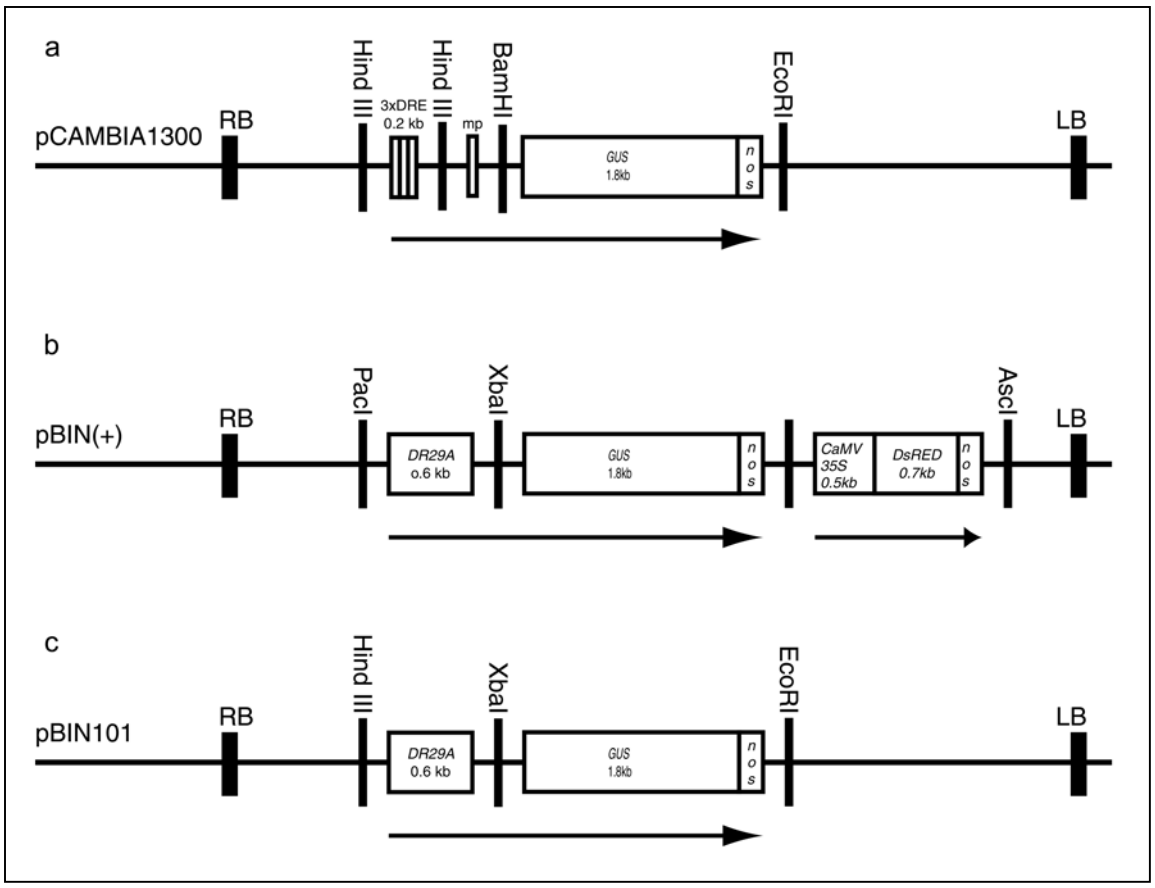

Figure 1. *AtDR29A* promoter derived constructs**.** (**a**) *GUS* under control of a chimeric promoter consisting of 3 DRE elements fused to the minimal (-61) *AtDR29A* promoter as described in (Yamaguchi-Shinozaki *et al.* 1994; Liu *et al.* 1998) (**b**) *GUS* reporter gene (Jefferson *et al.* 1987) placed under control of the *AtDR29A* (-694,1) promoter part, containing 2XDRE, as1 and ABRE. This construct also contained a reporter cassette, an enhanced *CaMV35S* promoter driving DsRED. (**c**) The same construct as (b) but lacking the *DsRED* reporter cassette.

To obtain a promoter that can be induced in roots a part of the *AtDR29A* promoter (*AtDR29A(-694,1)*), containing the root specific as1 promoter element and the two DRE elements, was used (Figure 1b). In the same plasmid also a selectable marker, enhanced *CaMV35S::DsRED*, was present. This pBIN(+)*AtDR29A(-694,1)::GUS-eCaMV35S::DsRED* construct (Figure 1b) was tested in 100 Arabidopsis plants with *A. rhizogenes* transformed roots (Figure 2).

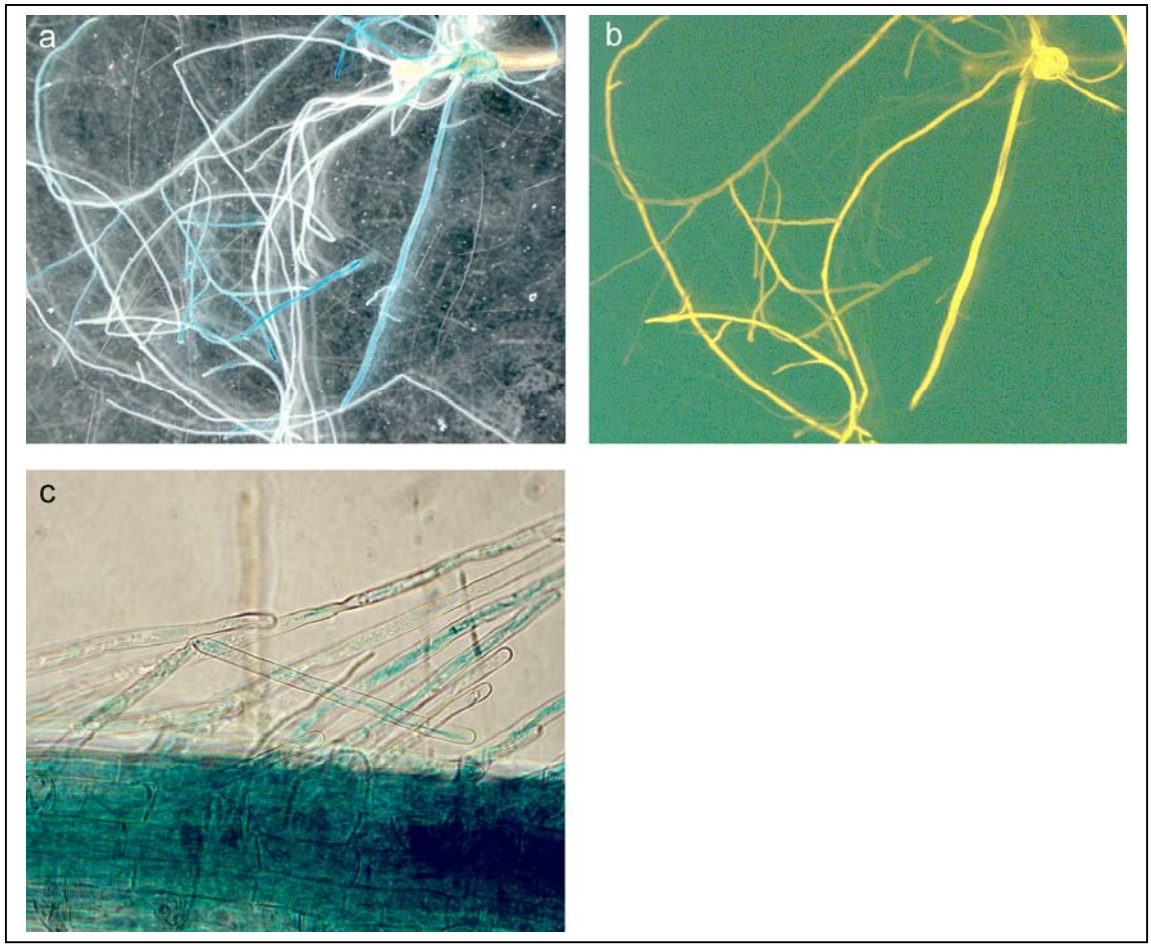

Figure 2. Histochemical localization of GUS activity in cold treated Arabidopsis roots expressing pBIN(+)*AtDR29A(-694)::GUS-eCaMV35S::DsRED*, stained for GUS for 12 hours (**a**,**c**). DsRED fluorescence in GUS stained roots (**b**).

The majority of the roots show DsRED fluorescence (Figure 2b), so the efficiency of co-transformation is high. Half of the plants (50) were cold induced (12h, 4°C) and the roots were screened for GUS activity. GUS activity was found in root as well root hairs (Figure 2c). Therefore it is very likely that the as1 element indeed confers the ability to be expressed in the root. Also it can be seen that DsRED fluorescence nicely matches the GUS staining (Figure 2a,b). However, also untreated (not cold induced) control plants as cold treated roots showed extensive GUS activity. No significant difference in GUS activity could be detected between contol and cold treated plants. This implies that the *AtDR29A(-694,1)* promoter is constitutively active in *A. rhizogenes* transformed Arabidopsis roots. A similar construct used in Arabidopsis did not result in constitutive root expression (Yamaguchi-Shinozaki *et al.* 1994; Liu *et al.* 1998). However, this construct lacked the *eCaMV35S::DsRED* reporter cassette and –stable transformed plant instead of *A. rhizogenes* transformed roots were used.

In parallel the construct was tested in 50 Medicago *A. rhizogenes* transformed roots (Figure 3a,b,c,d,e).

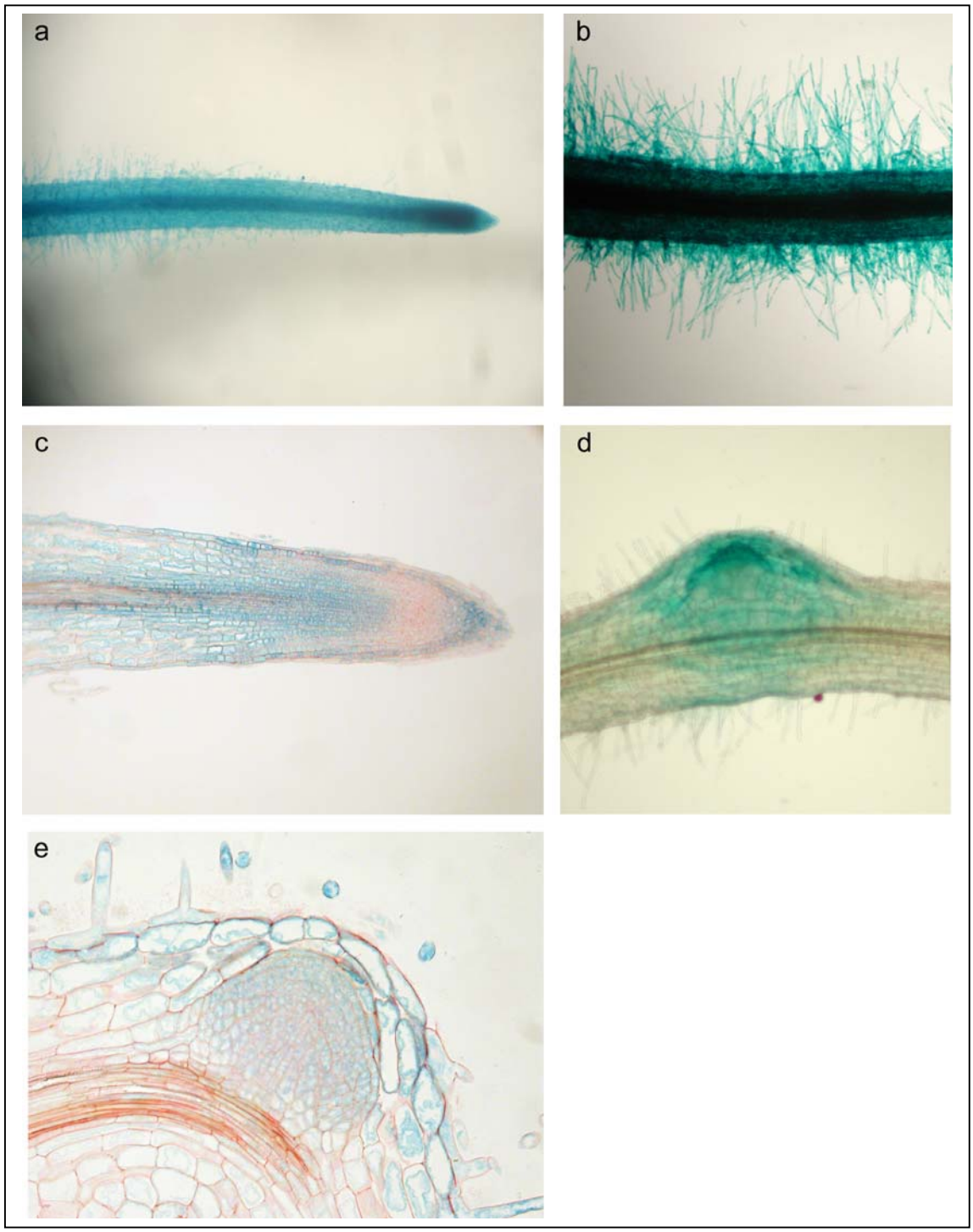

Figure 3. Histochemical localization of GUS activity in Medicago roots expressing pBIN(+)*DR29A(-694)::GUS-eCaMV35S::DsRED* stained for 21 hours (**a**,**b**,**c**) and a longitudinal sectioning of such roots (**c**). Lateral root formation stained for 6 hours (**d**,**e**) and (**e**) is a longitudinal section of such a formation stained for 21 hours.

Also in Medicago the construct appeared to be constitutively active in roots. The experiment was repeated with 40 more Medicago plants, giving comparable results. Therefore it can be concluded that *AtDR29A(-694,1)* (Figure 1b) is constitutively

active in Arabidopsis as well as Medicago roots. So this construct can not be used as an inducible promoter system in roots of these plants.

The DRE elements present in the promoters are cold responsive elements but can also be activated by dehydration. To exclude that the constitutive activity of the (Figure 1b) construct is caused by drought Medicago roots were not grown on paper as before, but between two wet papers. Sixty Medicago plants were transformed with this construct, grown between papers and screened for GUS activity. No significant difference in GUS activity could be detected between Medicago plants grown between 2 filter papers or on top of a filter paper (Figure 4). So drought is probably not the cause of the observed constitutive expression in roots.

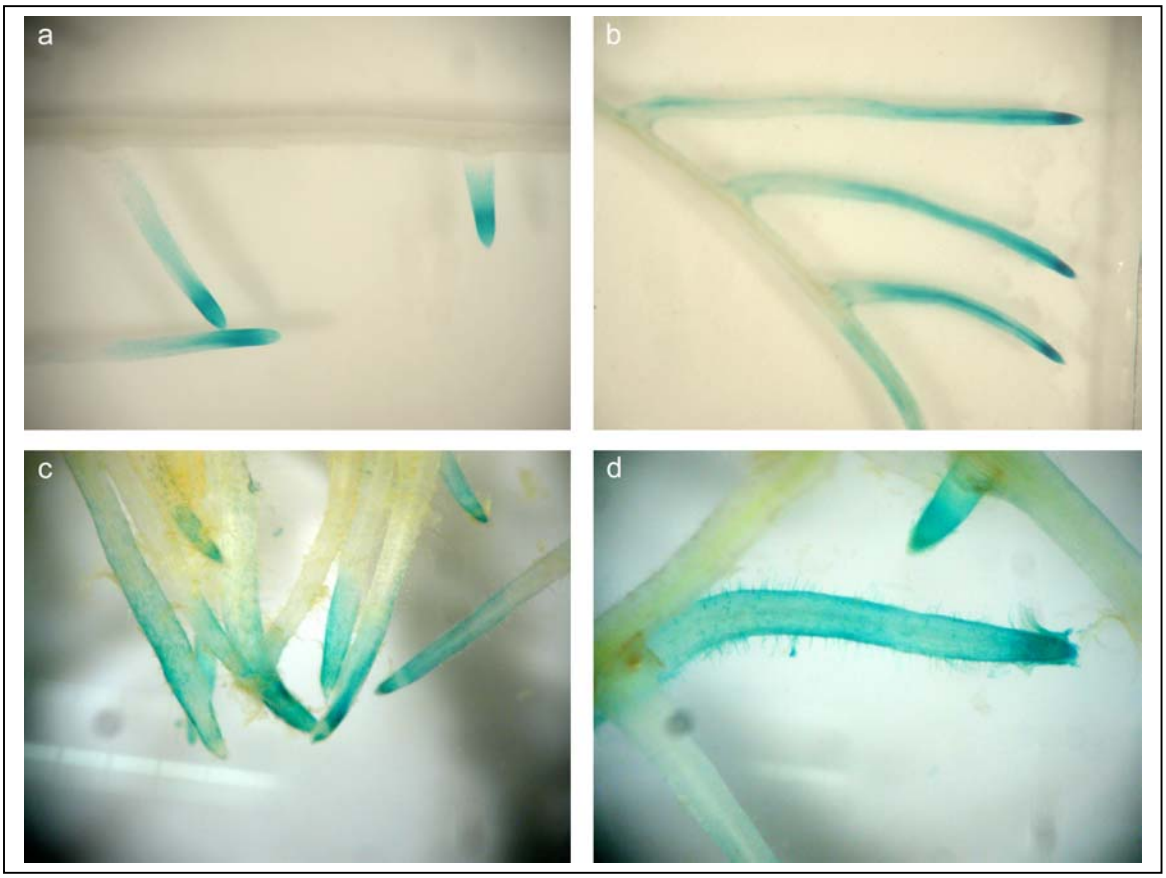

Figure 4. Histochemical localization of GUS activity in Medicago roots expressing pBIN(+)*AtDR29A(-694):GUS-eCaMV35S:DsRED*. Roots grown on paper and stained for 6 hours for GUS activity (**a**,**b**). Roots grown between papers and stained for 6 hours for GUS activity (**c**,**d**).

In line with the data described in Chapter 5 we expected that the constitutive expression of construct 1b might be caused by elements of the 35S promoter controlling expression of DsRED. To eliminate any influence of the *eCaMV35S* promoter on the *DR29A(-694,1)* promoter the *eCaMV35S::DsRED* cassette was removed creating pBIN101 *DR29A(-694,1)::GUS* (Figure 1c). This construct was tested in Medicago roots. 21 Medicago plants were transformed and 5 grown between - and 16 on top of paper. When the roots were large enough all 21 plants were analyzed for GUS activity. All plants had some roots displayed GUS activity (1 not) and the GUS activity was as high as in roots transformed with construct 1b

containing the *eCaMV35S* reporter. So the *DR29A(-694,1)* promoter is constitutively active in Medicago roots and therefore this promoter is not suited as cold inducible promoter system.

Discussion.

Here we show that the *DR29A(-694,1)::GUS* gene is constitutively active in Medicago as well as Arabidopsis roots. This is markedly different from the data reported by Yamaguchi-Shinozaki *et al.* who showed that a similar construct is not constitutively active in Arabidopsis roots (Yamaguchi-Shinozaki *et al.* 1994). This group used stable transformed Arabidopsis roots whereas we used *A. rhizogenes* based transformation. Therefore our roots have different auxin and cytokinin levels. To our knowledge increased levels of ABA have not been reported in *A. rhizogenes* transformed roots however it seems worthwhile to check whether removal of the ABA responsive ABRE element in *DR29A(-694,1)* eliminates the constitutive expression. Further we did not test in Arabidopsis the activity of *DR29A(-694,1)::GUS* in the absence of a 35S promoter (1c). Therefore it can not completely be excluded that this promoter is silent in Arabidopsis roots although it is constitutively active in Medicago roots.
When *eCaMV35S::DsRED* transformation reporter cassette is included the *DR29A(-694,1)* promoter becomes constitutively active in the root. This could be due to an effect of the two enhancer elements of e*CaMV35S* used to regulate the reporter gene *DsRED* (Fang *et al.* 1989; Beilmann *et al.* 1992). Therefore another promoter not showing this effect should replace the *eCaMV35S* used to control the reporter cassette. For example the *PsRH2* (chapter 2) or the Ubiquiti *AtUBQ10* promoter controlling the *DsRED* reporter gene as was used previously by Limpens *et al*. (Limpens *et al.* 2004).

Acknowledgements We like to thank Valerie Hecht for providing the Colombia *A. thaliana* genomic DNA and Kazuo Shinozaki for providing the pBI221(71x3/GUS Reporter).

Chapter 5

The Sinorhizobium meliloti inducible Medicago truncatula MtENOD12 promoter

Abstract

Medicago truncatula (Medicago) has the ability to establish an endosymbiotic relationship with the soil bacterium *Sinorhizobium meliloti*, resulting in nitrogen-fixing root nodules. The formation of these root nodules starts when the bacteria colonize the root surface and fast responses are induced in the epidermal cells containing root hairs. One of these responses is the activation of the *Medicago truncatula MtENOD12* gene within 3 to 6 hours after inoculation. Due to this relatively quick response of the *MtENOD12* promoter it could possibly be used as a *Rhizobium* inducible promoter system to study the effects of transgenes on infection thread and nodule formation in *M. truncatula* roots.

To determine the suitability of this promoter, a 0.8 kb upstream promoter region of *MtENOD12* was fused to the ß-glucuronidase (*GUS*) reporter gene and used to transform Medicago roots. *GUS* is induced after *Sinorhizobium meliloti* inoculation, at the site of infection, in nodule primordia and in the infection zone of nodules. Furthermore, non-symbiotic *MtENOD12* expression is observed in the root tip, which might cause a possible negative growth effect on the root if the encoded gene product has a negative effect on root development.

In conclusion the *MtENOD12* promoter has good potential as inducible promoter system to study effects of transgenes during early symbiotic events.

Keywords ENOD12*,* GUS, *Medicago truncatula*, Promoter analysis, Root epidermis, *Agrobacterium rhizogenes*

Gerard N.M. van der Krogt, Rossana Mirabella, Carolien Franken and Ton Bisseling

Introduction

As described in the previous chapters (3 and 4), inducible promoter systems have several advantages. Our research concentrates on the interaction of rhizobia and legumes. Therefore promoters of genes that are specifically activated during this interaction could be useful, in addition to promoters that can be activated by exogenously applied compounds. The Medicago *ENOD12* promoter could possibly be used as a rhizobial induced promoter. *ENOD12* has been identified in several legumes including pea, Medicago (*Medicago truncatula*), Alfalfa and Vetch (*Vicia sativa)*, and has been shown to be activated during early stages of the infection process (Scheres *et al.* 1990; Pichon *et al.* 1992; Allison *et al.* 1993; Journet *et al.* 1994). A Medicago *ENOD12* (*MtENOD12*) promoter fused to the ß-glucuronidase (*GUS*) gene has been studied in Medicago roots (Pichon *et al.* 1992; Journet *et al.* 1994). It was shown that this transgene is activated in the root epidermis within 3 to 6 hours after inoculation with *Sinorhizobium meliloti* and 2 to 3 hours after applying *S. meliloti* Nod factors (Pichon *et al.* 1992; Journet *et al.* 1994). This activation starts in the epidermal cells of the elongation zone just above the root tip, extends throughout the zone of root hair emergence and growth, but expression does not occur in the zone with mature root hairs. The region where *MtENOD12* can be induced includes root hairs that just reached their maximum size and in which cell biological changes can be induced with Nod factors. In addition to the expression in the root epidermis, *MtENOD12* activity is also induced in nodule primordia, and full-grown nodules. During the formation of a nodule primordium this gene is active in the primordial cells as well as in the root cortical cells through which the infection thread will migrate (Scheres *et al.* 1990). In nodules, *in situ* hybridization studies as well as *ENOD12::GUS* expression analysis have shown that this gene is active in zone II of the nodule, which is the zone where rhizobia are released from infection threads and multiply. *ENOD12* is not active in the meristem (zone I) nor in the nitrogen fixing zone III (Scheres *et al.* 1990; Pichon *et al.* 1992).

According to these observations the *MtENOD12* promoter could be a suitable inducible system to study the effects of transgenes on infection thread and nodule formation. To determine the suitability of this inducible system the *MtENOD12* promoter was fused to *GUS* and used to transform *M*. *truncatula* roots using the *Agrobacterium rhizogenes* co-transformation procedure (described in chapter 2). After *S. meliloti* inoculation the *GUS* expression patterns were analyzed. To be able to distinguish transformed from not transformed roots the *DsRED* reporter gene (Matz *et al.* 1999; Baird *et al.* 2000; Jach *et al.* 2001; Campbell *et al.* 2002) was included in the construct.

Materials and Methods

Bacterial strains and plant material

Agrobacterium strain MSU 440 containing the Ri plasmid pRiA4 of A. rhiz. strain A4 (Sonti *et al.* 1992) was used to transform *Medicago truncatula* Jemalong A17.
Rhizobium Sinorhizobium melilot 2011was used to inoculate Medicago roots.

Hairy root transformation

Root transformation was performed, with a few modifications, according to Stiller et al. (1997). Sterilized seeds (10 min in conc. H_2SO_4, five rinses with sterile water, 10 min commercial bleach, seven rinses with sterile water) were germinated in the dark on a wet filter paper on top of solid Fahråeus medium (0.9% Daishin agar (Brunswig)) at 4°C overnight. Subsequently, they were incubated upside down at 24°C for 1 day. The seed coats of the germinated seeds were removed and the seeds were transferred to filter paper, placed on top of agar plates, with the same medium and sealed for about two third with Parafilm. The dishes were incubated in a growth chamber in a vertical position with a 16/8 hour day/night cycle at 21°C. Five days later the plantlets, have unfolded cotyledons, root and a shoot. A fresh plate of *A. rhizogenes* is used and bacteria from this plate were streaked on the hypocotyl using a sterile curled glass pipette. Subsequently, the root is removed by cutting the hypocotyl with a scalpel in the area were the *A. rhizogenes* was streaked. By doing so, the freshly cut surface will be infected by *A. rhizogenes*. The hypocotyls are covered by an additional filter paper and cultivated for five days. Then filters plus plants were transferred to emergence medium plates (1x SH-A salts (major elements; minor elements; Iron compounds), 1x UM-C vitamins (100mg/l Myoinositol; 5mg/l Nicotinic acid; 10mg/l Pyriodoxine-HCl; 10mg/ml Thiamine-HCl; 2 mg/l Glycine (Clara L. Diaz pers. comm.)), 1% sucrose, 3mM MES, pH 5.8, 0.9% agar (Daishin), 300 µg/ml Cefotaxime). In most cases each root originates from a single transformed cell (see Chapter 2). After 6 to 18 days after infection with *A. rhizogenes* the newly formed roots can be analyzed.

Plant growth and *Rhizobium* inoculation

Transformed *M. truncatula* plants were grown on filter paper for 3 weeks. Subsequently they are transferred to gravel trays and grown for about one more week. The plants were inoculated with *Sinorhizobium melilot* 2011. The rhizobia were obtained by growing them on YEM plates at 28°C for 3 days and suspending the bacterial colonies in water to an OD_{600} of 0.1.

Constructs

All cloning work was carried out according to standard procedures (Maniatis *et al.* 2000) and all DNA fragments made by PCR were sequenced.

pBIN(+)*MtENOD12::GUS-eCaMV35S::DsRED* (Figure 1a)
The *MtENOD12* (0.8 kb) fragment was PCR amplified with the following oligonucleotides containing the extra restriction sites XbaI/HindIII; GCTCTAGATTTTAATGTTAGTGCATATAAC (underlined isXbaI), CCCAAGCTTGAAGGGTAAAATAGAAAA (underlined is HindIII), cloned in pGEM-T and subcloned (XbaI/HindIII) in pBIN-basis *eCaMV35S::DsRED* (the construction of pBIN-basis *eCaMV35S::DsRED* is described in chapter 4). This construct was combined (PacI/XbaI) with the *GUS* from pBIN(+) *AlcA::GUS* (the construction of pBIN(+) *AlcA::GUS* is described in chapter 3), creating pBIN-basis *MtENOD12::GUS-eCaMV35S::DsRED*. Finally the HindIII-*MtENOD12::GUS*-HindIII cassette was isolated (Hind III) and re-inserted in reversed in orientation, creating pBIN(+)*MtENOD12::GUS-eCaMV35S::DsRED* (Figure 1A).

pBIN101*MtENOD12::GUS* (Figure 1b)
This construct was made by isolating (HindIII/XbaI) the *MtENOD12* (0.8 kb) fragment . Subsequently this fragment was subcloned in pBIN101.3 (Clontech, USA)

Histochemical GUS analysis

GUS staining was performed according to Jefferson *et al.* (Jefferson *et al.* 1987) with a few alterations. Plant material was incubated in 0.05% (w/v) X-Gluc (Duchefa) in 0.1M sodium phosphate buffer with 3% sucrose, 5µM ferrocyanide, 5µM ferricyanide (pH 7). Vacuum infiltration was applied for 30 minutes and the sample was incubated at 37°C.

Sectioning

Samples were embedded in Technovit 7100 as described in the protocol from Kulzer. 10μm sections were made using a Leica microtome and mounted in Euparal (Agar Scientific LTD.).

Microscopy

For imaging a Nikon SMZ-U stereomicroscope and a Nikon optiphot-2 bright field microscope were used to analyze the GUS experiment. Photographs were made using a Nikon coolpix990 digital camera. For fluorescence imaging a Leica MZFLII stereomicroscope fitted with DsRED excitation/emission filters and equipped with a digital Leica DC300F camera was used. Images were processed using Photoshop 5.5 and illustrator 8.0.

Results

Previously a 2.3 kb long upstream region of *MtENOD12* was used to drive the expression of *GUS* (Pichon *et al.* 1992). Here an *MtENOD12* promoter construct was made by taking the –1 to –836 bp region of the promoter. The promoter part was fused to the coding part of *GUS* and placed in the binairy transformation vector pBIN101 (Figure 1a).

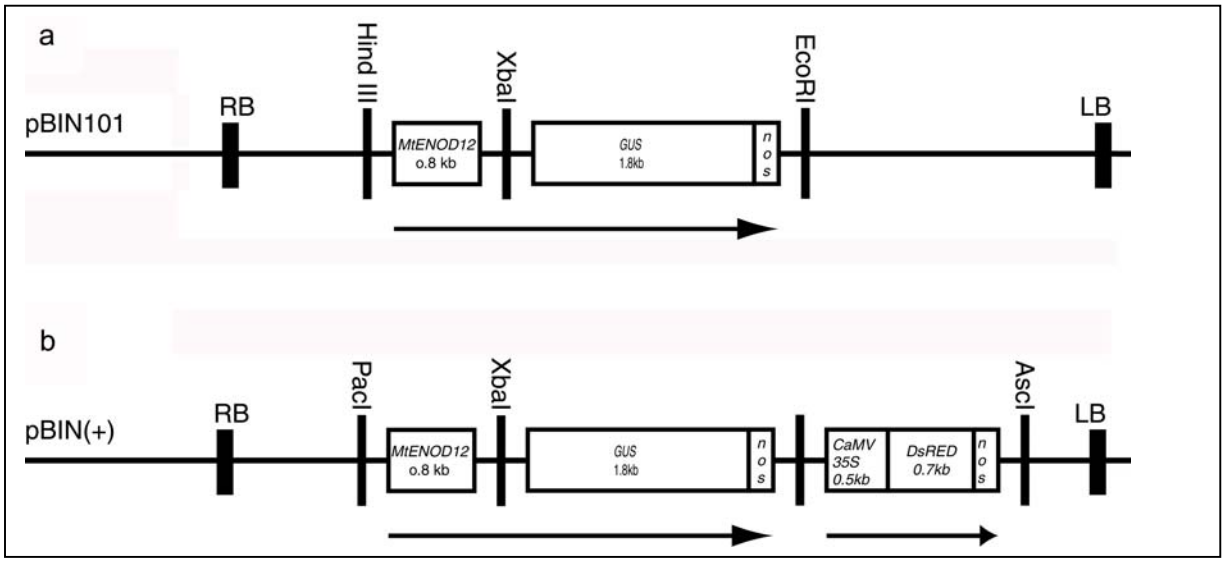

Figure 1. (**a**) The *GUS* reporter gene placed under control of the –1 to –836 region of the *MtENOD12* promoter. (**b**) The same construct as (a) only with a transformation reporter cassette inserted. This cassette contains an enhanced *CaMV35S* (*eCaMV35S*) promoter driving *DsRED*.

The *A. rhizogenes* based root transformation, as described in chapter 2, was used to transform 36 Medicago plants with the *MtENOD12::GUS* construct (1a). After 3 weeks the plants were transferred to gravel and grown for 3 days under nitrogen limiting conditions. Prior to inoculation a few plants were analyzed for GUS activity (Figure 2a,b). The remaining plants were inoculated with *S. meliloti* and after 14 days analysed for GUS activity (Figure 3a,b,c,d,e,f).

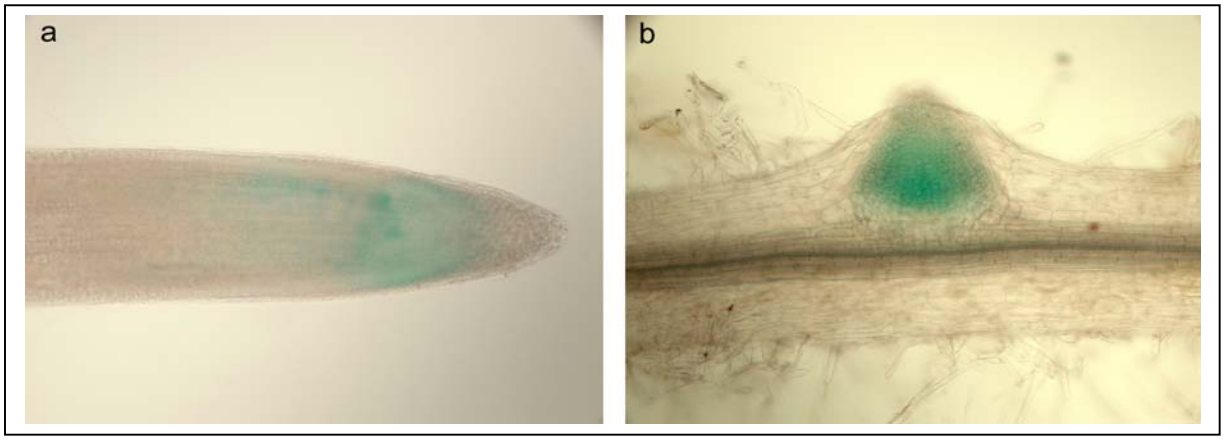

Figure 2. Uninoculated M*edicago* roots containing *MtENOD12::GUS*. GUS activity is found after 6 hours of staining in root tips (**a**) and lateral root primordia (**b**).

As is shown in Figure 2a,b GUS activity is found in the root tips and lateral root primordia of uninoculed roots upon 6 hours of GUS staining. Such staining has not been observed using the 2.3 kb long upstream region of *MtENOD12* driving GUS (Pichon *et al.* 1992).

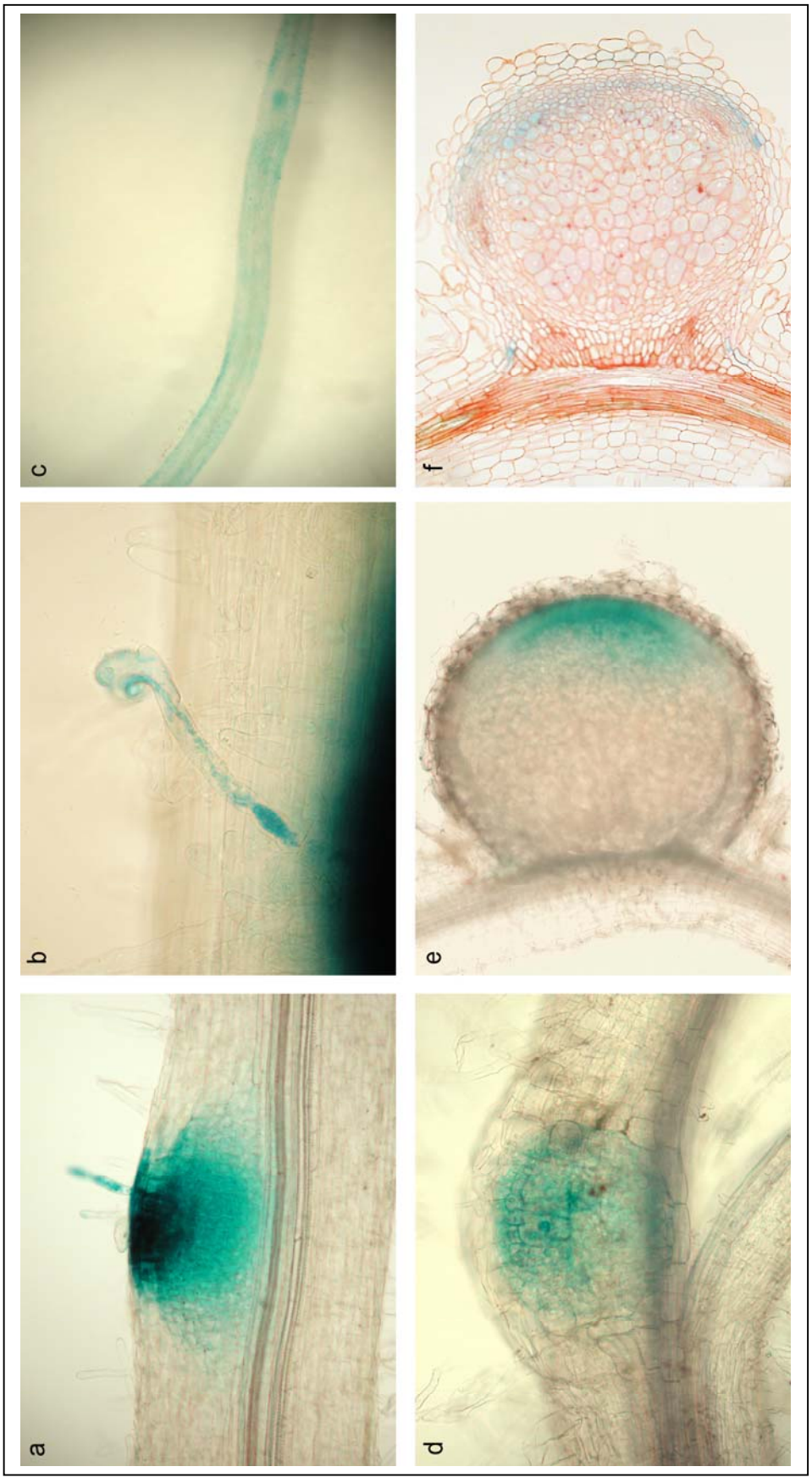
a
b
c
d
e
f

Figure 3. Medicago roots and root nodules expressing *MtENOD12::GUS* 14 days after inoculation with *S. meliloti*. GUS activity is generally found after 6 hours of staining in cells containing infection threads (**a**,**b**) and further after a prolonged staining (16 hours) also in epidermal cells, although at a lower level (**c**). (**d**) After 6 hours of staining GUS activity can be found in the nodule primordia. (**e**) Root nodules showing GUS activity restricted to the distal cell layers of the nodule, (**f**) is a section of such a nodule.

GUS activity is clearly found at sites of infection thread growth, in nodule primordia (Figure 5a,b,d) and also a low GUS activity is found in the whole epidermis (Figure 5c). Figure 5e,f shows the GUS activity in the nodule, 14 days after inoculation, where GUS activity is restricted to the apical part of the nodule, GUS activity is present in the distal part of zone II. An activity in the nodule similar as was found for the 2.3 kb long upstream region of *MtENOD12* (Pichon *et al.* 1992).

These results illustrate the suitability of the *MtENOD12* promoter as an inducible promoter. However if the promoter is fused to a gene of interest and expressed in roots using the *A. rhizogenes* based root transformation, no clear distinction can be made between co-transformed roots and those lacking the transgene. This is especially the case if the product of the gene of interest under control of the *MtENOD12* promoter is not directly detectable. To circumvent this problem a fluorescent reporter gene (*DsRED*), under control of the *eCaMV35S* promoter was included in the binary vector (Figure 1b). By screening for red fluorescence roots a selection for transgenic roots containing the *MtENOD12* construct can now be made (see Chapter 2 and 4).

20 Medicago *MtENOD12::GUS-eCaMV35S::DsRED* transformed plants were made. Based on *DsRED* expression, plants with transgenic roots were selected. These plants were grown in petridishes on filter paper placed on top of an agar-feeding layer. After 3 weeks the plants were transferred to gravel and subsequently inoculated with *S. meliloti.* DsRED expressing roots were analyzed for GUS activity (Figure 4).

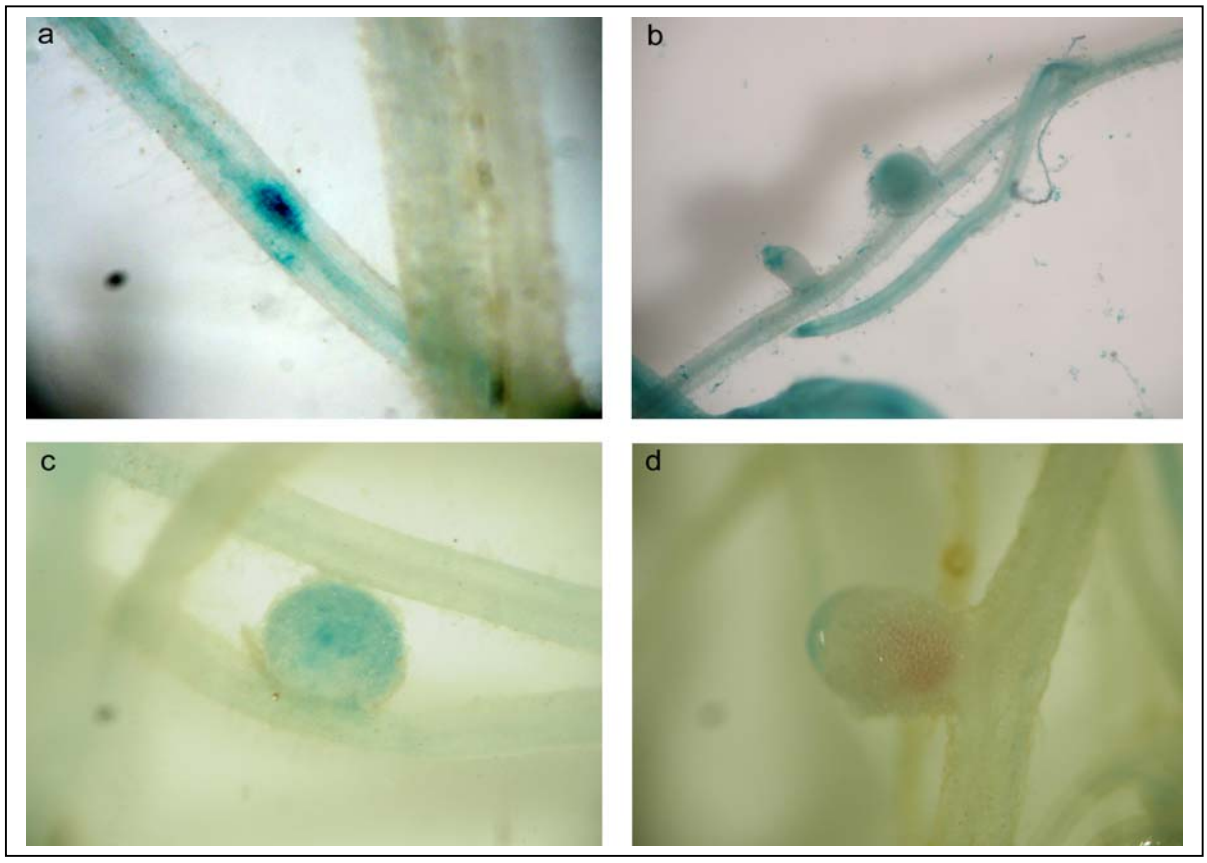

Figure 4. M*edicago* roots and root nodules expressing *MtENOD12::GUS-eCaMV35S::DsRED* after inoculation with *S. meliloti*. a,b,c and d show GUS expression patterns, after staining 6 hours. (**a**) Shows strong GUS activity in the vascular bundles of the root and in a nodule primordium. (**b**) Shows strong activity in the root tip. (**c**,**d**) Shows GUS activity in nodules.

DsRED fluorescence in roots expressing the *eCaMV35S::DsRED* reporter cassette is clearly visible (data not shown). However, the *GUS* expression patterns now found differs from that when the *DsRED* reporter cassette is not included. This reporter causes an additional strong GUS activity especially in the root vascular tissue Figure 4 a,b. This suggests that the *eCaMV35S* promoter of *DsRED* influences the expression pattern of *MtENOD12::GUS.*

To determine if there is an effect of the *eCaMV35S* promoter on the activity of the adjacent *MtENOD12* promoter the experiment was repeated and 9 plants were transformed using the same construct. After transformation all plants showed several *DsRed* expressing roots. These uninoculated plants were also analyzed for GUS activity which was mainly found in the vascular tissue. From this it can be concluded that the *MtENOD12* promoter is now constitutively active at a high level. Therefore the insertion of this DsRED reporter cassette markedly reduces the usefulness of *MtENOD12* as a rhizobial inducible promoter.

Discussion

The *MtENOD12* promoter is a suitable inducible promoter to study effects of transgenes in cells forming infection threads – and during nodule formation. This promoter is induced at the site of infection (Figure 3a,b), in nodule primordia (Figure 3d) and in nodules (Figure 3e). The strength of this promoter after induction equals that of the constitutive *CaMV35S* promoter, in epidermal cells (chapter 2) and in nodules, respectively (unpublished results).
However, using the 0.8 kb long *MtENOD12* promoter has the advantage of easier cloning and also a higher transformation rate due to a smaller fragment between the T-DNA borders. However, the *MtENOD12* promoter might be less suited if the gene of interest has a negative effect on root formation. Since the promoter used in this chapter is constitutively active in root tips and in lateral root primordia (Figure 3). However, since the non-symbiotic activity in the root tip is rather low a transgene might not accumulate to sufficient levels to block root development. Our results for the 0.8 kb *MtENOD12* promoter are similar to those found for the 2.3 kb *MtENOD12* promoter region. (Pichon *et al.* 1992). However, the low GUS activity found in the whole epidermis (Figure 3c) was not reported by Pichon. For the 2.3 kb promoter region the epidermal activity was restricted to a region that starts within the root elongation zone above the apical meristem, and it terminates at the start of the mature root hair zone (Pichon *et al.* 1992). Using a smaller promoter region could be the cause of the observed difference in the epidermal expression patterns. However, this extended epidermal expression found for the 0.8 kb long promoter could also be caused by a longer GUS staining than was done by Pichon et al.
If the *MtENOD12* promoter constructs are introduced in roots using the *A. rhizogenes* based root transformation, cotransformed roots cannot always be selected. When *eCaMV35S::DsRED* transformation reporter cassette is included we have shown that this is well possible. However when this reporter cassette is included the *MtENOD12* promoter becomes constitutively active in the root. This could be due to an effect of the two enhancer elements of e*CaMV35S* used to regulate the reporter gene *DsRED* (Fang *et al.* 1989; Beilmann *et al.* 1992). Therefore also here another promoter not showing this effect should replace the *eCaMV35S* used to control the reporter cassette. For example a *PsRH2* promoter controlling the *DsRED* reporter gene as was used previously by Limpens *et al*. (Limpens *et al.* 2004)

So the *MtENOD12* promoter is a suitable rhizobial inducible promoter to study effects of transgenes during the symbiotic events, but a marker gene allowing the selection of co transformed roots remains to be optimized.

Acknowledgements We would like to thank David Barker for providing the *MtENOD12* full-length construct and advise for using the 0.8 kb minimal *MtENOD12* promoter.

Chapter 6

In vivo actin visualization in *Vigna* protoplasts

Abstract

F-actin can be visualized in living cells using a fusion of a Fluorescent Protein (FP) and actin, Actin Binding Protein (ABP) or only its Actin Binding Domain (ABD). These constructs were successfully used in for example *Drosophila*, *Dictostelium* and mammalian cell types. In plants only fusions with ABP/ABD were successful. To obtain additional actin probes we set out to test more FP based F-actin constructs. These were tested for F-actin binding in Cowpea (*Vigna unguiculata L.)* mesophyll protoplasts. So different actins were fused to a FP; Human (Hsßact)*, Dictostelium* (DdAct15) and pea actin (PsAct1). *PsAct1* was isolated for this purpose from a pea root hair cDNA library. None of these FP-actin fusions resulted in an unaffected labelled F-actin skeleton. Therefore fusions of FP and ABPs/ABDs were tested, *Dictostelium* Cortexillin (DdCortN$_{1-233}$) and *Dictostelium* Talin (DdTalin$_{2302-2491}$) and also the Maize Actin Depolymerizing Factor (ZmADF3). Of these fusions DdTalin$_{2302-2491}$ yielded a good F-actin labelling in protoplasts.

Keywords Actin, Actin labeling, Cowpea (*Vigna unguiculata L.)* mesophyll, Cortexillin, Talin, ZmADF3.

Gerard N.M. van der Krogt, Rossana Mirabella, Jojanneke Rosendaal, Tijs Ketelaar, Az-Eddine Hardi and Ton Bisseling

Introduction

The actin skeleton is dynamic and involved in many cellular processes. Actin is synthesized as a monomeric globular protein (G-actin) that can form Filamentous polymers (F-actin). F-actin continuously assembles and disassembles, which results in dynamic filaments. The configuration of this skeleton is controlled by certain actin binding proteins, nucleating, bundling, stabilizing, severing F-actin and sequestering G-actin. Other actin binding proteins serve as motor proteins facilitating movement of cellular components along the filaments (Staiger *et al.* 2000; Esseling *et al.* 2001; Hussey *et al.* 2004).

The actin skeleton is involved in the *Rhizobium*-legume interaction (Cárdenas 1998; Ruijter *et al.* 1999) a symbiotic interaction that ultimately results in the formation of nitrogen fixing root nodules. This symbiosis is initiated by signaling molecules secreted by the rhizobia, so-called Nod factors. These Nod factors are lipochitooligosaccharides (LCOs). LCOs induce several responses in root hairs. Among these are, membrane depolarization within minutes (Felle 1995), calcium spiking within 6 to 10 min. (Cárdenas *et al.* 1999) and an increase of fine actin filaments in the subapical area of the root hair within 3-15 minutes (Ruijter *et al.* 1999), followed by a morphological change of the root hair, the so-called root hair deformation (Heidstra 1994; Esseling *et al.* 2003). Nod factor secreting rhizobia induce in some root hairs the formation of a curl. There, bacteria become entrapped in the cavity formed by the curl and an infection thread (IT) is formed (Gage *et al.* 1996; Cheng *et al.* 1998; Limpens *et al.* 2003). This IT is a tubular structure growing to the base of the root hair (Newcomb 1976; Callaham *et al.* 1981; Turgeon *et al.* 1985) guiding the bacteria through the root hair towards the dividing cortical cells, where bacteria are released into host cells. Also the IT itself and the sites were it penetrates cells is associated with F-actin (Davidson *et al.* 2001).

Un till recently all data on the role of actin in root hair deformation and the infection process were obtained with fixed cells, using actin antibodies or F-actin binding dyes. Therefore the dynamics of the skeleton during these processes could not be optimally studied. Recently it has become possible to visualize the actin skeleton in living plant cells by using fusions with Fluorescent Proteins (FPs) (Hussey *et al.* 1998; Kost *et al.* 1998; Ketelaar *et al.* 2004; Sheahan *et al.* 2004; Wang *et al.* 2004; Weerasinghe *et al.* 2005). The visualization of the actin skeleton can be achieved by a fusion of a FP and an Actin Binding Protein (ABP) or its Actin Binding Domain (ABD) or by a chimera of actin and FP. However, actin-FP fusions label actin filaments but are also present as monomeric actin. The monomeric form can be a relatively large proportion (up to 50%) of the total pool of cellular actin-FP and this can cause a high “background” (Theriot 1994; Schafer *et al.* 1995). If the ABP/ABD-FP affinity for actin filaments is high it would result in markedly lower “background” fluorescence and might be more useful to visualize the actin filaments. However a too high affinity for F-actin of ABP/ABD-FPs, combined with high expression levels might hamper the binding of F-actin regulating proteins. The usefulness of actin-FP or ABP/ABD-FP to visualize-actin filaments is determined by the efficiency by which the actin skeleton is labeled and interferes with the functioning of the skeleton.

Several actin-FP fusions have been described that were shown to be functional in mammalian, Drosophila or Dictostelium cells (Doyle *et al.* 1996; Westphal *et al.* 1996; Ballestrem *et al.* 1998; Chiodas *et al.* 1998; Verkhusha *et al.* 1999). In general these actin-FP fusions label the skeleton if an inducible or endogenous actin promoter is used. Further, the level of the tagged actin should not exceed 30% of the total actin present in the cell. So apparently actin-FP can be incorporated into the actin cytoskeleton but when its level is too high it disturbs proper functioning of the skeleton. This is also indicated by the disability of an actin fusion to complement an actin deficient yeast mutant (Doyle *et al.* 1996). Some actin isoforms are active in heterologous systems, however it appears that their expression levels are crucial (Kumar *et al.* 1997; Kandasamy *et al.* 2001; Gilliland *et al.* 2002; Ringli *et al.* 2002). For example Dictostelium FP-actin can be integrated in a mammalian actin cytoskeleton without any disturbance of cell functions (Chiodas *et al.* 1998).
In contrast to the successful application of actin-FP in animal systems, this has not been reported for plants. Kost *et al.* (Kost *et al.* 2000) describes an *Arabidopsis thaliana* actin FP fusion that incorporates into actin filaments, but it inhibits growth. The stable expression of GFP-AtAct2/7 in tobacco BY-2 suspension cells allowed visualization of filamentous structures. However, these transgenic BY-2 lines could not be maintained for extended periods, indicating that the fusion protein might interfere with cell viability or cell division. In addition, transient expression of the construct severely inhibited tobacco pollen germination and tube growth. In contrast, the ABP/ABD-FP approach was more successful in plants. The *Arabidopsis thaliana* actin depolymerizing factor (ADF) FP fusion labeled successfully the actin skeleton, although the filaments were thicker, and shorter and a reduced number of actin filaments were formed (Dong *et al.* 2001). Fusions containing complete actin binding proteins have the disadvantage that they could have maintained their biological activity by which expression of such fusions could affect the functioning of the cell even more. Using only an ABD of an actin binding protein could circumvent this problem. Therefore the ABD of mouse talin protein was fused to a FP and expressed in BY-2 tobacco suspension cells or in *A. thaliana* plants were it visualizes the F-actin, in general without affecting the functioning of cells. An exception to this is pollen tube growth as the construct can hamper growth, if expressed at a too high level (Kost *et al.* 1998; Cheung *et al.* 2004). Also this ABD-FP construct does not seem to label all filaments. An extensive F-actin network as was visualized in several plant cells with phalloidin or actin antibodies was not found using this construct (Ruijter *et al.* 1999; Kovar *et al.* 2001; Ketelaar *et al.* 2002). So although F-actin visualization in living plant cells is achieved to some extend, it is essential that it will be improved.

To compare the efficiency of F-actin labeling of different constructs a *Vigna* protoplasts test system seems appropriate. First; high transfection efficiency up to 80% can be obtained (Bokhoven *et al.* 1993). Second, a certain expression level appears sometimes to be crucial for proper labeling of the actin skeleton (Gillilland *et al.* 2002; Ringli *et al.* 2002). The protoplasts test system gives within each experiment cells with very different expression levels. Third, protoplasts can function rather normally without an actin cytoskeleton since protoplasts with a depolymerized actin skeleton are still able to synthesize viruses and make tubular structures enabling virus transportation (Pouwels *et al.* 2002). This suggests that the formation of a non-functional actin skeleton will not be lethal for protoplasts. Using this test system might

finally result in finding a candidate with potential to label F-actin in legume root hairs, during the *Rhizobium*-legume interaction.

Materials and Methods

Transient expression in protoplasts

Cowpea (*Vigna unguiculata L.)* mesophyll protoplasts were prepared essentially as described previously (Bokhoven et al. 1993) except that 10mM $CaCl_2$ was added to the enzyme solution. Ten to fifteen µg of purified plasmid DNA (concentrations were checked on gel and with spectophotometer) in 10-20 µl of water was added to 0.5-1x10^6 protoplasts.

Plasmid Constructs

All cloning work was carried out according to standard procedures (Maniatis *et al.* 2000) and all DNA fragments made by PCR were sequenced.

YFP-(SGLRSRAQASNSAVD)-PsAct1 (Figure 3a):
First, pEYFP(V68L/Q69K)-C1 was made. *EYFP*(V68L/Q69K) (0.7kb) was isolated form cameleon 2.1 (this YFP has a reduced pH sensitivity (Miyawaki *et al.* 1999)) using PCR in combination with the following oligonucleotides;
GGGGCTAGCCGGTCGCCACC**ATG***G*TGAGCAAGGGCGAGGA (underlined NheI, start codon bold),
TCGAGATCTGAGTCCGGACTT (underlined Bgl II) and used to replace *EGFP* in pEGFP-C1 (Clontech, USA).
In addition the ORF of *PsAct1* cDNA clone was PCR amplified using in combination with the following oligonucleotides;
CGCGTCGACGCCGATGCTGAGGATATT (underlined SalI)
CGGGATCC*TTA*GAAGCATTTTCTGTG (underlined BamHI, stop codon italic). This fragment (1.1 kb) was cloned using SalI/BamHI in pEYFP(V68L/Q69K)-C1 subsequently subcloned (NheI/BamHI) as a 1.8 kb EYFP fusion in pMON999 (XbaI/BamHI).

YFP-(SGLRSRAQAS)-PsAct1 (Figure 3b):
PsAct1 was amplified using PCR in combination with the following oligonucleotides;
TCCCCGCGGGGCCGATGCTGAGGATAT (underlined SacII)
CGGGATCC*TTA*GAAGCATTTTCTGTG (underlined BamHI, stop codon italic). This fragment (1.1 kb) was cloned using (SacII/BamHI) in pEYFP(V68L/Q69K)-C1 subsequently subcloned (NheI/BamHI) as a 1.8 kb EYFP fusion in pMON999 (XbaI/BamHI).

YFP-(SGLRSRA)-PsAct1 (Figure 3c):
PsAct1 was amplified using PCR in combination with the following oligonucleotides;
CCGCTCGAGTGGCCGATGCTGAGGATA (underlined XhoI)
CGGGATCC*TTA*GAAGCATTTTCTGTG (underlined BamHI, stop codon italic). This fragment (1.1 kb) was cloned (XhoI/BamHI) in pEYFP(V68L/Q69K)-C1 subsequently subcloned (NheI/BamHI) as a 1.8 kb EYFP fusion in pMON999 (XbaI/BamHI).

PsAct1-(P(A)$_{10}$SRS)-YFP (Figure 3d):
In this construct a linker, GGTACCCGCTGCTGCCGCCGCTGCAGCTGCTGCTGCATCTAGA (underlined KpnI and XbaI ,respectively) couples *PsAct1* to *smRSEGFP*. The *PsAct1* stop codon was there for eliminated. In addition the *smRSEGFP* was replaced with EYFP. EYFP was amplified from cameleon 2.0 (Miyawaki *et al.* 1997) using PCR in combination with the following oligonucleotides;
AATTCTAGAAGCAAGGGCGAGGAGCTGT (underlined XbaI), TTTGAGCTC*TTA*CTTGTACAGCTC (underlined SstI, stop codon italic) and used to replace *smRSEGFP*.

YFP-(SGLRSRA)-DdAct15 (Figure 3e):
DdAct15 (1.1 kb) was isolated by PCR on the template provided kindly by G. Gerisch, in combination with the following oligonucleotides;
GATCTCGAGCTATGGATGGTGAAGATGTTC (underlined XhoI),
CGGGATCC*TTA*GAAGCATTTTCTGTG (underlined BamHI, stop codon italic). This fragment (1.1 kb) was cloned (XhoI/BamHI) in pEYFP(V68L/Q69K)-C1 subsequently the 1.8 kb fusion was subcloned (NheI/BamHI) into (XbaI/BamHI) pMON999.

GFP-(SGLRSRAQA)-Hsßact (Fig 3f)
The p*EGFP-(SGLRSRAQA)- Hsßact* was kindly provided by J. Broers and F. Ramaekers. The *Hsßact* (1.1 kb) was cloned in pEGFP-C1 (Clontech) (Hind III/BamHI), creating a SGLRSRAQA linker. The *EGFP-(SGLRSRAQA)- Hsßact* was isolated (1.8 kb) (NheI/BamHI) and cloned into the pMON999 (XbaI/BamHI).

YFP-(SGLRSRAL)-DdTalin$_{2302-2491}$ (Figure 3g)
The *DdTalin* (0.6 kb) actin binding part (basepair 8023-8576; amino acid $_{2301-2492}$) was isolated by PCR on the *DdTalin* template kindly provided by J. Faix in combination with the following oligonucleotides;
CCGAGCTCTCATCGTAGATGCTAGTAGT (underlined SacI), CGGGATCC*TTA*ATTTTTATTATAATT (underlined BamHI, stop codon italic). This 0.57kb fragment was cloned (XhoI/BamHI) in pEYFP(V68L/Q69K)-C1 subsequently the 1.3 kb fusion was subcloned (NheI/BamHI) in pMON999 (XbaI/BamHI).

YFP-(GGSGGSRL)-DdCortN$_{1-233}$ (Figure 3h).
DdCortN$_{1-233}$ was isolated by PCR using cortexillin I, (kindly provided by Alexander Stock and Jan Faix), as template in combination with the following oligonucleotides;
GCGTCGACTCATGGCAGGTAAAGATTGG (underlined SalI),
CGAGCTCGGTACC*TTA*CTCTTCCTTGGCTCTATAG (underlined SacI, underlined dotted KpnI and the stop codon italic). This 0.7kb fragment was cloned (SalI/KpnI) in pEYFP(V68L/Q69K)-C1 subsequently the 1.4 kb fusion was subcloned (NheI/SacI) in pMON999 (XbaI/SacI).

YFP-(SGLRSRAQASNS)-ZmADF3 (Figure 3i):
ZmADF3 (0.4 kb) was isolated by PCR on the template provided kindly by P. Hussey in combination with the following oligonucleotides;
CCCGAATTCCATGGCGAACGCGAGATCGG (underlined EcoRI),
GCGGATCC*CTA*GCGTGCCCGATCCTT (underlined BamHI, stop codon italic). This fragment (0.4 kb) was cloned (EcoRI/BamHI) in pEYFP(V68L/Q69K)-C1 subsequently the 1.1 kb fusion was subcloned (NheI/BamHI) in pMON999 (XbaI/BamHI).

ZmADF3
ZmADF3 (0.4 kb) was isolated by PCR on the pMON999 *EYFP*(V68L, Q69K)-*(SGLRSRAQASNS)-ZmADF3* (Figure 2p) template in combination with the following oligonucleotides;
GGTCTAGA*ATG*GCGAACGCGAGATCG (underlined XbaI, start codon italic),
GCGGATCC*CTA*GCGTGCCCGATCCTT (underlined BamHI, stop codon italic). This fragment (0.4 kb) was cloned in pMON999 (XbaI/BamHI).

Alexa488-phalloidin and Rhodamin-phalloidin protoplast actin staining

Before staining the transfected cowpea protoplasts were prefixed with 500µM MBS-ester (m-maleimido benzoyl N-hydroxy succinimide ester) in protoplast medium for 3 minutes to stabilize the actin filaments and to stop cytoplasmic streaming. Subsequently, fixation was performed by adding slowly 4% paraformaldehyde and 0.1% glutaraldehyde in ASB (actin stabilizing buffer; 100mM PIPES pH 6.8, 1 mM $MgCl_2$ 1mM$CaCl_2$, 75 mM KCl) within a few minutes. After 20 minutes of incubation the fixed protoplasts were washed once in ASB for 4 minutes.
Next the plasmamembranes were permeabilized with 100µg/ml LP-choline (L-alpha-lyso-phosphatidylcholine) in ASB for 8 minutes and washed for 4 minutes with ASB. After that the protoplasts were labelled with 0.33µM Alexa fluor 488-phalloidin (Molecular probes) in ASB for 5 minutes and sealed with Citifluor-glycerol (an anti fading matter) on a microscope slide. Subsequently, the fixed and stained protoplasts were analysed using CSLM.

Cytochalasin D treatment.

Protoplasts were diluted 1:1 with Cytochalasin D (500µl fresh protoplast medium, 0.5µl Cytochalasin D 10 mM in 0.1% DSMO).

Confocal laser Scanning Microscopy (CLSM)

The Alexa488-phalloidin stained protoplasts were imaged using an Optiphot microscope (Nikon) connected to a Biorad MRC 600 CLSM with an Argon-Krypton laser and fitted with a 60x (NA 1.4) oil objective. The standard K1-K2 (FITC/TRITC) filter were used to detect the Alexa488-phalloidin (Molecular probes) and chloroplast fluorescence.
For the YFP, GFP and co-localization studies of YFP and rhodamin-phalloidin a Zeiss LSM510 CLSM implemented on an inverted microscope (Axiovert 100) fitted with a Zeiss plan neofluotar 10x (Na 0.5) air and a 40x (NA 1.30) oil immersion objective was used. To excite the fluorescent probes a 543nm, 488nm or 514nm Argon laser line was used. The light was reflected onto the sample by a dichroic mirror.For YFP the 514nm Argon laser line was used with a HFT514 dichroic mirror and a BP535-590IR emission filter. For GFP a 488nm Argon laser line with a HFT488 dichroic mirror and a BP505-530 emission filter was used.
For the colocalization of YFP and rhodamin-phalloidin (542nm absorbtion/565nm emission) the 514nm and 543nm laser was used with NT 80/20/543, NFT545, NFT635 VIS filters and the emission filters BP530-600 (YFP) and BP 565-595 (rhodamin-phalloidin). These settings were selected in order to distinguish between rhodamin fluorescence and the auto fluorescence. In cases the chlorophyll fluorescence was visualized, a LP650 emission filter was used. For all co-localisation studies, the multi-track mode of the LSM 510 was used, to exclude bleed through.
Images were processed using Photoshop 5.5 and illustrator 8.0.

Results

The actin skeleton of cowpea protoplasts

The ability of FP constructs to visualize the actin skeleton will be studied in *Vigna unguiculata L.* (cowpea) mesophyl protoplasts. Therefore we first studied the configuration of the endogenous actin skeleton of cowpea protoplasts to serve as reference. The actin cytoskeleton configuration was visualized by using Alexa488-phalloidin (Figure 1).

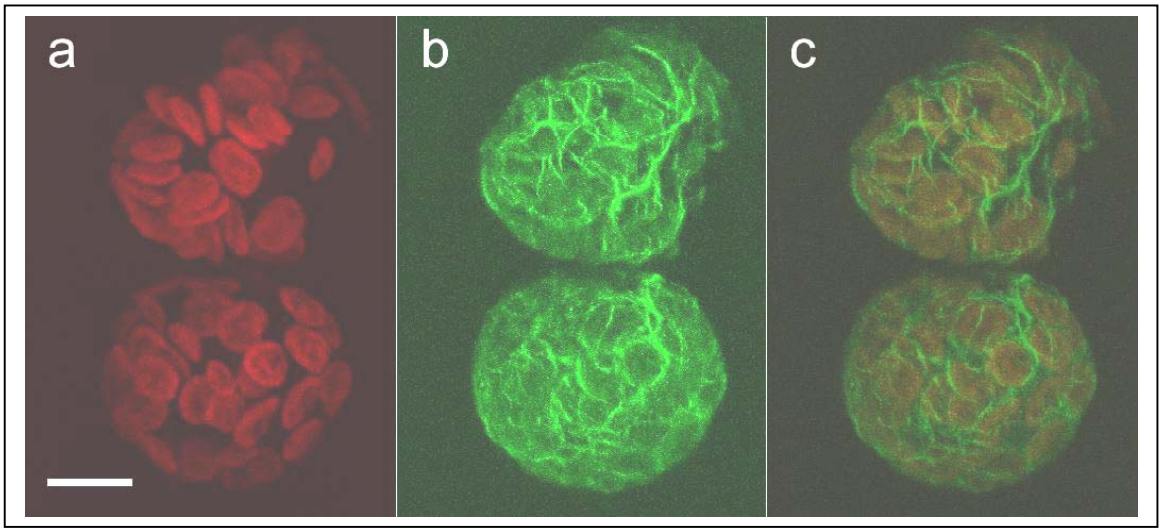

Figure 1. Confocal Z-stack of Alexa488-phalloidin labeled protoplasts. Pseudo colored Alexa488 (actin) fluorescence is indicated in green (**b**) whereas chloroplasts autofluorescence is visualized in red (**a**). **a** and **b** merged (**c**).
Bars = 10 µm.

As is shown in Figure 1b the actin cytoskeleton of these protoplasts is mainly composed of thick bundles. A meshwork of thin actin filaments as found in growing cells of other plant cell types, is not detected (Ruijter *et al.* 1999; Kovar *et al.* 2001; Ketelaar *et al.* 2002). This network just may not be present in cowpea protoplast or it has been lost during protoplast isolation or staining procedure. Nevertheless the protoplast expression system still seems an attractive system to get insight in the properties of FP fusions in a fast and efficient manner.
To make actin-FP fusions we isolated an actin clone from pea (Figure 2) and further we used 2 actin clones from heterologous systems (Figure 3). First the isolation of the pea actin clone will be described.

Isolation of a cDNA clone of a pea actin gene expressed in root hairs
We reasoned that an actin that is (specifically) formed in root hairs has the highest probability to be incorporated as actin-FP into the root hair actin skeleton. For this reason an available pea root hair cDNA library (Mylona 1996) was screened. A soybean actin cDNA clone (Hightower *et al.* 1985) was used to screen this cDNA library. This resulted in several cDNA clones but all encoding the same actin isoform, *PsAct1* (Figure 2).

Figure 2. *PsAct1* cDNA sequence and amino acid sequence.

After a second screening using the *PsAct1* as probe several additional clones were obtained, but sequencing showed that they all encode PsAct1 (data not shown). Pea most likely has several actin genes therefore this indicates that *PsAct1* is the most abundantly expressed actin gene in pea root hairs.
Arabidopsis has 8 actin genes and PsAct1 is most homologous (98% on protein level) to AtAct7 (Mckinney *et al.* 1998). *AtAct2, AtAct7* and *AtAct8* are all highly expressed in Arabidopsis roots and root hairs. *AtAct7* is the only actin in this gene family that is highly regulated by phytohormones. Its expression level is increased within minutes after auxin application (Kandasamy *et al.* 2003). AtAct7 plays also a special role in germination and control of root growth and most likely also is involved in creating cell polarity (Gilliland *et al.* 2003). An Arabidopsis *AtAct2* mutant showed severe root hair elongation defects. However this mutant could be rescued by over expressing *AtAct7* (Gillilland *et al.* 2002) and this supports our assumption that *PsAct1* is a good candidate to be tested as a FP-fusion.

Actin FP fusions

Actin FP fusions were made and put under control of an enhanced CaMV35S promoter, which is highly active in protoplasts (Bokhoven *et al.* 1993). For the fusions we used the isolated *PsAct1* cDNA clone, a dictyostelium actin (DdAct15) and a human actin (Hsßact) fused at their C or N-terminus, to a Green Fluorescent Protein (GFP) or Yellow Fluorescent Protein (YFP) (Figure 3a-f).

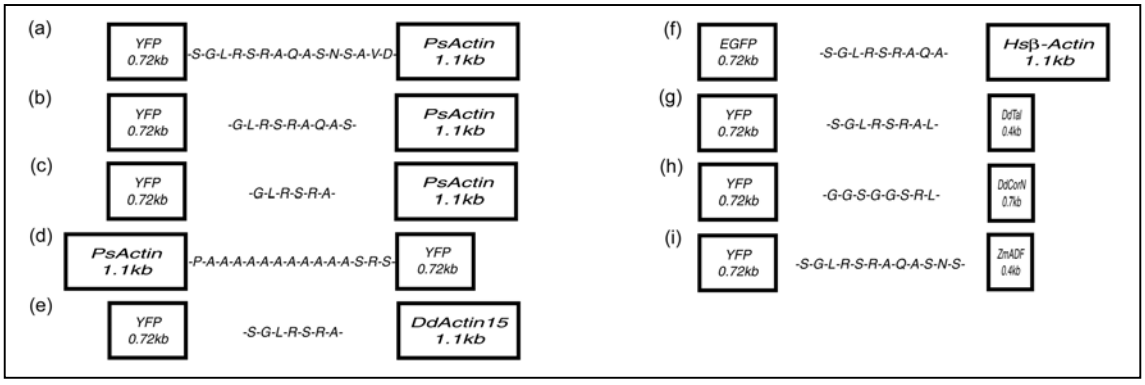

Figure 3. Constructs for *in vivo* labeling of the actin cytoskeleton.
The constructs contain an actin (a-f) or an ABP/ABD (g-i), respectively. These are linked to a FP and in between a linker is positioned. The latter is indicated by the one letter code of amino acids.
(**a**) YFP-(SGLRSRAQASNSAVD)-PsAct1. A similar fusion, GFP-$(GA)_5$-AtActin has shown to hamper plant cell growth (Kost *et al.* 2000).
(**b**) A similar construct as (a) but with a GLRSRAQAS linker.
(**c**) A similar construct as (a) but with a GLRSRA linker.
(**d**) A similar construct as (a) but with the C terminus of actin fused to a linker followed by an FP creating the PsAct1-$(P(A)_{10}$SRS)-YFP. Such an actin C' fusion, ScACT1-$(A)_{10}$-GFP fusion, has been shown to label only partially the actin filaments in yeast cells (Doyle *et al.* 1996).
(**e**) YFP-(SGLRSRA)-DdAct15. A similar fusion, GFP(S65T)-(KLEFK)-DdAct15 has been shown to be functional in its homologous background *Dictostelium disoideum* (Westphal *et al.* 1996).
(**f**) GFP-(SGLRSRAQA)-Hsß actin fusion.
A similar fusion, GFP-(GSTSG)-(Hsßact HSAC07) has been shown to be functional in several mammalian cell lines (Ballestrem *et al.* 1998).
(**g**) YFP-(SGLRSRAL)-DdTalin$_{2301-2492}$, a *Dictostelium disoideum* Talin ABD (DdTalin$_{2302-2491}$) fused to YFP. A similar fusion, GFP-$(GA)_5$-MmTN$_{345-2541}$, has been shown to enable F-actin visualization in Arabidopsis cortical root cells and tobacco pollen tubes (Kost *et al.* 1998).
(**h**) YFP-(GGSGGSRL)-DdCortN$_{1-233}$, a *Dictostelium disoideum* cortexillinI N terminus ABD (DdCortexellinN$_{1-233}$) (Weber *et al.* 1999) fused to YFP.
(**i**) YFP-(SGLRSRAQASNS)-ZmADF3, a *Zea maiz* ABP, Actin Depolymerizing Factor (ZmADF3) (Lopez *et al.* 1996) fused to YFP, A similar fusion, GFP-$(GA)_5$-AtADF, has been shown to alter F-actin morphology, reducing the number and /or the length of the filaments (Dong *et al.* 2001).

Actin visualization in cowpea protoplasts

The constructs indicated in Figure 3 were tested in cowpea protoplasts (Figure 4). For each construct transfections were repeated at least 3 times, parallel with controls for transfection efficiency. 10µg DNA of each construct, was used to transfect 1 million of protoplasts. 1 to 3 days after transfection the protoplasts were imaged.

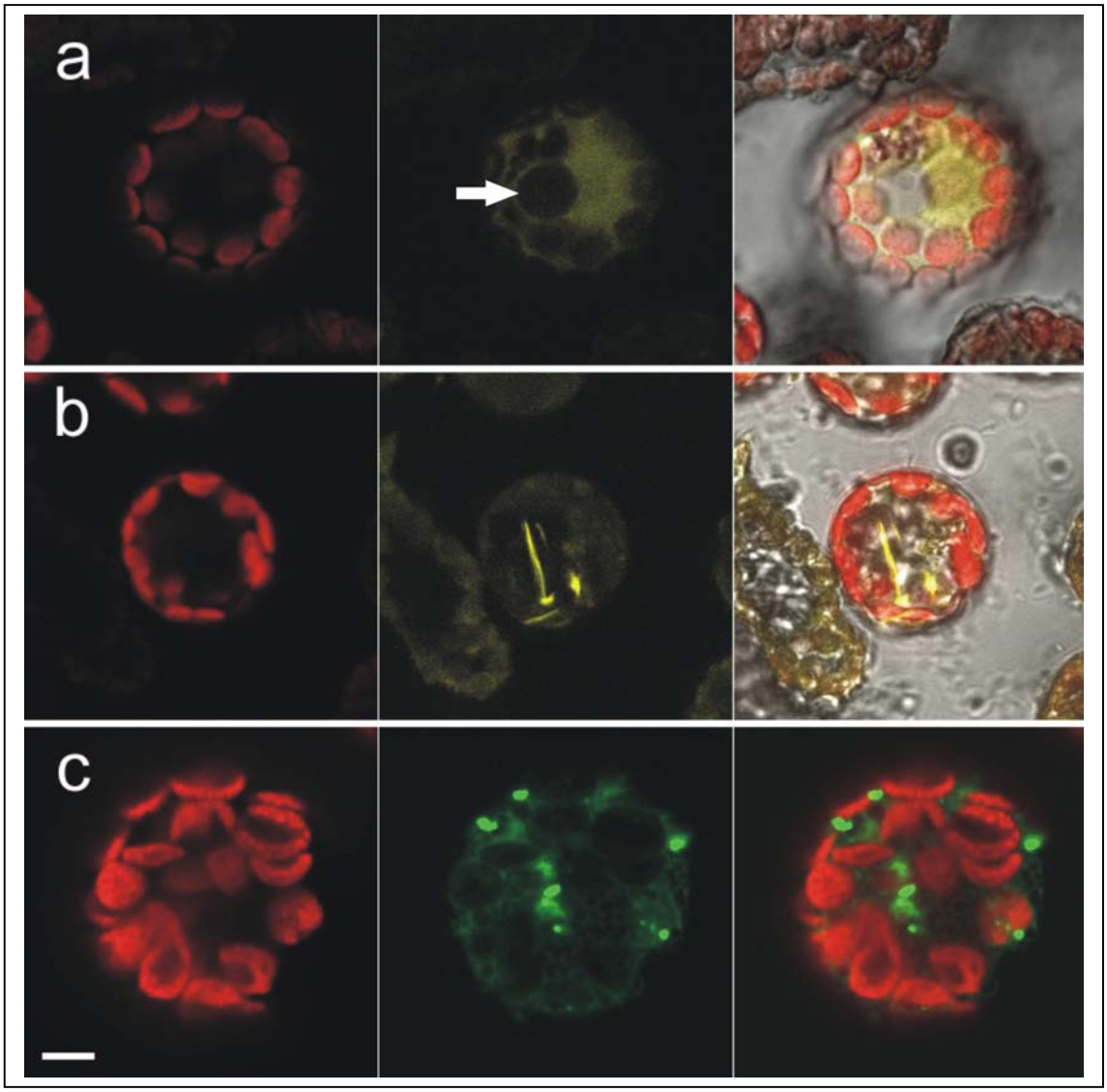

Figure 4. Confocal sections of PsAct1-YFP (Figure 3d) and GFP-Hsβact transfected protoplasts (Figure 3f). Pseudo colored from left to right; first chloroplasts in red, then YFP labeled actin yellow / GFP labeled actin in green followed by a merged image. (**a,b**) Protoplasts transfected with 10μg PsAct1-YFP, 1 (a) respectively 3 (b) days after transfection, (**c**) protoplast transfected with 20μg GFP-Hsβact and 2 days after transfection.
The arrow indicates the nucleus. Bars = 5 μm.

Two days after transfection all PsAct1 fusions (Figure 3a-d) resulted in cytoplasmic fluorescence and none of the proteins occurred in the nucleus. In contrast, free YFP mainly accumulates in the nucleus. This suggests that a fusion protein is made and free YFP is not (abundantly) present.
However, only the PsAct1-(P(A)$_{10}$SRS)-FP (Figure 3d) fusion did result in a few fluorescent filaments (Figure 4a,b). These fluorescent filaments were thick rods, rarely branched and were present in only about 5% of the cells. 3 days after transfection about 10% of the protoplasts showed such fluorescent rods (Figure 4b). This fluorescent skeleton is markedly different from the endogenous skeleton visualised by Alexa488 phalloidin (Figure 1) since that is composed of, shorter, thinner and more frequently branched filaments. In addition to the fluorescent rods, FP fluorescence is found in the cytoplasm. To determine if an increase in FP-actin

concentration can shift the equilibrium of FP-actin monomers to filamentous FP-actin the DNA concentration used to transfect was doubled. This had no effect on number of fluorescent filaments or on filament morphology, but only on the number of cells expressing PsAct1-FP. Namely, 2 days after transfection, about 10% of cells formed fluorescent rods with a similar morphology as those formed when lower amounts of DNA were used for transfection. So a higher expression level resulted in an increase of the number of protoplasts forming fluorescent rods, but it did not change rod morphology. Liu *et al*. have already shown that a similar PsActin fusion is able to polymerise *in vit*ro (Liu *et al.* 2004). However, this fusion was not shown to be able to form filaments in stably transformed BY2 plant cells. This pea actin is very homologous, 98% on protein level, to PsAct1. However among the few amino acids that differ there are prolines which could affect the structure.

Other actin fusions tested were FP-DdAct15 and FP-Hsßact. Both were shown to be functional in Dictostelium or mammalian cells, respectively (Westphal *et al.* 1996; Ballestrem *et al.* 1998; Chiodas *et al.* 1998). FP-DdAct15 (Figure 3e) resulted in cytoplasmic fluorescence. Whereas FP-Hsßact (Figure 3f) transfected protoplasts showed 2 days after transfection in about 1% of the protoplasts fluorescent patches (1-20 per cells) (Figure 4c). When 20μg DNA is used (in stead of 10) for transfection up to 5% of the protoplasts contained such patches. This is in accordance with previously published results showing that plant and animal actin do not tend to form hetero F-actin polymers (Ren *et al.* 1997; Jing *et al.* 2003; Staiger *et al.* 2004). The other actin fusions tested having only cytoplasmic fluorescence, did not form structures by an increase in DNA concentration.
In conclusion, only the PsAct1-FP construct resulted in fluorescent rods but the configuration of this fluorescent “skeleton” is markedly different from that visualized by phalloidin staining.
It has to be kept in mind that *PsAct1* is highly expressed in pea root hairs and is therefore the best candidate to be expressed as a fusion in legume root hairs. However, due to this also *PsAct1* based constructs might be less suited to be used in mesophyll protoplasts.

To determine if PsAct1-FP is indeed associated with F-actin, it was tested whether YFP co-localizes with phalloidin visualized F-actin. Rhodamin-phalloidin and not Alexa488-phalloidin labeling was used for co-localization since its fluorescence can be distinguished better from that of YFP.

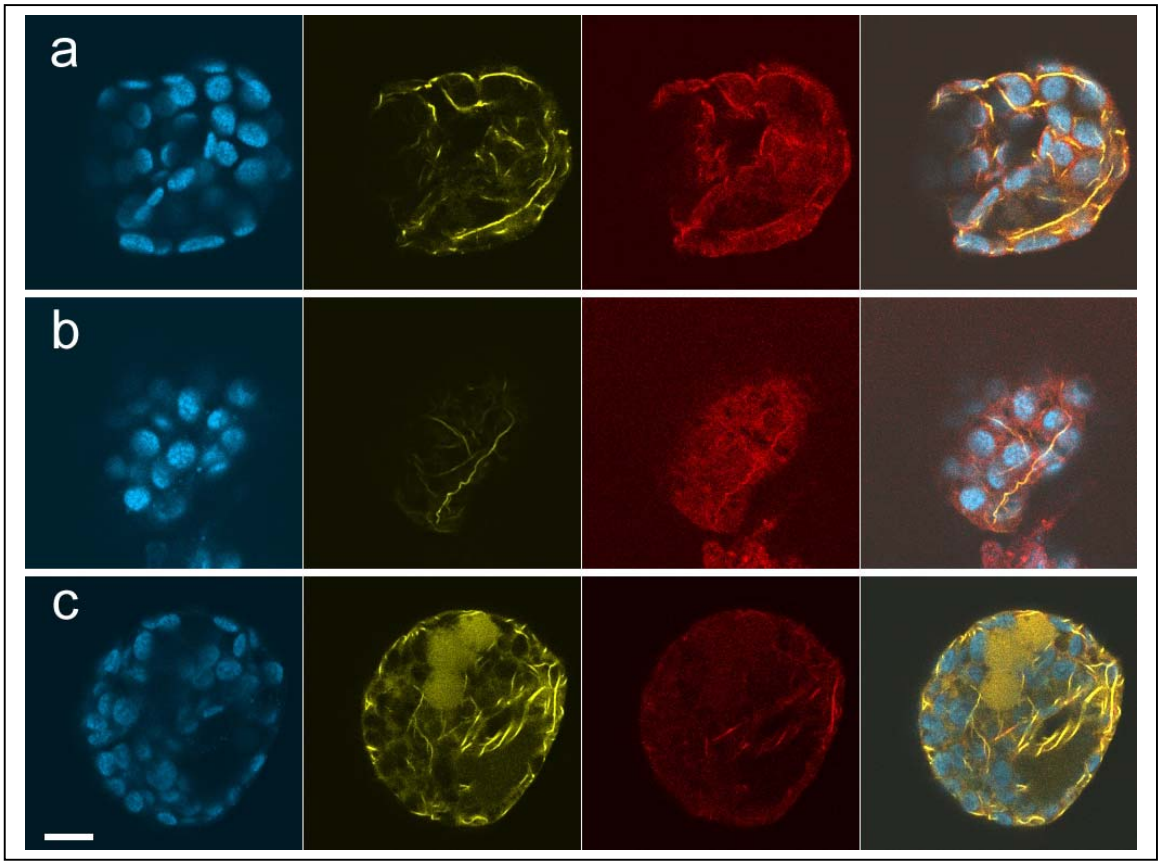

Figure 5. Confocal images of fixed cowpea protoplast transfected with, row (**a**) PsAct1-YFP, (**b**) YFP-DdTalin$_{2303-2491}$, (**c**) YFP-ZmADF3 and stained with rhodamin-phalloidin.; From left to right in pseudo colors; first chloroplasts in blue, second YFP labeled actin yellow , third Rhodamin-phalloidin labeled actin red and followed by a merged image.
Bar = 5 µm.

PsAct1-FP containing rods and phalloidin labeled rods do co-localize (Figure 5a). However, the background of Rhodamin fluorescence complicates the visualization of all Rhodamin-phalloidin labeled filaments. Only the more intensely labeled rods show co-localization with the FP filaments. This co-localization and absence of only Rhodamin-phalloidin labeled filaments implies that actin-FP has been incorporated in the actin skeleton, but the configuration of this skeleton is markedly altered, in comparison with that of untransfected protoplasts (Figure 1). This might mean that PsAct1-FP hampers F-actin formation, for example by reducing G-actin incorporation at the barbed-end and therefore causing a disassembly of the (endogenous) filaments due to a continuous disassembly at the pointed-end.
To study whether the actin-FP skeleton is still dynamic we treated the protoplasts with cytochalasin D. Cytochalasin D promotes actin depolymerization by binding to the barbed-end of an actin filament. In this way it blocks actin polymerization and due to the continuous de-polymerization of the F-actin pointed-end filaments will disappear as previously was shown in cowpea protoplast (Pouwels *et al.* 2002).

FP-PsAct1 transfected protoplasts, formed a similar fluorescent skeleton as shown in Figure 4a,b. Two days after transfection 5µM cytochalasin D was added, but this did not affect the fluorescent skeleton (even till 30 minutes after application). This

indicates that incorporation of PsAct1-FP in F actin markedly reduces the turnover of F-actin.
Since expression of actin-FP fusions altered actin organisation and decreased actin dynamics it will markedly affect the viability of cells. Therefore we searched for another approach to visualise the actin skeleton and studied whether fusions of a FP and an Actin Binding Protein (ABP) or its Actin Binding Domain (ABD) could be used.

ABD/ABP FP fusions
The ABDs that were used for fusion with FP are the from *Dictostelium disoideum* talin and cortexillin, respectively. Further, *Zea mays* ZmADF3, an ABP, was fused to an FP.
Talin has an F-actin binding domain of 191 aa at its C terminus, which can be used to label F-actin (Muguruma *et al.* 1990; Hemmings *et al.* 1996). The cortexelin F-actin binding domain (227 amino acids (aa)) is located at its N terminus (1-227). This region was previously used in a similar FP fusion (Stock *et al.* 1999; Weber *et al.* 1999).
The constructs FP-DdTalin$_{2303-2491}$ (Figure 3g) and FP-DdCortN$_{1-233}$ (Figure 3h) were introduced in protoplasts to test whether they could visualize the actin cytoskeleton. Only FP-DdTalin$_{2303-2491}$ resulted in fluorescent filaments (Figure 6a,b).

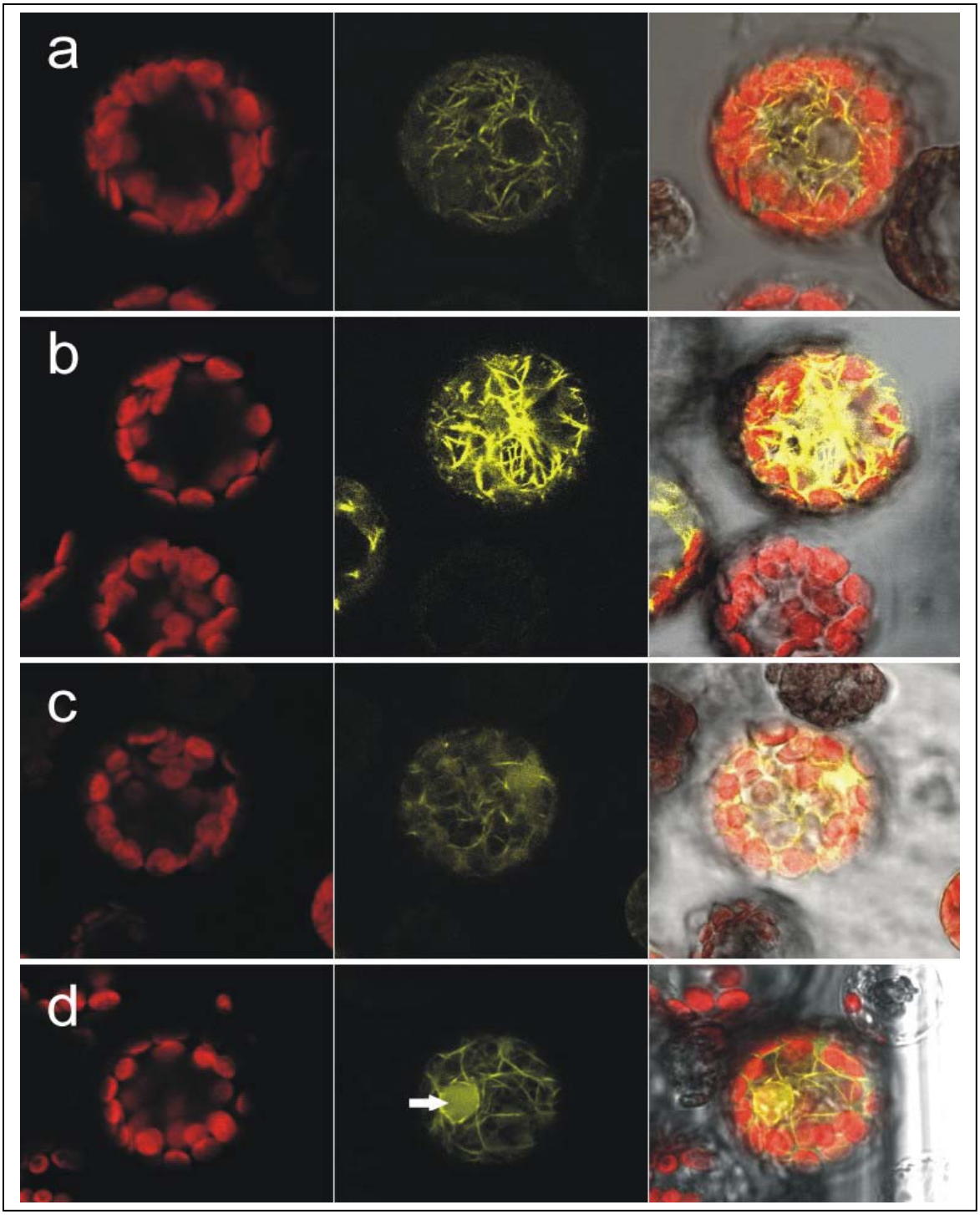

Figure 6. Confocal images of cowpea protoplasts transfected with various FP-ABP/ABD. From left to right in pseudo colors; first; chloroplasts red, second YFP labeled actin yellow and followed by a merged image. (**a,b**) YFP-DdTalin$_{2303-2491}$, 1(a) respectively 2(b) days after transfection. (**c,d**) YFP-ZmADF3, 1(c) respectively 2(d) days after transfection.
The arrows indicate the nuclei. Bars = 5 µm.

FP-DdTalin$_{2303-2491}$ labels (1 day after transfection) in about 50% of the cells a fluorescent network. This network consists of a meshwork of thin and thick filaments (Figure 6a,b). This network seems to differ from the endogenous network (Figure 1) by showing more and also thicker filaments. After 2 days the number of filaments per cell has increased and about 70% of cells show a fluorecent skeleton.

In addition to the talin and cortexelin based fusions the *Zea mays* ZmADF3 full-length protein (140 aa) was used since in vitro studies have shown that it binds to F-actin and it occurs at rather high levels in tips of growing root hairs (Jiang *et al.* 1997). The construct FP-ZmADF3 (Figure 3i) was transfected into protoplasts and resulted in fluorescent filaments (Figure 6c,d). FP-ZmADF3 is mainly cytoplasmic, but labels 2 days after transfection, in about 30% of the cells, a fluorescent network of filaments. This network differs from that labeled by FP-DdTalin$_{2303-2491}$ since fewer fluorescent filaments are present (Figure 6c,d1-3). This difference could be caused by the activity of ADF, stimulating F-actin shortening, bundling and reorganization, as has been shown by Dong *et a*l. (Dong *et al.* 2001). Also an increased cytoplasmic fluorescence is often found, compared to the talin construct. This could indicate a lower F-actin affinity of the FP-ZmADF3 fusion. Fluorescence is now also found in the nucleus (Arrow in Figure 6). This nuclear localization is not found with the other constructs tested. ZmADF3 has no clear nuclear localization signal sequence (Chang-Jie *et al.* 1997), but has been shown to occur in the nucleus (Dong *et al.* 2001).
Confocal images of fixed cowpea protoplast transfected with FP-DdTalin$_{2303-2491}$ or FP-ZmADF3 and stained with rhodamin-phalloidin (Figure 5b,c) showed FP rods and phalloidin labeled rods co-localizing. Therefore also the FP-DdTalin$_{2303-2491}$, FP-ZmADF3 constructs label F-actin. However, the visualization with Rhodamin-phalloidin is too poor to answer the question if only a certain fraction of the F-actin is labeled by the fusions. It is known that phalloidin and ADF compete for the same binding site on the F-actin, giving a poor phalloidin labeling (McGough *et al.* 1997; Dong *et al.* 2001).

To obtain a better insight in whether ZmADF3 affects the configuration of the actin skeleton co-transfections using ZmADF3 (without a FP) and FP-DdTalin were performed (Figure 7).

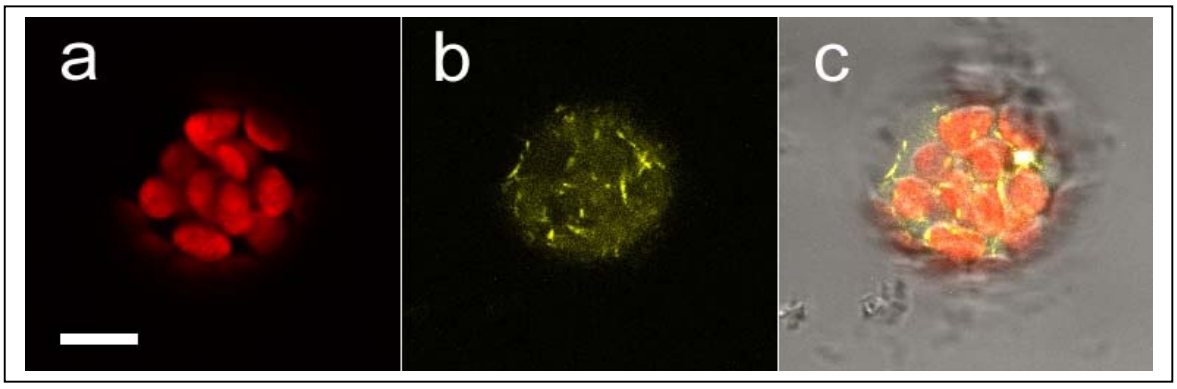

Figure 7. Confocal image of cowpea protoplasts co-transfected with 10μg YFP-DdTalin and ZmADF3. Pseudo colored; chloroplasts red (**a**), YFP labeled actin yellow (**b**) and a merged (**c**).
Bars = 5 μm.

Small rods labeled by FP-DdTalin are visible in the cytoplasm, and these are noticeably shorter than the fluorescent filaments in protoplasts transfected with only FP-DdTalin$_{2303-2491}$ or FP-ZmADF3. So clearly overexpression of ZmADF3 has an effect on the F-actin configuration. However, the effect of FP-ZmADF3 and ZmADF3 seems to differ, probably caused by a higher activity of the latter.

If ZmADF3 has indeed an effect on the skeleton, ZmADF3 activity might stimulate YFP-PsAct1 incorporation in the F-actin skeleton. To test this, a co-transfection of ZmADF3 and FP-PsAct1 was performed resulting in similar fluorescent filaments as formed by transfection with solely FP-PsAct1 (Figure 4a,b). The PsAct1-FP filaments are now formed faster, namely 1 day after transfection and further more protoplasts have such filaments..
Based on these results we conclude that FP-ZmADF3 markedly affects the configuration of the F-actin.

To determine if the $DdTalin_{2303-2491}$ and ZmADF3 based fusions are indeed associated with F-actin, transfected protoplasts were stained with rhodamin-phalloidin (Figure 5b, c). The FP-$DdTalin_{2303-2491}$ and rhodamin-phalloidin stained filaments almost completely co-localize (Figure 5b). However, small filaments cannot be observed due to the background of rhodamin fluorescence.
Also FP-ZmADF3 does show such a co-localization with rhodamin-phalloidin (Figure 5c), so also FP-ZmADF3 labels F-actin. However, with this construct only a subset of the filaments is labeled with phalloidin. This is probably caused by the fact that phalloidin and the ZmADF3 compete for the same binding site on F-actin as was described by others (McGough *et al.* 1997; Dong *et al.* 2001).

To determine if the $DdTalin_{2303-2491}$ and ZmADF3 based fusions have maintained their dynamic property transfected protoplasts were treated with cytochalasin D.
It was already shown for FP-$DdTalin_{2303-2491}$ transfected protoplasts that treatment with cytochalasin D (60µM) eliminates the fluorescent filaments within 30 minutes and the fluorescent skeleton reappears within 2 hours. So association with FP-$DdTalin_{2303-2491}$ did not markedly affect actin turnover (Pouwels *et al.* 2002).
After treatment with cytochalasin D (5µM) of FP-ZmADF3 transfected protoplasts the fluorescent filaments disappeared within 15 minutes and then reappeared within about 20 minutes. So also the FP-ZmADF3 labeled skeleton maintained its dynamic property.

Discussion

A useful probe to label F-actin in living cells has to fulfil in principle two main requirements. First, it should label preferably the complete F-actin skeleton of the cell and second; it should neither affect the configuration nor the dynamics of the endogenous F-actin skeleton. If we apply these criteria to the actin probes we tested in this chapter the following can be concluded:
PsAct1-YFP fusion is shown to cause a marked change of the configuration of the endogenous F-actin skeleton, which in addition, also has lost its dynamic properties. For this reason this probe is not useful to label F-actin in cowpea protoplasts. On the other hand FP-actin fusions were successfully used to label F-actin in stably transformed yeast and various animal systems (Doyle *et al.* 1996; Westphal *et al.* 1997; Ballestrem *et al.* 1998; Verkhusha *et al.* 1999). However, up till now, in spite of many attempts (pers. comm.), a successful visualisation of the actin skeleton using an actin-FP construct has not been reported for plant cells. This suggests that plant actins might be different from that of other organisms and more easily affected in its

function when fused to FP. This is also indicated by the fact that heterologous actin does not incorporate into plant F-actin (Hepler *et al.* 1993; Ren *et al.* 1997; Liu *et al.* 2004; Staiger *et al.* 2004). The only exception is an Alexa fluor 488 labelled rabbit actin (Molecular probes USA) that could form filaments in onion epidermal cell (Paves *et al.* 2004).
Although the PsAct1-FP construct was not useful in cowpea protoplasts this does not exclude that it can be used to visualize F-actin in root hairs. To test this, the *PsAct1-FP* fusion was used to transform *Lotus japonicus* (Lotus) roots using the *PsRh2* promoter (see Chapter 2). However it did not yield any fluorescent roots (unpublished results). PsAct1 has the highest homology to AtAct7, and it is shown that AtAct7 is required for normal callus formation (Kandasamy *et al.* 2001). For this reason an altered PsAct1, a PsAct1- FP, might hamper normal callus formation. To obtain *PsAct1-FP* transformed roots we used *A. rhizogenes* root transformation, a procedure based on root formation from callus formed on hypocotyl (see also Chapter 2). Therefore expressing PsAct1-FP could result in a selection for callus (roots) that does not express the transgene.
The lack of success with FP-actin in living plant cells shows that currently the ABP/ABD-FP approach is the best method to obtain a FP labeled F-actin skeleton. Two ABP/ABD-FP constructs, of the ones tested, resulted in F-actin labelling in protoplasts, namely FP-ZmADF and FP-DdTalin$_{2303-2491}$. FP-ZmADF is not a good probe, as it affects the configuration of the F-actin. In contrast FP-DdTalin$_{2303-2491}$ labels an F-actin skeleton that resembles very the skeleton of untransformed protoplasts and it does not influence the dynamic properties of the F-actin. So fulfilling both prerequisites set at the beginning. DdTalin$_{2303-2491}$ ABD used for the FP fusion is 37% homologous on amino acid level to the *Muscus musculus* talin ABD MmTn$_{2345-2541}$ used in a similar F-actin probe by Kost *et a*l. (Kost *et al.* 1998). However, MmTn$_{2345-2541}$-FP induces changes in F-actin bundling, its dynamic properties, causes defects in cell development and may not faithfully label all microfilament arrays in stably transformed plant cells (Marthur *et al.* 1999; Marthur *et al.* 2003; Marthur *et al.* 2003; Ketelaar *et al.* 2004; Wang *et al.* 2004). Whether the DdTalin$_{2303-2491}$-FP fusion will not cause these problems in stably transformed plant cells remains to be studied. However, when this construct was used to transform Lotus roots (using the *PsRH2* promoter), no FP labeled F-actin was obtained (unpublished results). However very recently a paper appeared using *35S::Talin-GFP* to visualize successfully F-actin in Lotus root-hairs (Weerasinghe *et al.* 2005). Although a fine F-actin cytoskeleton extending to the tip of roothairs as found by Weerasinghe *et al.* was not visualized (Weerasinghe *et al.* 2005). So although FP-DdTalin$_{2303-2491}$ is a good F-actin probe in protoplasts, more studies on its usefulness in plants still have to be done.
Additional ABP/ABD-FP probes have been made by others,for example a T-plastin ABD-FP fusion to visualize F-actin in onion epidermal cells (Timmers *et al.* 2002). However, in animal, plant and yeast cells the plastin ABD-FP fusion labels only specific parts of the F-actin skeleton. Further these studies involved transient expression and so the cells forming a labeled skeleton did not have to divide. Therefore an evaluation of the plastin based constructs requires studies in stable transformed plants
Very promising ABP/ABD-FP fusions are based on Fimbrin 1 (AtFim1) (Ketelaar *et al.* 2004; Sheahan *et al.* 2004; Wang *et al.* 2004). These fusions were successfully used in stably transformed plants and allow the visualization of the more fine and dynamic

F-actin network even in root hairs. Up to now this fusion is the only described F-actin probe that does not disturb root hair growth when expressed at rather low levels, although it fails to decorate the fine, dynamic actin in the subapex of growing root hairs. Therefore Fimbrin might be less fit for visualizing F-actin filament dynamics in legume roots upon *Rhizobium* infection. So although F-actin visualization in plant cells is achieved to some extend, it is essential that it will be improved.

Acknowledgements We like to thank Jan Faix (Cell Biology department Planegg, Germany) for providing the Talin/cortexillin clones, Patrick Hussey (University of Durham, UK) for providing the ZmADF3 clone, Roger Tsien (Howard Hughes Medical Institute, University of California, San Diego) for providing the cameleon 2.1, Gunther Gerish (Max Planck Institute für Biochemie, Martinsried, Germany) for providing the DdAct15, Frans Ramaekers and Jos Broers for providing the EGFP-Hsßact and Andrea Jahrhaus for making the pEYFP(V68L/Q69K)-C1 clone.

Chapter 7

Innovative microscopy in living plant cells; GFP-based FRET microscopy in living plant cells

Published in modified form in Trends in Plant Science July 1999, Vol. 4, No. 7

Abstract

In vitro studies on isolated biomolecules are often difficult to extrapolate to *in vivo* function because of the complex organization of cells. On the other hand, *in vivo* study of molecular behaviour is technically demanding, as it requires sensitive methods to detect molecules with a high spatial resolution, and further they should not disturb cell performance. The combination of Green Fluorescent Protein (GFP) technology with Fluorescence Resonance Energy Transfer (FRET) offers the possibility to study interaction of molecules in living cells and is used to design vital sensors to detect for example Ca^{2+}. Here we showed for the first time that its feasible to use fluorescent protein based FRET in *Lotus japonicus* (Lotus) root hairs. The Yellow-cameleon-2 (Ycam2.0) FRET construct was used to image [Ca^{2+}] in Lotus root hairs. Ycam2.0 was placed under a root epidermis specific promoter (*PsRH2)* and expressed in *Agrobacterium rhizogenes* transformed roots of Lotus. Subsequently, calcium concentrations (Ycam2.0 FRET efficiencies), were imaged using Fluorescence Spectral Imaging Microscopy (FSPIM). This enabled us to visualize a calcium gradient at apex tip of growing root hairs. However the number of transgenic *Agrobacterium rhizogenes* transformed roots obtained was very low. This was probably caused by the fact that Ycam2.0 is toxic for plant cells above a certain threshold.

Keywords Hairy roots, *Lotus japonicus*, FLIM, FRET, FSPIM

Theodorus W.J. Gadella, Jr, Gerard N.M. van der Krogt and Ton Bisseling

Introduction

The fate and function of biomolecules in living plant cells is a challenging area of plant science. On the one hand, *in vitro* studies on isolated biomolecules are often difficult to extrapolate to *in vivo* function because of the complex organization and high degree of compartmentalization in living plant cells. On the other hand, the *in vivo* study of molecular function is technically demanding, as it requires the simultaneous capability of detecting molecules with high (subcellular) spatial resolution, high sensitivity, high specificity and yet with minimal perturbation of the cell state, in addition to obtaining information about the molecular state or molecular environment. The combination of green fluorescent protein (GFP) technology with fluorescence resonance energy transfer (FRET) microscopy offers these capabilities, and thereby creates new horizons for molecular plant cell biology, particularly in the field of signal transduction.

GFP and chromophore mutants

The GFP from the jellyfish *Aequorea victorea* is a 21 kDa apo-protein that spontaneously folds into a bright-green fluorescing structure. The gene encoding GFP can be expressed in many (non-jellyfish) cell types, enabling the use of GFP as a molecular marker for gene expression. By fusing the gene encoding GFP with a gene encoding an endogenous protein, and the subsequent expression of the chimera, fluorescent fusion proteins can be produced and targeted to specific subcellular organelles. Consequently, the fate of these fusion proteins and the organelle dynamics can be monitored in living plants at the single cell level with high specificity, sensitivity and spatial resolution, and with minimal perturbation of the cell. For example, the recent studies of Golgi-stack movements along endoplasmic reticulum strands (Boevink *et al.* 1998) and the use of GFP-fusion proteins for studying the dynamics of the actin (Kost *et al.* 1998) and tubulin (Marc *et al.* 1998) cytoskeleton in living plant cells. Nowadays, as a result of site-directed mutagenesis, GFPs come in many flavours, fluorescing at different colours, and codon usage has been optimized for plants (eliminating a cryptic splice site) (Haseloff *et al.* 1997). The chromophore of the wild-type GFP is formed from three amino acids (Ser65, Tyr66, Gly67) and mainly absorbs UV (397 nm) but also blue light (475 nm), and emits green fluorescence (505 nm). The most employed mutants are the enhanced green fluorescent protein, EGFP, which lacks the UV absorption of wild-type GFP; the blue fluorescent protein, BFP; the cyan fluorescent protein, CFP; and the most red-shifted, the yellow fluorescent protein, YFP (Box 1).

Box 1. Chromophore mutants of the green fluorescent protein (GFP)[a]

Essential amino acid substitutions, the resulting changed chemistry of the chromophore and the wavelengths for maximal absorbance and fluorescence are indicated.

- **Enhanced green fluorescent protein** (EGFP)
  Ser65 to Thr, Phe64 to Leu.
  Phenolate anion in chromophore.
  Absorbance/emission = 488/509 nm.
- **Yellow fluorescent protein** (YFP)
  Ser65 to Gly, Ser72 to Ala, Thr203 to Tyr.
  Phenolate anion in chromophore with stacked π-electron system (to Tyr203).
  Absorbance/emission = 514/527 nm.
  The addition of Val68 to Leu, Gln69 to Lys to YFP yields a more pH-insensitive (above pH 6.8) enhanced version of YFP with slightly red-shifted spectral properties:
  Absorbance/emission = 516/529 nm (Ref. 15).
- **Blue fluorescent protein** (BFP)
  Tyr66 to His, Tyr145 to Phe.
  Imidazole in chromophore.
  Absorbance/emission = 382/446 nm.
- **Cyan fluorescent protein** (CFP)
  Phe64 to Leu, Ser65 to Thr, Tyr66 to Trp, Asn146 to Ile, Met153 to Thr, Val163 to Ala, Asn212 to Lys.
  Indole in chromophore.
  Absorbance/emission = 434, 452/476, 505 nm.

[a]Some of the chromophore mutants of GFP are known under different names. Therefore, the abbreviations used here refer to chromophore mutant classes. For an overview of GFP chromophore mutants see Ref. 5.

In line with the applications mentioned already, the spectroscopic mutants of GFP can be used to perform double labelling or colocalization studies (Ellenberg *et al.* 1999). But the use of fluorescence resonance energy transfer (FRET) between these different GFPs is far more powerful, enabling the study of protein–protein interactions, protein conformational changes and proteolytic processing with high (subcellular) resolution and sensitivity in living cells.

The FRET principle

FRET is the phenomenon whereby a fluorescent molecule – the donor – transfers energy by a nonradiative (through space) mechanism to a neighbouring chromophore – the acceptor (Figure 1 and Box 2; for reviews see References (Wu *et al.* 1994; Clegg 1996)). The absorption spectrum of the acceptor chromophore must overlap with the fluorescence emission spectrum of the donor. When the spectral overlap is more extensive, the efficiency of the FRET process will be higher and consequently, FRET can occur over longer distances. FRET is highly dependent on the proximity between the donor and acceptor, and, in general, only occurs when the molecules are separated by <10 nm. It is characterized by the Förster radius (R_0; Figure 1).

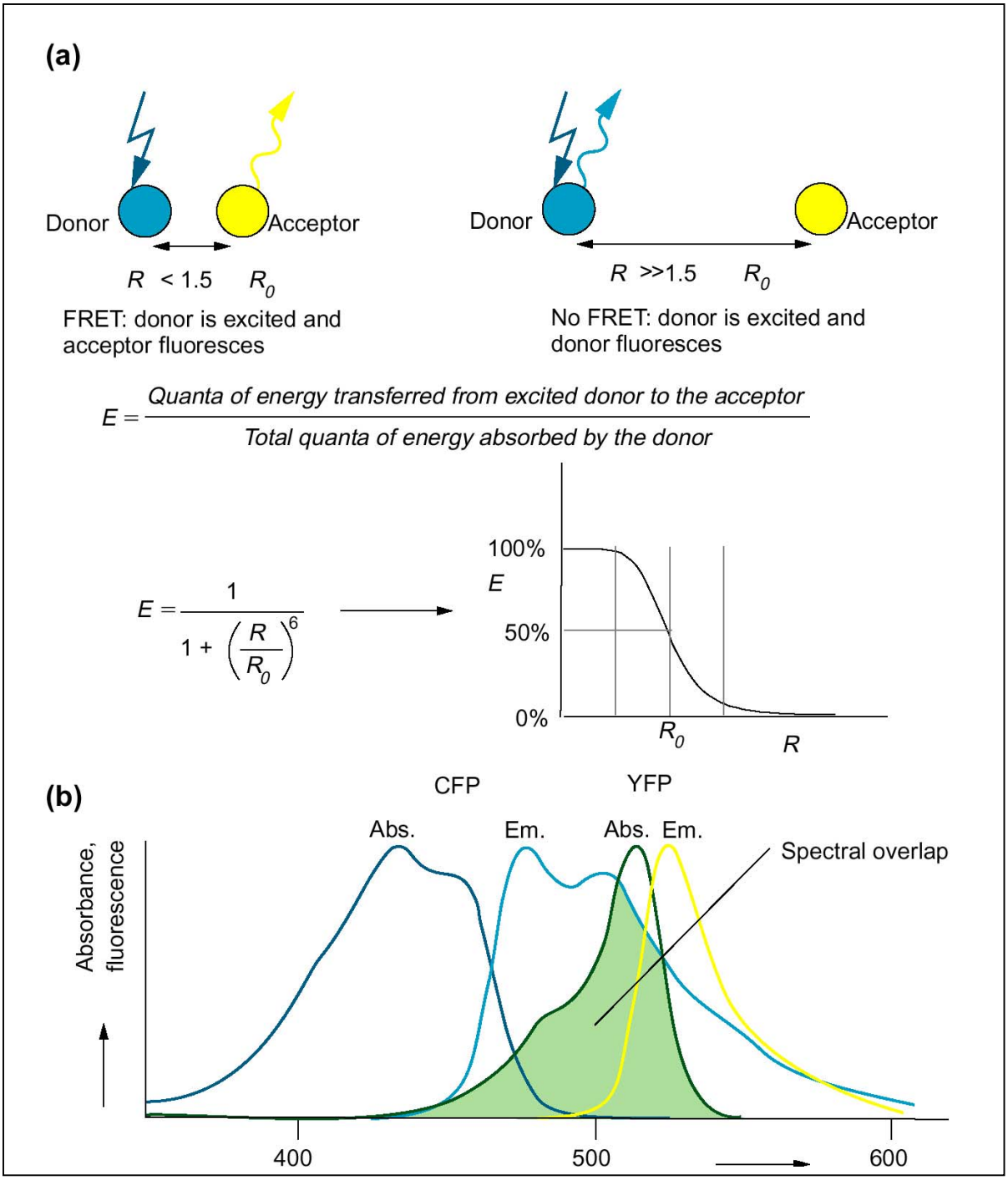

Figure 1. (**a**) Definition of fluorescence resonance energy transfer (FRET) and its relation to donor–acceptor proximity. R_0 = the Förster radius for energy transfer, generally between 3–6nm. The R_0 value is the distance between donor and acceptor at which the FRET efficiency (E) is 50% (i.e. 50% of the excitation energy absorbed by the donor is transferred to the acceptor). When donor and acceptor are separated by 1.5 x R_0 or more, the FRET efficiency is dropped to, 8%. When donor and acceptor are separated by <0.5 x R_0, the FRET efficiency is .98.5%. For this reason, FRET provides an excellent way of studying whether molecules indeed interact. (**b**) Prerequisites for FRET: (1) donor must be fluorescent; (2) there must be a spectral overlap between donor fluorescence and acceptor absorbance the spectral overlap for the cyan fluorescent protein (CFP) and the yellow fluorescent protein (YFP) is indicated in green; Abs., absorbance; Em., emission; (3) the distance between donor and acceptor must be <2 x R_0; (4) the angle between donor and acceptor transition moments should not be 90^0 ($k^2 \neq 0$, where k^2 = the dipole orientation factor). See References (Wu *et al.* 1994; Clegg 1996) for a quantitative description of R_0.

R_0 values for common donor–acceptor pairs (reviewed by (Wu *et al.* 1994)) usually vary between 3 and 6 nm and can be determined experimentally. They depend on the spectral overlap, the relative orientation of the donor and acceptor chromophores, and the quantum yield of the donor fluorophore (Clegg 1996). Chromophore-mutated GFPs show an excellent spectral overlap and, hence, good FRET pairs can be made using the available GFPs (Pollok *et al.* 1999). For example, the BFP is a good donor to the Ser65 to Thr-mutated EGFP. The R_0 value for this pair is 4.0–4.3 nm depending on the exact amino acid substitutions. Superior to the BFP–GFP pair is the use of the CFP–YFP pair, with an R_0 value of 4.9–5.2 nm depending on the choice of the types of CFP and YFP (Tsien 1998). With such high R_0 values, even at a separation of 8 nm between CFP and YFP, a 10% FRET efficiency can be observed. Furthermore, with the CFP–YFP FRET pair, cytotoxic UV excitation (required for the BFP–GFP pair) can be avoided.

FRET measurement

FRET is manifested by a decrease in the fluorescence intensity (or quantum yield) of the donor fluorophore. If the acceptor chromophore is a fluorophore, FRET will increase the fluorescence of the acceptor (the so-called sensitized emission). With digital imaging techniques it is possible to quantify the altered ratio of donor:acceptor fluorescence and to determine the FRET efficiency. However, the ratio of the measured donor:acceptor fluorescence intensity also depends on the microscope optics and the local relative concentrations of the donor and acceptor. Therefore the actual microscopic FRET measurements are rather complex, requiring (at least) three separate images, collected at different excitation and emission filter–wavelength combinations, and several instrumental correction factors (Gordon *et al.* 1998; van Rheenen *et al.* 2004). For many plant cell types another complicating factor is the direct absorption (or filtering) of fluorescence by chlorophyll pigments, which decreases blue fluorescence intensity (such as for BFP and CFP), which can be misinterpreted as a reduced donor fluorescence quantum yield caused by FRET. FRET also decreases the fluorescence lifetime (the average time that the molecule spends in the excited state) of the donor (Clegg 1996).

Box 2. How can FRET be quantified experimentally?

- The donor fluorescence intensity (or quantum yield) is reduced:

$$E = 1 - \frac{I_{D,+A}}{I_{D,-A}}$$

($I_{D,+A}$ Donor fluorescence in the presence of the acceptor; $I_{D,-A}$ donor fluorescence in the absence of the acceptor).

- The donor fluorescence lifetime (τ) is reduced:

$$E = 1 - \frac{\tau_{D,+A}}{\tau_{D,-A}}$$

($\tau_{D,+A}$ donor fluorescence lifetime in the presence of the acceptor; $\tau_{D,-A}$ donor fluorescence lifetime in the absence of the acceptor).

- The acceptor (if fluorescent) becomes more fluorescent (sensitized):

$$E = \frac{\varepsilon_A}{\varepsilon_D}\left(\frac{I_{A,+D}}{I_{A,-D}} - 1\right)$$

($I_{A,+D}$ acceptor fluorescence in the presence of the donor; $I_{A,-D}$ acceptor fluorescence in the absence of the donor; ϵ_D and ϵ_A are the extinction coefficients of the donor and acceptor at a wavelength where both the donor and acceptor absorb. Note that donor fluorescence must be subtracted to get $I_{A,+D}$).

Unlike fluorescence intensity, the fluorescence lifetime (or τ) is not dependent on local chromophore concentration, direct absorption of donor fluorescence (e.g. by

chlorophyll) or on (moderate levels of) photobleaching, and consequently provides quantitative information about the FRET efficiency. For this reason, fluorescence lifetime imaging microscopy (FLIM; Figure 2), producing high resolution micrographs in which each pixel value represents the local fluorescence lifetime, is ideal for studying FRET in single cells (Gadella *et al.* 1995; Bastiaens *et al.* 1999; Gadella 1999).

Yellow-cameleon-2 fusion protein

The Yellow-cameleon-2 (Ycam2.0) fusion protein was developed as a calcium indicator (Miyawaki *et al.* 1997). In addition to CFP and YFP units at either end of the molecule, the fusion protein also contains the calcium binding protein calmodulin and the M13 calmodulin-binding protein. Upon binding calcium to the calmodulin part of the molecule, the M13 unit binds to the calmodulin unit, inducing a significant change in the distance or relative orientation of the CFP and YFP cylinders at the ends of the molecule (Figure 3b). As a result, the FRET efficiency from CFP to YFP increases upon calcium binding (Miyawaki *et al.* 1997; Miyawaki *et al.* 1999). Because the acceptor:donor molecular ratio in cameleon is always 1:1 (because they are fused into one protein), the YFP:CFP fluorescence intensity ratio can be directly related to the cytosolic calcium concentration. The Ycam indicator is responsive to calcium in living cells of intact plants (Figure 2).

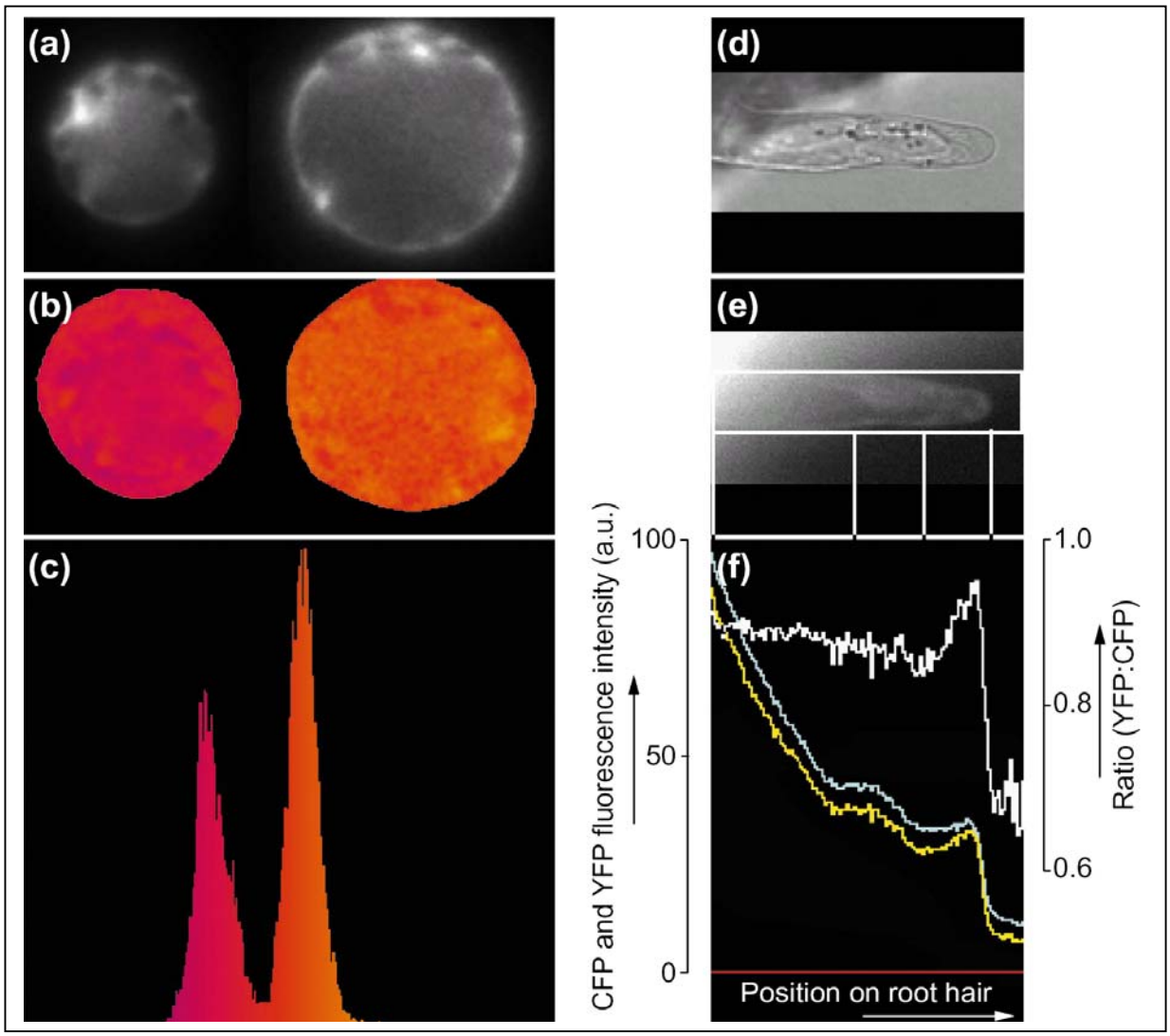

Figure 2. Fluorescence resonance energy transfer (FRET) microscopy in yellow-cameleon. (Ycam) (**a–c**) Fluorescence lifetime imaging microscopy (FLIM) analysis of the cyan fluorescent protein (CFP) fluorescence of living Cowpea (*Vigna unguiculata*) mesophyll protoplasts expressing Ycam2.0 , a fusion protein containing both CFP and yellow fluorescent protein (YFP) (left protoplast) or expressing unfused cytosolic CFP (right protoplast). Only the CFP fluorescence emission is monitored. (**a**) Fluorescence intensity image, (**b**) fluorescence lifetime image, (**c**) temporal histogram and pseudocolour scale of the fluorescence lifetime pixel values of (**b**). The left protoplast was transfected with Ycam2.0 (Miyawaki *et al.* 1997) under a modified 35S promoter using the pMON dicot expression vector (see Chapter 2). The right protoplast was transfected using the same vector but containing only CFP (Phe64 to Leu, Ser65 to Thr, Tyr66 to Trp, Asn146 to Ile, Met153 to Thr, Val163 to Ala, Asn212 to Lys). The protoplasts were excited using the 457 nm argon-ion laser line modulated at 40 MHz, and the CFP fluorescence was selectively imaged using a 470–500 nm bandpass emission filter (the microscope set up, lifetimeimage calculation and image processing are described in (Gadella 1999). From the pseudocoloured lifetime images, it can be inferred that the CFP lifetime of the cameleon-fusion protein is about 2.1 ns (= 2.1 x 10^{-9} s) whereas the CFP lifetime of unfused CFP is 2.6 ns. The reduced CFP lifetime in the Ycam is caused by intramolecular FRET, occurring at an efficiency of ~25% (Box 2). This example clearly shows that fluorescence lifetimes can be very accurately measured in living plant cells and that they are independent of the local fluorophore concentration. (**d–f**) Fluorescence spectral imaging microscopy (FSPIM) analysis of Ycam2.0 expressed in root hairs of *Lotus japonicus* (Lotus). (**d**) Phase contrast image of the root hair, (**e**) fluorescence intensity image and (f) the profile plots over the root hair axis of the CFP (cyan) and YFP (yellow) intensity and the YFP:CFP ratio (white). The roots were transformed using *Agrobacterium rhizogenes* (see Chapter 2) carrying the Ycam2.0 gene under the *PsRH2* root epidermis specific promoter (see Chapter 2). The root was excited using a mercury lamp and a 430–440 nm bandpass filter. The fluorescence emission was filtered through a 455 nm longpass filter and transferred on to a Chromex (Albuquerque, NM, USA) 250IS imaging spectrograph coupled to a Photometrics (Tucson, AZ, USA) CH250 CCD camera providing spatially resolved (along the root hair axis) fluorescence emission spectra. The entrance slit of the spectrograph is superimposed on (**e**). The CFP, YFP and autofluorescence spectral components were calculated from the multicomponent spectra using a linear four-component spectral-fitting procedure, similar to a procedure described in (Gadella *et al.* 1997). The vertical lines drawn between (**e**) and (**f**) indicate the border of the entrance slit, the left and right borders of the nucleus and the tip of the root hair, respectively. As expected, the YFP:CFP fluorescence ratio, which is directly related to the cytosolic calcium concentration, is independent of the relative abundance of the fluorescent indicator. This can be seen by comparing the plot profiles of the CFP and YFP fluorescence intensity with the ratio plot profile.

The roots of Lotus plants have been transformed with the Ycam2.0 construct and the CFP and YFP-fluorescing components measured as a function of distance over the axis of a young, growing root hair by fluorescence spectral imaging microscopy (FSPIM) (Gadella *et al.* 1997). Polar growth at the root hair tip is regulated by a local increased calcium concentration (Wymer *et al.* 1997). Indeed, the ratio of YFP:CFP fluorescence increases significantly towards the root hair tip (Figure 2). This reflects an increased calcium concentration inducing an enhanced FRET efficiency in the cameleon molecule.

Outlook

Of course, GFP-based FRET indicators can be used for many other purposes (Figure 3).

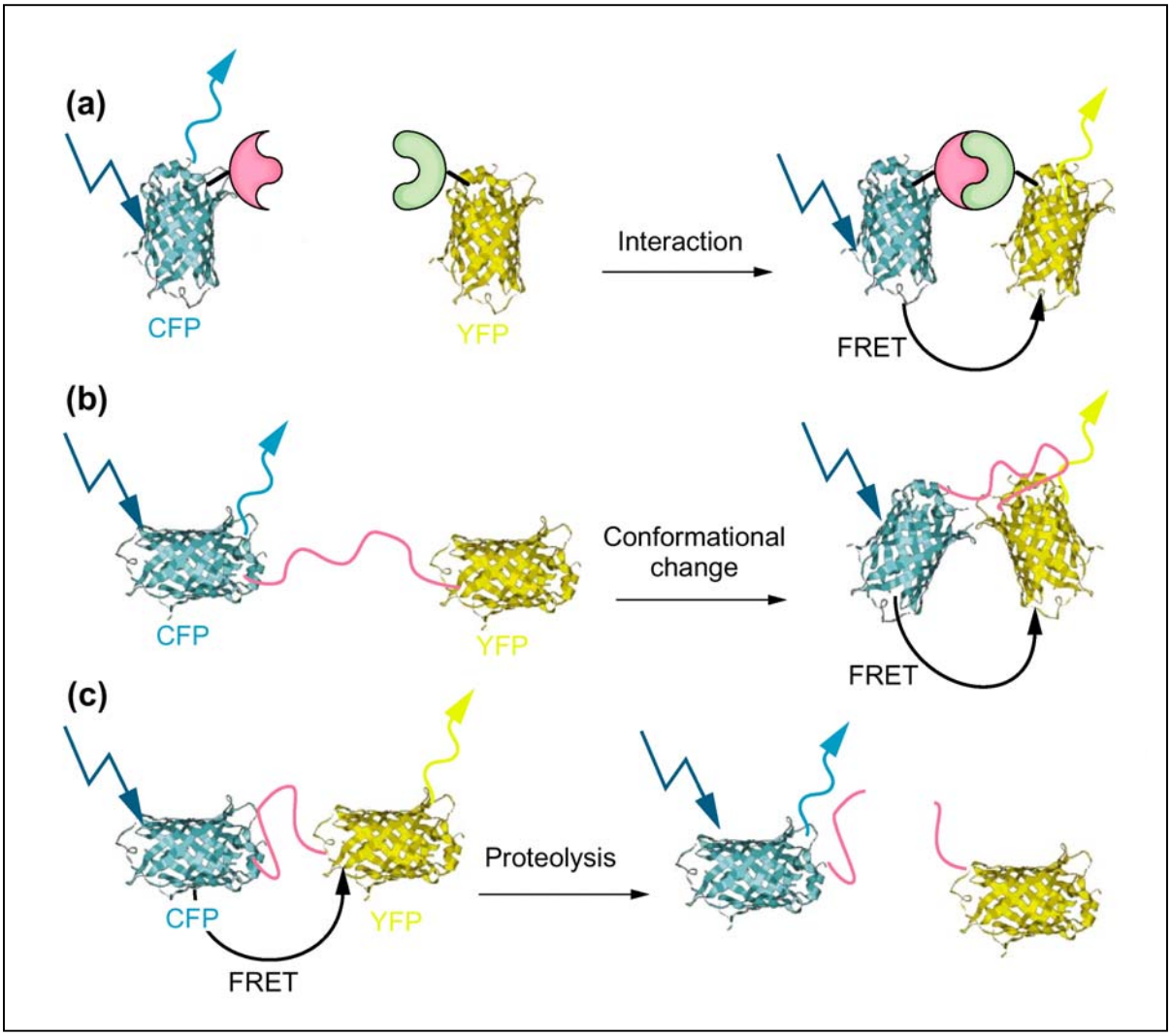

Figur 3. Possible use of green fluorescent protein (GFP)-based fluorescence resonance energy transfer (FRET) microscopy indicators. (**a**) Protein–protein interactions. (**b**) Monitoring of the conformational state of fusion proteins. (**c**) Proteolytic cleavage of fusion proteins. Abbreviations: CFP, cyan fluorescent protein; YFP, yellow fluorescent protein; dark blue arrow indicates excitation; cyan and yellow arrows indicate fluorescence; non-CFP or YFP fusion-proteins are represented in pink and green.

Firstly and most importantly, FRET can be used for monitoring protein–protein interactions. Two separate fusion proteins – one containing CFP and the other, its putative interacting partner containing YFP – are co-expressed in the plant cell type of choice (i.e. by using appropriate promoters). If intermolecular FRET is detected, it provides direct proof of the close proximity (i.e. <8 nm) of the CFP and YFP cylinders and consequently of the existence of the protein–protein interaction. Because, in general, the relative abundance of donor and acceptor for co-transformations is unknown or variable depending on the subcellular location, FLIM would be the most suitable technique for studying intermolecular FRET (Bastiaens and Squire 1999; Gadella 1999). This strategy was successful for demonstrating the interaction between the CFP–calmodulin and the M13–YFP fusion proteins in mammalian cells (Miyawaki et al. 1997), and the interaction between the Bcl-2 and the Bax mitochondrial proteins using BFP and GFP fusions (Mahajan 1998). The attractive

features of the microscopic measurement of FRET, are that, in addition to studying whether proteins do interact, it is possible to determine:

- If the interaction changes with time (because the FRET measurement is non-destructive).
- To what extent the proteins do interact.
- Where they interact (which cell types and at what subcellular location).

Another advantage of the method is that researchers are no longer restricted to the artificial nuclear environment (in another species) as they are for the yeast two-hybrid screening method. The second area of application is the study of molecular conformational changes, such as the Ycam (Miyawaki et al. 1997; Miyawaki et al. 1999). The strategy is to construct a sandwich-like fusion of CFP, a protein of interest and YFP. It is essential that the protein of interest can be induced to undergo a conformational change that alters the proximity and/or relative orientation of the CFP and YFP cylinders, changing the intramolecular FRET efficiency. Ligand or ion-binding domains of receptors or channels are interesting protein candidates, or, for instance, protein sequences with a phosphorylation site. Using such fusion proteins, ligand or ion-binding, or phosphorylation can be studied in living plant cells with high spatial resolution by monitoring (local) alterations in FRET-efficiency. The third area of application is the study of proteolytic processing of proteins *in vivo*. Again, a tandem fusion of CFP–YFP (or BFP–GFP) and a protein of interest (or part thereof) is constructed (Pollok and Heim 1999). When the protein of interest is intact, FRET can be observed, but as soon the protein becomes cleaved and the parts dissociate, FRET is lost. The approach has proved useful for studying proteolytic processing in living mammalian cells during apoptosis (Xu 1998). As with any technique there are potential sources that can introduce artefacts. For instance, the pH-sensitivity of some of the GFPs (especially the YFP with a pK of near 6.9) might cause problems, restricting their applicability to subcellular areas with a pH >7 (i.e. not in vacuoles). Therefore the pH sensitivity of YFP was reduced significantly by introducing an extra mutation (Gln69Arg) (Miyawaki et al. 1999). However, as described by others, the pH sensitivity of certain GFP variants can be utilized to provide subcellular targetable pHindicators (Miesenbock et al. 1998). Another obvious problem can be the bulkiness of the CFP–YFP cylinders (2 x 3 nm), which might yield inactive or incorrectly folded fusion proteins. In spite of the many successful bioactive fusion GFP-proteins published to date, there is no guarantee that novel fusion proteins are biofunctional. Hence, the FRET-approach for monitoring protein–protein interactions outlined here must include separate checks for the biofunctionality of the interacting fusion proteins. This prohibits the use of the FRET method as a quick screening method like the yeast two-hybrid system. The main advantage of the GFP-based FRET indicators is that they employ the machinery of the plant cell for their synthesis and subcellular targeting. By using cell-type specific promoters (see Chapter 2) and/or fusion to targeting sequences, the indicators can be produced specifically in the cell type and subcellular location of choice. Hence the potential for studying dynamic cell biological processes, such as intracellular signalling, is much greater than for microinjected or passively loaded chemical fluorescent indicators, which are usually restricted to the cytoplasm of the outer cell layers of the plant. Therefore, in spite of the fact that the experiments shown in Figure 2 represent only the first described *in vivo* FRET measurements between CFP and YFP in plants, the future potential is extensive.

Additional comments

Here we describe the successful use of Ycam to visualize the Ca^{2+} gradient at the apex of growing Lotus root hairs. Although this experiment provides the prove of principle that Ycam can be used to visualize Ca^{2+} in root hairs, it turned out to be difficult to use it in the *Rhizobium*-legume interaction. We did several transformation experiments with Medicago (*Medicago truncatula*) and Lotus (*Lotus japonicus*) and for both species we obtained only a limited number of transgenic roots in which Ycam was visible; for Medicago 1 out of 40 plants- (~400 roots) and for Lotus respectively, 1 out of 60 plants (~600 roots). These roots were obtained by *A. rhizogenes* based root transformation. Although these roots can be kept in culture, such cultured roots cannot be used for *Rhizobium*-root interaction studies. Therefore transgenic roots obtained in this way can only be used in a single experiment. The very low number of transgenic roots in which Ycam is visible, indicates that the window in which Ycam is detectable and not toxic to the cells is very narrow. Toxicity could be caused by the calmodulin moiety of Ycam that can interact with numerous endogenous proteins, for example kinases and ion channels. In addition calmodulin binds Ca^{2+} by which it can affect the concentration of this second messenger in the cell. For these reasons it is very likely that Ycam is toxic for cells and can only be present below a certain concentration (Heim and Griesbeck, 2004). Our data are consistent with studies of Downie and Oldroyd (pers. com.). They have made a stable transformant of Medicago using a similar Cameleon construct and only obtained a single transformant with detectable Cameleon fluorescence. The relatively low number of papers reporting the successful use of Cameleon in plants and mammals also suggest a negative effect of Cameleon on the viability of cells.
The low efficiency by which Ycam transformed roots can be obtained implies that *A. rhizogenes* based root transformations is not very useful to study Ca^{2+} in living cells during the *Rhizobium* legume interaction. It will be far more attractive to make a stably transformed plant line as this can be used in multiple experiments. A second disadvantage of hairy roots is the relatively large size of the composite plants by which they are difficult to handle during microscopy. For this reason imaging of early responses during the *Rhizobium* root hair interactions should preferably be done with stably transformed lines.

Acknowledgements We gratefully acknowledge the kind donation of the Ycam2.0 construct by Dr R.Y. Tsien (Howard Hughes Medical Institute, University of California, San Diego, USA).

Chapter 8

Concluding remarks

Gerard N.M. van der Krogt and Ton Bisseling

The aim of this thesis is to explore the potential of *in vivo* imaging to obtain insight in the early stages by which the *Rhizobium*-legume symbiosis is established.
The *Rhizobium*-legume symbiosis starts in root epidermal cells especially in root hairs. In these cells subcellular changes are induced by Nod factors that are secreted by the rhizobia. Since these root hair cells are well accessible for microscopy, our studies have been primarily focused on these cells. Important Nod factor induced responses are $[Ca^{2+}]$ influx at root hair tips, $[Ca^{2+}]$ spiking around and in the nucleus and changes in the actin configuration (Cárdenas *et al.* 1999; Ehrhardt *et al.* 1996; Wais *et al.* 2000; Walker *et al.* 2000; Ruijter *et al.* 1999). Therefore our exploring studies have been focused on imaging of $[Ca^{2+}]$ and the actin skeleton.
Currently, the majority of vital reporters is derived from fluorescent proteins (FPs) and the genes encoding such reporters are introduced in the genome of the cells /organisms that are studied. Therefore a major prerequisite for such studies is an efficient transformation procedure.

Transformation
We have tested the *Agrobacterium rhizogenes* root (hairy root) transformation procedure, as it is markedly faster than the *Agrobacterium tumefaciens* based transformation. *A. rhizogens* transformation has been shown to be an important tool to study the *Rhizobium*-legume interaction (Smit *et al.* 2005; Limpens *et al.* 2003).
In this thesis it is shown that both Lotus (*Lotus japonicus*) and Medicago (*Medicago truncatula*) can be transformed with a high frequency. In both cases co-transformation efficiencies of 80%. can be reached. Further, transgenic roots are obtained relatively fast as the first co-transformed roots are available within 4 weeks. Since each root is in general the result of an individual tansformation event and expression levels of the transgene varies per root, a collection of roots is obtained that mimics an “allelic series”. These characteristics show that this transformation procedure has in principle the potential to be a useful tool in studying the early responses induced by Nod factor.
The importance of this transformation procedure is underlined by studies that do not have to provide insight in the real time dynamics of a process. For example it has been shown to be an efficient tool to:

- determine the sub cellular location of GFP tagged proteins (examples are *NSP1*, *NSP2*, *DMI2*, *DMI1* and *DMI3*) (Smit *et al.* 2005; Kalo *et al.* 2005; Ane *et al.* 2004; Endre *et al.* 2002; Levy *et al.* 2004; Mitra *et al.* 2004)
- complement mutants disturbed in the symbiosis, for example (Smit *et al.* 2005; Kalo *et al.* 2005).
- determine RNAi induced phenotypes (especially when knock-down phenotypes accumulate in the root (like aberrant and aborted infection threads in *Lyk3* and *DMI2* knock down) (Limpens *et al.* 2003).

In contrast to the above-mentioned successes, our studies showed that the *A. rhizogenes* root transformation is sub-optimal for studies on dynamic processes during early stages of the *Rhizobium*-legume. A principle problem is the morphology of the transgenic roots formed from the callus at the site of transformation. In general, imaging of responses induced by Nod factors, can be best performed in a liquid environment, for example in a Fahråeus slide-like container (Fåhreaeus 1957). The traditional Fahråeus assay starts with 2-day-old seedlings that have been germinated in a special way by which the small roots are very straight and can be efficiently transferred to Fahråeus slides. The root hairs of such seedlings are also located in clear zones, encompassing just emerging - to full-grown root hairs. In addition these root hairs are also very straight. This in contrast to *A. rhizogenes* induced roots, which are long, have a wavy morphology and an altered morphology of the root hairs. It turned out to be difficult (but not impossible) to use these roots for real time imaging. Also due to the large size of the Medicago shoots that formed the *A. rhizogenes* induced roots hampers good handling on the microscope stage. However, trimming of the shoot is no option as this blocks normal nodule formation on *A. rhizogenes* induced as well as untransformed roots (Ramos and Bisseling 2003).
The constructs that we tested in *A. rhizogenes* induced roots, the [Ca^{2+}] reporter Cameleon (Nagai *et al.* 2000; Miyawaki *et al.* 1997), resulted in a very low frequency of roots expressing the transgene. Such reporters can most likely only be expressed below a certain concentration as they influence the biological system. Cameleon for example has the potential to buffer the Ca^{2+} concentration. But on top of this the calmodulin and the M13 calmodulin-binding domain could also perturb functioning of the endogenous calmodulins or calmoduline binding proteins (Heim and Griesbeck 2004). Therefore it seems probable that the expression level has to be within a narrow concentration window allowing imaging and not affecting root hair growth. This hypothesis is supported by the low frequency of co-transformation that we observed as well as that *A. tumefaciens* based transformation of Medicago with a Cameleon construct only resulted in a single line in which Ca^{2+} could be imaged (Allen Downie pers. comm.). Similar low (or even lower) *A. rhizogenes* based transformation frequencies were obtained by us with ROP GTPases, actin and actin binding protein based constructs.
To obtain a sufficient number of seeds of an *A. tumefaciens* transformed Medicago will take about 1.5 year. Although this is a relatively long period, our experience with *A. rhizogenes* transformed roots indicated that this will be a better approach. First transgenic Medicago‘s in which the reporter does not affect root (hair) development while imaging is possible might be difficult to obtain. However, a single success can be used “indefinitely”. However, *A. rhizogenes* transformed roots can still be useful to get a first clue which kind of reporter and which variants might be worthwhile for studies in stable transformants.

Inducible promoters
In both, *A. rhizogenes* as well as *A. tumefaciens* based transformation it will be attractive to have inducible promoters available. In either case regeneration of root/embryo’s does involve a callus phase. Therefore it will be important to extend studies on inducible promoters to the callus phase. Of the promoters tested here the ethanol inducible promoter system has the highest potential to be <u>not</u> auto-induced in the callus phase and therefore the best nominee for future use.

Final conclusions

Vital imaging will be of increasing importance as is illustrated by recent localization studies (Kalo *et al.* 2005; Smit *et al.* 2005). For example the Lotus DMI homologs (Castor and Pollex) seem to be located in plastids and in case this true, Nod factor signaling will move from plasmamembrane, to plastids, to nuclei. Further the location of the primary transcription factor NSP2 is in the ER surrounding the nucleus. After application of Nod factor NSP2-FP diminishes in the nuclear envelope and increases in the nucleus. However, it is not possible yet to differentiate between the retargeting or newly synthesized NSP2 or a reallocation of the old protein. However, new FP variants PA-FP (Photo Activatable Fluorescent Protein) or the fluorescent timer, DsRED-E5 (Patterson *et al.* 2002; Mirabella *et al.* 2004) might allow approaches to tackle such questions.

References

Adams, S. R., A. T. Harootunian, Y. J. Buechler, S. S. Taylor and R. Y. Tsien (1991). "Fluorescence ratio imaging of cyclic AMP in single cells." Nature 349: 694-7.

Allison, L. A., G. B. Kiss, P. Bauer, M. Poiret, M. Pierre, A. Savoure, E. Kondorosi and A. Kondorosi (1993). "Identification of two alfalfa early nodulin genes with homology to members of the pea Enod12 gene family." Plant Molecular Biology 21: 375-80.

Ane, J.M., G.B. Kiss, B.K. Riely, R.V. Penmetsa, G.E. Oldroyd, C. Ayax, J. Levy, F. Debelle, J.M. Baek, P. Kalo, C. Rosenberg, B.A. Roe, S.R. Long, J. Denarie, D.R. Cook. (2004). "Medicago truncatula DMI1 required for bacterial and fungal symbioses in legumes." Science 303(5662): 1364-7.

Andersen, S. U., C. Cvitanich, B. K. Hougaard, A. Roussis, M. Gronlund, D. B. Jensen, L. A. Frokjaer and E. O. Jensen (2003). "The glucocorticoid-inducible GVG system causes severe growth defects in both root and shoot of the model legume *Lotus japonicus*." Plant-Microbe Interactions 16(12): 1069-76.

Aoyama, T. and N. H. Chua (1997). "A glucocoticoid-mediated transcriptional induction system in transgenic plants." The Plant Journal 11(3): 605-12.

Bader, J. E. and A. G. Beck-Sickinger (2004). "Fluorescence resonance energy transfer to study receptor dimerization in living cells." Methods in Molecular Biology 259: 335-52.

Baird, G. S., D. A. Zacharias and R. Y. Tsien (1999). "Circular permutation and receptor insertion within green fluorescent proteins." Proceedings of the National Academy of Sciences of the USA 96(20): 11241-6.

Baird, G. S., D. A. Zacharias and R. Y. Tsien (2000). "Biochemistry, mutagenesis, and oligomerization of DsRED, a red fluorescent protein from coral." Proceedings of the National Academy of Sciences of the USA 97(22): 11984-89.

Ballestrem, C., B. Wehrle-Haller and B. Imhof (1998). "Actin dynamics in living mammalian cells." Journal of cell science 111: 1649-58.

Bastiaens, P. I. H. and A. Squire (1999). "Fluorescence lifetime imaging microscopy: spatial resolution of biochemical processes in the cell." Trends in Cell Biology 9: 48–52.

Bauchrowitz, M. A., D. G. Barker and G. Truchet (1996). "Lectin genes are expressed throughout root nodule development and during nitrogen-fixation in the *Rhizobium-Medicago* symbiosis." The Plant Journal 9: 31-43.

Baumberger, N., C. Ringli and B. Keller (2001). "The cimeric leucine-rich repeat/extensin cell wall protein LRX1 is required for root hair morphogenesis in *Arabidopsis thaliana*." Genes and Development 15(9): 1128-1139.

Beilmann, A., K. Albrecht, S. Schultze, G. Wanner and M. Pfitzner (1992). "Activation of a truncated PR-1 promoter by endogenous enhancers in transgenic plants." Plant Molecular Biology 18: 65-78.

Benfey, P. N., L. Ren and N.-H. Chua (1989). "The CaMV35S enhancer contains at least two domains which can confer different developmental and tissue-specific expression patterns." EMBO Journal 8: 2195-202.

Bevan, M. W. (1984). "Binary agrobacterium vectors for plant transformation." Nucleic Acids Research 12: 8711-21.

Bladergroen, M. R. and H. P. Spaink (1998). "Genes and signal molecules involved in the rhizobia-leguminoseae symbiosis." Curr. Opin. Plant Biol. 1(4): 353.

Boevink, P., K. Oparka, S. Santa Cruz, B. Martin, A. Betteridge and C. Hawes (1998). "Stacks on tracks: the plant Golgi apparatus traffics on an actin/ER network." The Plant Journal 15(3): 441-7.

Boisson-Dernier, A., M. Chabaud, F. Garcia, G. Becard, C. Rosenberg and D. G. Barker (2001). "Agrobacterium rhizogenes-Transformed roots of *Medicago truncatula* for the study of nitrogen-fixing and endomycorrhizal symbiotic associations." Molecular Plant-Microbe Interactions 14(6): 695-700.

Bokhoven, H., J. Verver, J. Wellink and A. Kammen (1993). "Protoplasts transiently expressing the 200K coding sequence of cowpea mosaic virus B-RNA support replication of m-RNA." Journal of General Virology 74: 2233-41.

Bokman, S. H. and W. W. Ward (1981). "Renaturation of *Aequorea victoria* green-fluorescent protein." Biochemical and Biophysical Research Communications 101: 1372-80.

Bucher, M., S. Brunner, P. Zimmermann, G. I. Zardi, N. Amrhein, L. Willmitzer and J. W. Riesmeier (2002). "The expression of an extensin-like protein correlates with cellular tip growth in tomato." Plant Physiology 128: 911-23.

Caddick, M. X., A. J. Greenland, I. Jepson, K. P. Krause, N. Qu, K. V. Riddell, M. G. Salter, W. Schuch, U. Sonnewald and A. B. Tomsett (1998). "An ethanol inducible gene switch for plants used to manipulate carbon metabolism." Nature Biotechnology 16: 177-80.

Caitoira, R., C. Galera, F. de Billy, R. V. Penmetsa, E. P. Journet, F. Maillet, C. Roosenberg, D. Cook, C. Gough and J. Denarie (2000). "Four genes of *Medicago truncatula* controlling components of a Nod factor transduction pathway." Plant Cell 12: 1647-65.

Caitoira, R., A. C. J. Timmers, F. Maillet, C. Galera, R. V. Penmetsa, D. Cook, J. Denarie and C. Gough (2001). "The *HCL* gene of *Medicago truncatula* controls *Rhizobium*-induced roothair curling." Development 128: 1507-18.

Callaham, D. A. and J. G. Torrey (1981). "The structural basis of infection of root hairs of *Trifolium repens* by *Rhizobium*." Canadian Journal of Botany 59: 1647-64.

Campbell, R. E., O. Tour, A. E. Palmer, P. A. Steinbach, G. S. Baird, D. A. Zacharias and R. Y. Tsien (2002). "A monomeric red fluorescent protein." Proceedings of the National Academy of Sciences of the USA 99: 7877-82.

Cárdenas, L., J. A. Feijo, J. G. Kunkel, F. Sanchez, T. Holdaway-Clarke, P. K. Hepler and C. Quinto (1999). "*Rhizobium* nod factors induce increases in intracellular free calcium and extracellular calcium influxes in bean root hairs." The Plant Journal 19(3): 347-52.

Cárdenas, L., Vidali, L., Dominguez, J., Perez, H., Sanchez, F., Hepler, P. K. and C. Quinto (1998). "Rearrangement of Actin Microfilaments in Plant Root Hairs Responding to *Rhizobium etli* Nodulation Signals." Plant Physiology. 116: 871-7.

Catoira, R., C. Galera, F. de Billy, R. V. Penmetsa, E. P. Journet, F. Maillet, C. Rosenberg, D. Cook, C. Gough and J. Denarie (2000). "Four genes of *Medicago truncatula* controlling components of a nod factor transduction pathway." Plant Cell 12: 1647-65.

Chabaud, M., Larsonneau, C., Marmouget, C. and T. Huguet (1996). "Trasformation of barrel medic (*Medicago truncatula Gaertn.*) by *Agrobacterium tumefaciens* and regeneration via somatic embryogenesis of transgenic plants with the *MtEnod12* nodulin promoter fused to the *gus* reporter gene." Plant Cell Reports 15: 305-10.

Chalfie, M., Y. Tu, G. Euskirchen, W. W. Ward and D. C. Prasher (1994). "Green fluorescent protein as a marker for gene expression." Science 263: 802-5.

Chang-Jie, J., A. G. Weeds and P. J. Hussey (1997). "The maize actin-depolymerizing factor, ZmADF3 redistributes to the growing tip of elongating root hairs and can be induced to translocate into the nucleus with actin." The The Plant Journal 12(5): 1035-43.
Chen, S., D. Hofius, U. Sonnewald and F. Bornke (2003). "Temporal and spatial control of gene silencing in transgenic plants by inducible expression of double-stranded RNA." The Plant Journal 36: 731-40.
Cheng, H. P. and G. C. Walker (1998). "Succinoglycan is required for initiation and elongation of infection threads during nodulation of alfalfa by *Rhizobium* meliloti." Journal of Bacteriology 180(19): 5183-91.
Cheung, A. Y. and H. M. Wu (2004). "Over expression of an Arabidopsis formin stimulates supernumerary actin cable formation from pollen tube cell membrane." Plant Cell 16(1): 257-69.
Chiang, C. C. and L. A. Hadwiger (1990). "Cloning and characterization of a disease resistance response gene in pea inducible by Fusarium solani." Molecular Plant-Microbe Interactions 3: 78-85.
Chiodas, A., A. Jungbluth, A. Sechi, J. Murphy, A. Ulrich and G. Marriott (1998). "The suitability and application of a GFP-actin fusion protein for long-term imaging of the organization and dynamics of the cytoskeleton in mammalian cells." European Journal of Cell Biology 77: 81-90.
Choi, C. Q. and S. Nash (2004). "GloFish draw suit; Watchdog groups want FDA to regulate first genetically modified pet in US." The Scientist: http://www.biomedcentral.com/news/20040107/01.
Clegg, R. M. (1996). Fluorescence resonance energy transfer, in *Fluorescence Imaging Spectroscopy and Microscopy*, John Wiley & Sons.
Cody, C. W., D. C. Prasher, W. M. Westler, F. G. Prendergast and W. W. Ward (1993). "Chemical structure of the hexapeptide chromophore of the *Aequorea* green-fluorescent protein." Biochemistry 32: 1212-18.
Cook, D. R. (1999). "*Medicago truncatula* - a model in the making!" Curr. Opin. Plant Biol.. 2: 301-304.
Cullen, B. R. (1987). "Use of eukaryotic expression technology in the functional analysis of cloned genes." Methods in Enzymology 152: 684-704.
Dandie, C. E., S. M. Thomas and N. C. McClure (2001). "Comparison of a range of green fluorescent protein-tagging vectors for monitoring a microbial inoculant in soil." Letters of Applied Microbiology 32(1): 26-30.
Davenport, D. and J. A. C. Nicol (1955). "Luminesence in Hydromedusae." Proceedings of the Royal Society of London 144: 399-411.
Davidson, A. L. and W. Newcomb (2001). "Changes in actin microfilament arrays in developing pea root nodule cells." Canadian Journal of Botany 79: 767-76.
Davis, S. J. and R. D. Vierstra (1998). "Soluble, highly fluorescent variants of green fluorescent protein (GFP) for use in higher plants." Plant Mol Biol 36(4): 521-8.
Deveaux, Y., A. Peaucelle, G. R. Roberts, E. Coen, R. Simon, Y. Mizukami, J. Traas, J. A. H. Murray, J. H. Doonan and P. Laufs (2003). "The ethanol switch: a tool for tissue-specific gene induction during plant development." The Plant Journal 36: 918-30.
Diaz, C. L., L. S. Melchers, P. J. J. Hooykaas, B. J. J. Lugtenberg and J. W. Kijne (1989). "Root lectine as a determinant of host-plant specificity in the *Rhizobium*-legume symbiosis." Nature 338: 579-81.
Dong, C.-H., B. Kost, G. Xia and N.-H. Chua (2001). "Molecular identification and characterization of the Arabidopsis AtADF1, AtADF5 and AtADF6 genes." Plant Molecular Biology 45: 517-27.
Doyle, T. and D. Botstein (1996). "Movement of yeast cortical actin cytoskeleton visualized in vivo." Proceedings of the National Academy of Sciences of the USA 93: 3886-91.
Drew, C. D. (1997). "Oxygen deficiency and root metabolism: Injury and acclimation under hypoxia and anoxia." Annual Review of plant physiology and Plant Molecular Biology 48: 223-50.
Ehrhardt, D. W., E. M. Atkinson and S. R. Long (1992). "Depolarization of alfalfa root hair membrane potential by *Rhizobium meliloti* Nod factors." Science 256(5059): 998-1000.
Ehrhardt, D. W., R. Wais and S. R. Long (1996). "Calcium spiking in plant root hairs responding to *Rhizobium* nodulation signals." Cell 85(5): 673-81.
Ellenberg, J., J. Lippincott-Schwartz and J. F. Presley (1999). "Dual-colour imaging with GFP variants." Trends in Cell Bilogy 9: 52-56.
Endre G., A. Kereszt, Z. Kevei, S. Mihacea, P. Kalo, G.B. Kiss. (2002). "A receptor kinase gene regulating symbiotic nodule development." Nature 417(6892): 910-1.
Engelen, F. A., J. W. Molthoff, A. J. Conner, J. P. Nap, A. Pereira and W. J. Stiekema (1995). "pBINPLUS; an improved plant transformation vector based on pBIN19." Transgenic Research 4: 288-90.
Esseling, J., F. G. P. Lhuissier and A. M. C. Emons (2003). "Nod Factor induced root hair curling: Continuous polar growth towards the point of Nod Factor application." Plant Physiology 132: 1982-88.
Esseling, J., N. Ruijter and A. M. Emmons (2001). The root hair actin cytoskeleton as a backbone, highway, morphogenetic instrument and target for signalling. Cell and molecular biology. R. W. Ridge and A. M. C. Emons. Tokyo Berlin New York, Springer Verlag**:** 19-52.
Fåhreaeus, G. (1957). "The infection of clover root hairs by nodule bacteria studied by a simple glass technique." Journal of General Microbiology 16: 374-381.
Fang, R.-X., F. Nagy, S. Sivasubramaniam and N. H. Chua (1989). "Multiple cis regulatory elements for maximal expression of the cauliflower mosaic virus 35S promoter in transgenic plants." The Plant Cell 1: 141-50.
Felle, H. H., Kondorosi, E., Kondorosi, A. and Schultze, M. (1995). "Nod signal-induced plasma membrane potential changes in alfalfa root hairs are differently sensitive to structural modifications of the lipochitooligosaccharide." The Plant Journal 7: 939-47.
Förster, T. (1948). "Zwischenmolekulare Energie Wanderungen und Fluoreszenz." Annals of Physics 2: 57-75.
Fricker, M. D., C. Plieth, H. Knight, E. Blancaflor, M. R. Knight, N. S. White and S. Gilroy (1999). Fluorescenct and luminescent probes for biological activity. Fluorescence and luminescence techniques for probe ion activities in living plant cells. W. T. Mason. London, Academic press**:** 569-96.
Fromm, M., L. Taylor and V. Walbot (1985). "Expression of genes transferred into monocot and dicot cells by electroporation." Proceedings of the National Academy of Sciences of the USA 82: 5824-28.
Gadella, T. W., Jr., G. N. M. v. d. Krogt and T. Bisseling (1999). "GFP-based FRET microscopy in living plant cells." Trends Plant Science 4(7): 287-91.
Gadella, T. W., G. Vereb, A. E. Hadri, H. Rohrig, J. Schmidt, M. John, J. Schell and T. Bisseling (1997). "Microspectroscopic imaging of nodulation factor-binding sites on living Vicia sativa roots using a novel bioactive fluorescent nodulation factor." Biophysical Journal 72(5): 1986-96.

Gadella, T. W. J., Jr (1999). Fluorescence lifetime imaging microscopy (FLIM): instrumentation and applications, Academic Press.
Gadella, T. W. J., Jr and T. M. Jovin (1995). "Oligomerization of epidermal growth factor receptors (EGFR) on A431 cells studied by timeresolved fluorescence imaging microscopy. A stereochemical model for tyrosine kinase receptor activation." Journal of Cell Biology 129: 1543-58.
Gage, D. J., T. Bobo and S. R. Long (1996). "Use of green fluorescent protein to visualize the early events of symbiosis between *Rhizobium meliloti* and alfalfa (*Medicago sativa*)." Journal Bacteriology 178(24): 7159-66.
Gatz, C. (1996). "Chemically inducible promoters in transgenic plants." Current Opinion in Biotechnology 7: 168-72.
Gatz, C. (1997). "Chemical control of gene expression." Annual Review of Plant Physiology and Plant Molecular Biology 48: 89-108.
Geurts, R. (1998). A genetic approach to study rhizobial Nod factor and Mycorrhizal fungi activated signalling. Laboratory of Molecular Biology. Wageningen, The Netherlands, Wageningen Agricultural University**:** 110.
Geurts, R., E. Fedorova and T. Bisseling (2005). "Nod factor signalling genes and their function in the early stages of *Rhizobium* infection." Current Opinion in Plant Biology 8(4): 346-52.
Gilliland, L. U., K. K. Muthugapatti, L. C. Pawloski and R. B. Meagher (2002). "Both vegetative and reproductive actin isovariants complement the stunned root hair phenotype of the Arabidopsis *act2-1* mutation." Plant Physiology 130: 2199-209.
Gilliland, L. U., L. C. Pawloski, M. K. Kandasamy and R. B. Meagher (2003). "Arabidopsis actin gene ACT7 plays an essential role in germination and root growth." The Plant Journal 33(2): 319-28.
Goedhart, J. (2001). Advanced Fluorescence Microscopic Methods For The Study Of Single Living Root Hairs. Probing Nod Factor Perception in Legumes by Fluorescence Microspectroscopy. Wageningen**:** 10-12.
Gong, Z., H. Wan, T. L. Tay, H. Wang, M. Chen and T. Yan (2003). "Development of transgenic fish for ornamental and bioreactor by strong expression of fluorescent proteins in skeletal muscle." Biochemical and Biophysical Research Communications 308: 58-63.
González, D., A. Sawyer and W. W. Ward (1997). "Spectral pertrubations of mutants of recombinant *Aequorea victoria* green-fluorescent protein (GFP)." Photochem Photobiol 65:21S.
Goodchild, D. J. and F. J. Bergersen (1966). "Electron microscopy of the infection and subsequent development of soybean nodule." Journal of Bacteriology 92: 204-13.
Gordon, G. W., G. Berry, X.H. Liang, B. Levine and B. Herman (1998). "Quantitative fluorescence resonance energy transfer measurements using fluorescence microscopy." Biophysical Journal 74: 2702-13.
Gordon, G. W., G. Berry, X. H. Liang, B. Levine and B. Herman (1998). "Quantitative fluorescence resonance energy transfer measurements using fluorescence microscopy." Biophysical Journal 74: 2702-13.
Gory, L., M. C. Montel and M. Zagorec (2001). "Use of green fluorescent protein to monitor Lactobacillus sakei in fermented meat products." FEMS Microbiology Letters 194(2): 127-33.
Govers, A., J. Biesheuvel, G. J. Wijers, F. J. Gommers, F. J. Bakker, J. Bakker, A. Schots and J. Helder (1998). "In planta monitoring of two constitutive promoters, CaMV 35S and TR2i, in developing feeding cells induced by Globodera rostochiensis using green fluorescent protein in combination with confocal laser scanning microscopy." Molecular Plant Pathology 52(188): 275-84.
Griesbeck, O., G. S. Baird, R. E. Campbel, D. A. Zacharias and R. Y. Tsien (2001). "Reducing environmental sensitivity of yellow fluorescent protein. Mechanism and applications." Journal Biological Chemistry 276: 29188-194.
Gualtieri, G., O. Kulikova, E. Limpens, K. Dong-Jin, D. R. Cook, T. Bisseling and R. Geurts (2002). "Microsynteny between pea and *Medicago truncatula* in the Sym2 region." Plant Molecular Biology 50: 225-35.
Hadri, A.-E., Spaink, H. P., Bisseling, T. and Brewin, N. J. (1998). "Diversity of Root Nodulation and Rhizobial Infection Processes." In Rhizobiacee.Spaink, H.P., Kondorosi, A. and Hooykaas, P.J.J. (ed.), Kluwer Academic publisher, Dordrecht 1: 347-.
Handberg, K. and J. Stougaard (1992). "*Lotus japonicus*, an autogamous diploid legume species for classical and molecular genetics." The Plant Journal 2: 487-94.
Hanson, G. T., R. Aggeler, D. Oglesbee, M. Cannon, A. Capaldi, R. Y. Tsien and S. J. Remington (2004). "Investigating mitochondrial redox potential with redox-sensitive green fluorescent protein indicators." The Journal of Biological Chemistry 279(13): 13044-53.
Hanson, M. R. and R. H. Kohler (2001). "GFP imaging: methodology and application to investigate cellular compartmentation in plants." Journal of Experimental Botany 52(356): 529-39.
Haseloff, J., K. R. Siemering, D. C. Prasher and S. Hodge (1997). "Removal of a cryptic intron and subcellular localization of green fluorescent protein are required to mark transgenic Arabidopsis plants brightly." Proceedings of the National Academy of Sciences of the USA 94(6): 2122-7.
Haugland, R. P. (2002). Handbook of fluorescence probes and research products.
Heidstra, R. and T. Bisseling (1996). "Nod factor-induced host responses and mechanisms of Nod factor perception." New Phytologist 133: 25-43.
Heidstra, R., Geurts, R., Franssen, H., Spaink, H., van Kammen, A. and Bisseling, T. (1994). "Root hair deformation activity of nodulation factors and their fate on *Viciae Sativa*." Plant Physiology 105: 787-97.
Heim, R., A. B. Cubitt and R. Y. Tsien (1995). "Improved green fluorescence." Nature 373: 663-64.
Hemmings, L., D. J. Rees, V. Ohanian, S. J. Bolton, A. P. Gilmore, B. Patel, H. Pridle, J. E. Trevithick, R. O. Hynes and D. R. Critchley (1996). "Talin contains three actin-binding sites each of which is adjacent to a vinculin-binding site." Journal of cell science 109(11): 2715-26.
Hepler, P. K., A. L. Cleary, B. E. S. Gunning, P. Wadsworth, G. O. Wasteneys and D. H. Zang (1993). "Cytoskeletal dynamics in living plant cells." Cell Biology International 17: 127-42.
Herman, B. (1989). "Resonance energy transfer microscopy." Methods in Cell Biology 30: 219-43.
Hightower, R. C. and R. B. Meagher (1985). "Divergence and differential expression of soybean actin gene." EMBO Journal 4(1): 1-8.
Hussey, J., M. J. Deeks, T. J. Hawkins and T. Ketelaar (2004). Polar cell growth and the cytoskeleton biology. London, Blackwell Publishers.
Hussey, P. J., M. Yuan, G. Calder, S. Khan and C. W. Lioyd (1998). "Microinjection of pollen-specific actin-depolymerizing factor, ZmADF1, reorientates F-actin strands in Tradescantia stamen hair cells." The Plant Journal 14: 353-357.
Hutter, H. (2004). "Five-colour in vivo imaging of neurons in *Caenorhabditis elegans*." Journal of Microscopy 215: 213-18.
Imaizumi-Anraku, H., N. Takeda, M. Charpentier, J. Perry, H. Miwa, Y. Umehara, H. Kouchi, Y. Murakami, L. Mulder, K. Vickers, J. Pike, J. A. Downie, T. Wang, S. Sato, E. Asamizu, S. Tabata, M. Yoshikawa, Y. Murooka, G. J. Wu,

M. Kawaguchi, S. Kawasaki, M. Parniske and M. Hayashi (2005). "Plastid proteins crucial for symbiotic fungal and bacterial entry into plant roots." Nature 433(7025): 527-31.
Jach, G., E. Binot, S. Frings, K. Luxa and J. Schell (2001). "Use of red fluorescent protein from *Discosoma sp.* (dsRED) as a reporter for plant gene expression." The Plant Journal 28(4): 483-91.
Jayaraman, S., P. Haggie, R. M. Wachter, S. J. Remington and A. S. Verkam (2000). "Mechanism and cellular applications of a green fluorescent protein-based halide sensor." The Journal of Biological Chemistry 275(9): 6047-50.
Jefferson, R. A., T. A. Kavanagh and M. W. Bevan (1987). "GUS fusion - ß-glucuronidase as a sensitive and versatile gene fusion marker in higher plants." EMBO Journal 6: 3901-07.
Jiang, C.-J., A. G. Weeds and P. J. Hussey (1997). "The maize actin-depolymering factor, ZmADF3, redistributes to the growing tip of elongating hairs and can be induced to translocate into the nucleus with actin." The Plant Journal 12(5): 1035-43.
Jing, Y., K. Yi and H. Ren (2003). "Actins from plant and animal sources do not tens to form heteropolymers in vitro and function differently in plant cells." Protoplasma 222: 183-91.
Journet, E. P., N. El-Gachtouli, V. Vernoud, F. de Billy, M. Pichon, A. Dedieu, C. Arnould, D. Morandi, D. G. Barker and V. Gianinazzi-Pearson (2001). "*Medicago truncatula* ENOD11. A novel RPRP-encoding early nodulin gene expressed during mycorrhization in abuscule-containing cells." Molecular Plant-Microbe Interaction 14(6): 737-48.
Journet, E. P., M. Pichon, A. Dedieu, F. Billy, G. Truchet and D. G. Barker (1994). "*Rhizobium meliloti* Nod-factors elicit cell-specific transcription of the ENOD12 gene in transgenic alfalfa." The Plant Journal 6: 241-49.
Kalo, P., C. Gleason, A. Edwards, J. Marsh, R. M. Mitra, S. Hirsch, J. Jakab, S. Sims, S. R. Long, J. Rogers, G. B. Kiss, J. A. Downie and G. E. D. Oldroyd (2005). "Nodulation signalling in legumes requires NSP2, a member of the GRAS family of transcriptional regulators." Science 308: 1786-89.
Kandasamy, M. K., L. U. Gilliland, E. C. McKinney and R. B. Meagher (2001). "One plant actin isovariant , ACT7, is induced by auxin and required for normal callus formation." Plant Cell 13: 1541-54.
Kato, N., D. Pontier and E. Lam (2002). "Spectral profiling for the simultaneous observation of four distinct fluorescent proteins and detection of protein-protein interaction via fluorescence energy transfer in tobacco leaf nuclei." Plant Physiology 129: 931-42.
Ketelaar, T., E. G. Allwood, R. Anthony, B. Voigt, D. Menzel and P. J. Hussey (2004). "The actin-interacting protein AIP1 is essential for actin organization and plant development." Current Biology 14: 145-49.
Ketelaar, T., R. G. Anthony and P. J. Hussey (2004). "Green fluorescent protein mTalin causes defects in actin organization and cell expansion in Arabidopsis and inhibits actin depolymerizing factor's actin depolymerizing activity *in vitro*." Plant Physiology 136: 3990-98.
Ketelaar, T., C. Faivre-Moskalenko, J. J. Esseling, N. C. A. de Ruijter, C. S. Grierson, M. Dogterom and A. M. C. Emons (2002). "Positioning of nuclei in Arabidopsis root hairs: An actin-regulated process of tip growth." The Plant Cell 14: 2941-55.
Kim, L., S. Kircher, R. Toth, E. Adam, E. Schafer and F. Nagy (2000). "Light-induced nuclear import of phytochrome-A:GFP fusion proteins is differentially regulated in transgenic tobacco and Arabidopsis." The Plant Journal 22(2): 125-33.
Kost, B., P. Spielhofer and N. H. Chua (1998). "A GFP-mouse talin fusion protein labels plant actin filaments in vivo and visualizes the actin cytoskeleton in growing pollen tubes." The Plant Journal 16(3): 393-401.
Kost, B., P. Spielhofer, J. Mathur, C.-H. Dong and N.-H. Chua (2000). Non-invasive F-actin visualization in living plant cells using a GFP-mouse talin fusion. Actin: a dynamic framework for multiple plant cell functions. C. J. Staiger, F. Baluska, D. Volkmann and P. W. Barlow. Dordrecht/Boston/London, Kluwer academic publishers. 89**:** 661.
Kovar, D. R., B. C. Gibbon, D. W. McCurdy and C. J. Staiger (2001). "Flulorescent-labbeld fimbrin decorates a dynamic actin filament network in living plant cells." Planta 213: 390-95.
Kumar, A., A. Crawford, L. Close, M. Madison, J. Lorenz, T. Doetschman, S. Pawlowski, J. Duffy, J. Neumann and J. Robbins (1997). "Rescue of the cardiac alpha-actin-deficient mice by enteric smooth muscle gamma-actin." Proc Natl Acad Sci USA 94: 4406-4411.
Kurkdjian, A. C. (1995). "Role of the differentiation of root epidermal cells in Nod factor from *Rhizobium meliloti*-induced depolarization of *Medicago sativa*." Plant Physiology 107: 783-90.
lally, D., P. Ingmire, H. Y. Tong and Z. H. He (2001). "Antisense expression of a cell wall-associated protein kinase, Wak4, inhibits cell elongation and alters morphology." The Plant Cell 13: 1317-31.
Lam, E., P. N. Benfey, P. M. Gilmartin, R.-X. Fang and N.-H. Chua (1989). "Site-specific mutations alter *in vitro* factor binding and change promoter expression pattern in transgenic plants." Proceedings of the National Academy of Sciences of the USA 86: 7890-94.
Lazarowitz, S. G. and R. N. Beachy (1999). "Viral movement proteins as probes for intracellular and intercellular trafficking in plants." The Plant Cell 11: 535-548.
Levy J., C. Bres, R. Geurts, B., B. Chalhoub, O. Kulikova, G. Duc, E.P. Journet, J.M. Ane, E. Lauber, T. Bisseling, J. Denarie, C. Rosenberg, F. Debelle. (2004) "A putative Ca^{2+} and calmodulin-dependent protein kinase required for bacterial and fungal symbioses." Science 303(5662): 1361-4.
Limpens, E. and T. Bisseling (2003). "Signalling in Symbiosis." Current Opinion in Plant Biology 6: 343-50.
Limpens, E., C. Franken, P. Smit, J. Willemse, T. Bisseling and R. Geurts (2003). "LysM domain receptor kinases regulating rhizobial Nod factor-induced infection." Science 302: 630-3.
Limpens, E., J. Ramos, C. Franken, V. Raz, B. Compaan, H. Franssen, T. Bisseling and R. Geurts (2004). "RNA interference in Agrobacterium rhizogenes-transformed roots of Arabidopsis and *Medicago truncatula*." Journal of Experimental Botany 55(399): 983-92.
Liu, A. X., S. B. Zhang, X. J. Xu, D. T. Ren and G. Q. Liu (2004). "Soluble expression and characterization of a GFP-fused pea actin isoform (PEAc1)." Cell Research 14(5): 407-14.
Liu, Q., M. Kasuga, Y. Sakuma, H. Abe, S. Miura, K. Yamaguchi-Shinozaki and K. Shinozaki (1998). "Two transcription factors, DREB1 and DREB2, with an EREB/AP2 DNA binding domain separate two cellular transduction pathways in drought- and low-temperature-responsive gene expression, respectively, in Arabidopsis." The Plant Cell 10: 1391-406.
Long, S. R. (1996). "*Rhizobium* symbiosis: nod factors in perspective." Plant Cell 8(10): 1885-98.
Lopez, I., R. G. Anthony, S. K. Maciver, C.-J. Jiang, S. Khan, A. G. Weeds and P. J. Hussey (1996). "Pollen specific expression of maize genes encoding actin depolymerizing factor-like proteins." Plant Biology 93: 7415-20.
Lutcke, H. A., K. C. Chow, F. S. Mickel, K. A. Moss, H. F. Kern and G. A. Scheele (1987). "Selection of AUG initiation codoms differs in plants and animals." The EMBO Journal 6(1): 43-48.

Lyznik, L. A., R. D. Ryan, S. R. Ritchie and T. K. Hodges (1989). "Stable co-transformation of maize protoplasts with gusA and neo genes." Plant Molecular Biology 13: 151-61.
Madsen, E. B., L. H. Madsen, S. Radutoiu, M. Olbryt, M. Rakwaslska, K. Szczyglowski, S. Sato, T. Kaneko, S. Tabata, N. Sandal and N. Stougaard (2003). "A receptor kinase gene of the LysM type is involved in legume perception of rhizobial signals." Nature 425: 637-40.
Maniatis, T., E. F. Fritsch and J. Sambrook (2000). Molecular cloning: A laboratory Manual. Cols spring harbour, NY, Cold Spring Harbour Laboratory Press.
Marc, J., C. L. Granger, J. Brincat, D. D. Fisher, T. Kao, A. G. McCubbin and R. J. Cyr (1998). "A GFP-MAP4 reporter gene for visualizing cortical microtubule rearrangements in living epidermal cells." Plant Cell 10(11): 1927.
Marthur, J., N. Marthur, B. Kernebeck and M. Hulskamp (2003). "Mutations in actin related proteins 2 and 3 affect cell shape development in Arabidopsis." Plant Cell 15: 1632-45.
Marthur, J., N. Marthur, V. Kirik, B. Kernebeck, B. P. Srinivas and M. Hulskamp (2003). "Arabidopsis CROOKED encodes for the smallest subunit of Arp2/3 complex and controls cell shape by region specific fine F-actin formation." Development 130: 3137-46.
Marthur, J., P. Spielhofer, B. Kost and N.-H. Chua (1999). "The actin cytoskeleton is required to elaborate and maintain spatial patterning during trichome cell morphogenesis in *Arabidopsis thaliana*." Development 126: 5559-68.
Matz, M. V., A. F. Fradkov, Y. A. Labas, A. P. Savitsky, A. G. Zaraisky, M. L. Markelov and S. A. Lukyanov (1999). "Fluorescent proteins from nonbioluminescent Anthozoa species." Nature Biotechnology 17: 969-73.
McGough, A., B. Pope, W. Chiu and A. Weeds (1997). "Cofilin changes the twist of F-actin: implications for actin filament dynamics and cellular function." Journal of Cell Biology 13: 771-81.
Mckinney, E. C. and R. B. Meagher (1998). "Members of the Arabidopsis gene family are widely dispersed in the genome." Genetics 149: 663-675.
Miesenbock, G., D. A. De Angelis and J. E. Rothman (1998). "Visualizing secretion and synaptic transmission with pH-sensetive green fluorescent proteins." Nature 394: 192-5.
Mirabella, R., H. Franssen and T. Bisseling (2002). LCO signalling in the interaction between *Rhizobium* and legumes, Oxford university press.
Mitra R.M., C.A. Gleason, A. Edwards, J. Hadfield, J.A. Downie, G.E. Oldroyd, S.R. Long. (2004) "A Ca2+/calmodulin-dependent protein kinase required for symbiotic nodule development: Gene identification by transcript-based cloning." Proceedings of the National Academy of Sciences of the USA 101(13): 4701-5.
Miyawaki, A., O. Griesbeck, R. Heim and R. Y. Tsien (1999). "Dynamic and quantitative Ca2+ measurements using improved cameleons." Proceedings of the National Academy of Sciences of the USA 96(5): 2135-40.
Miyawaki, A., J. Llopis, R. Heim, J. M. McCaffery, J. A. Adams, M. Ikura and R. Y. Tsien (1997). "Fluorescent indicators for Ca2+ based on green fluorescent proteins and calmodulin." Nature 388(6645): 882-7.
Miyawaki, A., A. Sawano and T. Kogure (2003). "Lighting up cells: labelling proteins with fluorophores." Nature Cell Biology supplements: S1-S7.
Mizuno, H., A. Sawano, P. Eli, H. Hama and A. Miyawaki (2001). "Red fluorescent protein from Discosoma as a fusion tag and partner for fluorescence resonance energy transfer." Biochemistry 40: 2502-10.
Muguruma, M., S. Matsumura and T. Fukazawa (1990). "Direct interactions between talin and actin." Biochemical and Biophysical Research Communications 171(3): 1217-23.
Mylona, P. (1996). Studies on legume root hair development: correlations with the infection process by *Rhizobium* bacteria. Department of Molecular Biology. Wageningen, Agricultural University Wageningen**:** 104.
Mylona, P., M. Moerman, W. C. Yang, T. Gloudemans, J. Van de Kerckhove, A. van Kammen, T. Bisseling and H. J. Franssen (1994). "The root epidermis-specific pea gene RH2 is homologous to a pathogenesis-related gene." Plant Molecular Biology 26(1): 39-50.
Mylona, P., Pawlowski, K., Bisseling, T. (1995). "Symbiotic Nitrogen Fixation." Plant Cell 7: 869-85.
Nagai, T., K. Ibata, E. S. Park, M. Kubota, K. Mikoshiba and A. Miyawaki (2002). "A variant of yellow fluorescent protein with fast and efficient maturation for cell-biological applications." Nature Biotechnology 20: 87-90.
Nagai, T., A. Sawano, E. S. Park and A. Miyawaki (2001). "Circularly permuted green fluorescent proteins engineered to sense Ca2+." Proceedings of the National Academy of Sciences of the USA: 3197-202.
Nagai, T., S. Yamada, T. Tominaga, M. Ichikawa and A. Miyawaki (2004). "Expanded dynamic range of fluorescent indicators for Ca(2+) by circularly permuted yellow fluorescent proteins." Proceedings of the National Academy of Sciences of the USA 101(29): 10554-9.
Nagai, Y. M., R. Myazaki, T. Aoki, S. Zama, K. Inouye, M. Hirose, Iino and M. Hagiwara (2000). "A fluorescent indicator for visualizing cAMP induced phosphprylation in vivo." Nature Biotechnology 18: 313-16.
Newcomb, W. (1976). "A correlated light and electron microscopic study of symbiotic growth and differentiation in Pisum sativum root nodules." Canadian Journal of Botany 54: 2163-86.
Odell, J. T., F. Nagy and N. H. Chua (1985). "Identification of DNA sequences required for activity of the cauliflower mosaic virus 35S promoter." Nature 313: 810-12.
Oldroyd, G. E. D. and R. Geurts (2001). "*Medicago truncatula*, going where no plant has gone before." Trends in plant science 6(12): 552-4.
Oldroyd, G. E. D. and S. R. Long (2003). "Identification and characterization of *nodulation signalling pathway 2*, a gene of *Medicago truncatula* involved in Nod factor Signalling." Plant Physiology 131: 1027-32.
Ormö, M., A. B. Cubitt, K. Kallio, L. A. Gross, R. Y. Tsien and S. J. Remington (1996). "Crystal structure of the Aequorea victoria green fluorescent protein." Science 273: 1392-95.
Palmer, A.E., C. Jin, J.C. Reed, R.Y. Tsien (2004). "Bcl-2-mediated alterations in endoplasmic reticulum Ca2+ analyzed with an improved genetically encoded fluorescent sensor." Proceedings of the National Academy of Sciences of the USA 101(50): 17404-09.
Patterson, G. H., S. M. Knobel, W. D. Sharif, S. R. Kain and D. W. Piston (1997). "Use of the green-fluorescent protein and its mutants in quantative fluorescence microscopy." Biophysical Journal 73: 2782-90.
Paves, H. and E. Truve (2004). "Incorporation of mammalian actin into microfilaments in plant cell nucleus." BMC Plant Biology 4(7): 1-9.
Pichon, M., E. P. Journet, A. Dedieu, F. de Billy, G. Truchet and D. G. Barker (1992). "*Rhizobium meliloti* elicits transient expression of the early nodulin gene *ENOD12* in the differentiating root epidermis of transgenic alfalfa." Plant Cell 4(10): 1199-211.
Pollok, B. A. and R. Heim (1999). "Using GFP in FRET-based applications." Trends in Cell Biology 9: 57-60.

Ponsioen, B., J. Zhao, J. Riedl, F. Zwartkruis, G. N. M. v. d. Krogt, M. Zaccolo, M. W.H., B. J.L. and J. K. (2004). "Detecting cAMP-induced Epac activation by fluorescence resonance energy transfer; EPAC as a novel cAMP indicator." EMBO reports 5(12): 1176-80
Potter, F. J., J. T. Wiskich and I. B. Dry (2001). "The production of an inducible antisense alternative oxidase (Aox1a) plant." Planta 212: 215-21.
Pouwels, J., G. N. M. v. d. Krogt, J. V. Lent, T. Bisseling and J. Wellink (2002). "The cytoskeleton and the secretary pathway are not involved in targeting the cowpea mosaic virus movement protein to the cell periphery." Virology (297): 48-56.
Prasher, D. C., V. K. Eckenrode, W. W. Ward, F. G. Prendergast and M. J. Cormier (1992). "Primary structure of the Aequorea victoria green-fluorescent protein." Gene 111: 229-33.
Quaedvlieg, N. E., H. R. Schlaman, P. C. Admiraal, S. E. Wijting, J. Stougaard and H. P. Spaink (1998). "Fusions between green fluorescent protein and beta-glucuronidase as sensitive and vital bifunctional reporters in plants." Plant Molecular Biology 38(5): 861-73.
Ramos, J., T. Bisseling (2003). "A method for the isolation of root hairs from the model legume *Medicago truncatula*." Journal of experimental Botany 54(391): 2245-50.
Radutoiu, S., L. H. Madsen, E. B. Madsen, H. H. Felle, Y. Umehara, M. Gronlund, S. Sato, Y. Nakamura, S. Tabata, N. Sandal and N. Stougaard (2003). "Plant recognition of symbiotic bacteria requires two LysM receptor-like kinases." Nature 425: 585-92.
Ren, H., B. C. Gibbon, S. L. Ashworth, D. M. Sherman, M. Yuan and S. C.J. (1997). "Actin purified from maize pollen functions in living plant cells." Plant Cell 9: 1445-57.
Rhodes, C. A., K. S. Lowe and K. L. Ruby (1988). "Plant regeneration from protoplasts isolated from embryogenic maiz culture cells." biotechnology 6: 56-60.
Ringli, C., N. Baumberger, A. Diet, B. Frey and B. Keller (2002). "ACTIN2 is essential for bulge site selection and tip growth during root hair development of Arabidopsis." Plant Physiology 129: 1464-72.
Rizzo, M. A., G. H. Springer, B. Granada and D. W. Piston (2004). "An improved cyan fluorescent protein variant useful for FRET." Nature Biotechnology 4: 445-9
Roslan, H. A., M. G. Salter, C. D. Wood, M. R. H. White, K. P. Croft, F. Robson, G. Coupland, J. Doonan, P. Laufs, A. B. Tomsett and M. X. Caddick (2001). "Characterization of the ethanol-inducible alc gene expression system in *Arabidopsis thaliana*." The Plant Journal 28(2): 225-35.
Roth, A. F. and W. W. Ward (1983). "Conformational stability after protease treatment in Aequorea GFP." Photochemistry and Photobiology 37S:S71.
Roth, L. E. and G. Stacey (1989). "Bacterium release into host cells of nitrogen-fixing soybean nodules: the symbiosome membrane comes from three sources." European Journal of Cell Biology 49: 13-23.
Ruijter, N. C. A., T. Bisseling and A. M. C. Emons (1999). "*Rhizobium* nod factors induce an increase in sub-apical fine bundels of actin filaments in vicia sativa root hairs within minutes." Molecular Plant-Microbe Interactions 12(9): 829-32.
Ruijter, N. C. A., Rook, M.B., Bisseling, T., Emons, A.M.C. (1998). "Lipochito-oligosaccharides re-initiate root hair tip growth in Vicia sativa with high calcium and spectrin-like antigen at the tip." The Plant Journal 3(13): 341-50.
Sagan, M. and D. Morandi, Tarenghi, E. and Duc, G. (1995). "Selection of nodulation and mycorrhizal mutants in the model plant *Medicago truncatula* (*Gaertn*) after g-ray mutagenesis." Plant Science 111: 63-.
Salter, M. G., J. A. Paine, K. V. Riddell, I. Jepson, A. J. Greenland, M. X. Caddick and A. B. Tomsett (1998). "Characterization of the ethanol-inducible alc gene expression system for transgenic plants." The Plant Journal 16: 127-132.
Schaarschmidt, S., N. Qu, D. Strark, U. Sonnewald and B. Hause (2004). "Local induction of the *alc* gene switch in transgenic tobacco plants by acetaldehyde." Plant Physiology 11:1566-77.
Schafer, D. A. and J. A. Cooper (1995). "Control of actin assembly at filamt ends." Annual Review of Cell and Developmental Biology 11: 497-518.
Schenk, R. U. and A. C. Hilderbrandt (1972). "Medium and techniques for induction and growth of monocotyledonous and dicotyledonous plant cell cultures." Canadian Journal of Botany 50: 199-204.
Scheres, B., v. d. C. Wiel, A. Zalensky, B. Horvath, H. P. Spaink, H. Eck, F. Zwartsluis, A.-M. Wolters, T. Gloudemans, A. v. Kammen and T. Bisseling (1990). "The ENOD12 gene product is involved in the infection process during the pea-*Rhizobium* interaction." Cell 60: 281-94.
Schneider, K., J. Mathur, K. Boudonck, B. Wells, L. Dolan and K. Roberts (1998). "The ROOT HAIRLESS 1 gene encodes a nuclear protein required for root hair initiation in Arabidopsis." Genes & Development 12(13): 2013-21.
Schultze, M. and A. Kondorosi (1998). "Regulation of symbiotic root nodule development." Annual review of genetics 32: 33-57.
Seo, M. and T. Koshiba (2002). "Complex regulation of ABA biosynthesis in plants." Trends in plant science 7(1): 41-8.
Shaner, N. C., R. E. Campbell, P. A. Steinbach, B. N. G. Giepmans, A. E. Palmer and R. Y. Tsien (2004). "Improved monomeric red, orange and yellow fluorescent proteins derived from Discosoma sp. red fluorescent protein." Nature Biotechnology 12:1567-72
Sheahan, M. B., C. J. Staiger, R. J. Rose and D. W. McCurdy (2004). "A green fluorescent protein fusion to actin binding domain 2 of Arabidopsis fimbrin highlights new features of a dynamic actin cytoskeleton in living plant cells." Plant Physiology 136: 3968-78.
Siemering, K. R., R. Golbi, R. Server and J. Haseloff (1996). "Mutations that supress the thermosensivity of green fluorescent protein." Curr Biol 6(12): 1653-1663.
Smit, P., J. Raedts, V. Portyanko, F. Debelle, C. Gough, T. Bisseling and R. Geurts (2005). "NSP1 of the GRAS protein family is essential for rhizobial nod factor-induced transcription." Science 308: 1789-91.
Sonti, R. V., M. Chiurazzi, D. Wong, C. S. Davies, G. R. Harlow, D. W. Mount and E. R. Singer (1992). "Arabidopsis mutant deficient in T-DNA integration." Proceedings of the National Academy of Sciences of the USA 92(25): 11786-90.
Staiger, C. J., F. Baluska, D. Volkmann and P. W. Barlow (2000). Developments in plant and soil sciences. Dordrecht, Boston, London, Kluwer academic publishers.
Staiger, C. J. and P. J. Hussey (2004). "Actin and actin-modulating proteins." Annual Plant Reviews 10: 32-80.
Stiller, J., L. Martirani, S. Tuppale, R. Chian, M. Chiurazzi and P. M. Gresshoff (1997). "High frequency transformation and regeneration of transgenic plants in the model legume *Lotus japonicus*." Journal Experimental Botany 48(312): 1357-65.

Stock, A., M. O. Steinmetz, P. A. Janmey, U. Aebi, G. Gerisch, A. Kammerer, I. Weber and J. Faix (1999). "Domain analysis of cortexillin I: actin-bundeling, PIP2-binding and the rescue of cytokinesis." The EMBO Journal 18(19): 5274-84.
Sujatha, J., P. Haggie, M. Rebekka, R. M. Wachter, S. J. Remington and A. S. Verkman (2000). "Mechanism and cellular applications of a green fluorescent protein-based halide sensor." The Journal of Biological Chemistry 275(9): 6047-50.
Sweetman, J. P., C. Chu, N. Qu, A. J. Greenland, U. Sonnewald and I. Jespon (2002). "Ethanol vapor is an efficient inducer of the alc gene expression system in model and crop plant species." Plant Physiology 129: 943-48.
Terrada, R. and K. Shimamoto (1990). "Expression of CaMV 35S-GUS gene in transgenic rice plants." Molecular & General Genetics 20: 389-92.
Theriot, J. A. (1994). "Regulation of the actin cytoskeleton in living cells." Seminars in Cell and Developmental Biology 5: 193-99.
Timmers, A. C. J., A. Niebel, C. Balague and A. Dagkesamanskaya (2002). "Differential localisation of GFP fusions to cytoskeleton-binding proteins in animal, plant and yeast cells." Protoplasma 220: 69-78.
Trieu, A. T., S. H. Burleigh, I. V. Kardailsky, I. E. Maldonado-Mendoza, W. K. Versaw, L. A. Baylock, H. Shin, T. J. Chiou, H. Katagi, G. R. Dewbre, D. Wiegel and M. J. Harrison (2000). "Technical advanceTransformation of *Medicago Trancatula* via infiltration of seedlings or flowering plants with Agrobacterium." The Plant Journal 22: 531-41.
Trinh, T. H., P. Ratet, E. Kondorosi, P. Durand, K. Kamate, P. Bauer and A. Kondorosi (1998). "Rapid and efficient transformation of diploid *Medicago truncatula* and *Medicago sativa* spp. falcata lines improved in somatic embryogenesis." Plant Cell Reports 17: 345-55.
Truong, K., A. Sawano, H. Mizuno, H. Hama, K. I. Tong, T. K. Mal, A. Miyawaki and M. Ikura (2001). "FRET base in vivo Ca2+ imaging by a new calmoduline-GFP fusion molecule." Nature Structural Biology 8: 1069-73.
Tsien, R. Y. (1998). "The green fluorescent protein." Annual Review of Biochemistry 67: 509-44.
Turgeon, B. G. and W. D. Bauer (1985). "Ultrastructure of infection-thread development during the infection of soybean by *Rhizobium japonicum*." Planta 163: 328-49.
van der Wal, J., R. Habets, P. Varnai, T. Balla and K. Jalink (2001). "Monitoring phospholipase C activation kinetics in live cells by FRET." Journal of Biological Chemistry 276: 15337-44.
van Rheenen, J., M. Langeslag and K. Jalink (2004). "Correcting confocal acquisition to optimize imaging of fluorescence resonance energy transfer by sensitized emission." Biophysical Journal 86: 2517-29.
van Rheenen, J., E. A. Mulugeta, H. Janssen, J. Calafat and K. Jalink (2005). "PIP_2 signaling in lipid domains: a critical re-evaluation." The EMBO Journal 24: 1664-73.
Varian Australia Pty Ltd, M., Victoria 3170, Australia "Varian manual."
Verkhusha, V. V., S. Tsukita and H. Oda (1999). "Actin dynamics in lamellipodia of migrating border cells in the drosophila ovary reveald by GFP-actin fusion protein." Federation of European Biochemical Societies 445: 395-401.
Verveer, P. J., F. S. Wouters, A. R. Reynolds and P. I. Bastiaens (2000). "Quantitative imaging of lateral ErbB1 receptor signal propagation in the plasma membrane." Science 290: 1567-70.
Wais, R. J., C. Galera, G. Oldroyd, R. Catoira, R. V. Penmetsa, D. Cook, C. Gough, J. Denarie and S. R. Long (2000). "Genetic analysis of calcium spiking responses in nodulation mutants of *Medicago truncatula*." Proceedings of the National Academy of Sciences of the USA 97(24): 13407-12.
Walker, S. A., V. Viprey and J. A. Downie (2000). "Dissection of nodulation signaling using pea mutants defective for calcium spiking induced by nod factors and chitin oligomers." Proceedings of the National Academy of Sciences of the USA 97(24): 13413-8.
Wang, Y.-S., C. M. Motes, D. R. Mohamalawari and E. B. Blancaflor (2004). "Green fluorescent protein fusions to Arabidopsis Fimbrin 1 for spatio-temporal imaging of F-actin dynamics in roots." Cell Motility and cytoskeleton 59: 79-93.
Weber, I., G. Gerisch, C. Heizer, J. Murphy, K. Badelt, A. Stock, J.-M. Schwartz and J. Faix (1999). "Cytokinesis mediated through the recruitment of cortexillins into the cleavage furrow." The EMBO journal 18(3): 586-94.
Weerasinghe, R. R., D. M. Bird and N. S. Allen (2005). "Root-knot nematodes and bacterial Nod factors elicit common signal transduction events in *Lotus japonicus*." Proceedings of the National Academy of Sciences of the USA 22(8): 3147-52.
Westphal, M., A. Jungbluth, M. Heidecker, B. Muhlbauer, C. Heizer, J.-M. Schwartz, G. Marriott and G. Gerisch (1996). "Microfilament dynamics during cell movement and chemotaxis monitored using a GFP-actin fusion protein." Current Biology 7: 176-83.
Wu, P. and L. Brand (1994). "Resonance energy transfer: methods and applications." Analytical Biochemistry 218: 1-13.
Wymer, C. L., T. N. Bibikova and S. Gilroy (1997). "Cytoplasmic free calcium distribution during the development of root hairs of *Arabidopsis thaliana*." The Plant Journal 12: 427-39.
Yamaguchi-Shinozaki, K. and K. Shinozaki (1993). "Characterization of the expression of the desiccation-responsive rd29 gene of *Arabidopsis thaliana* and analysis of it's promoter in transgenic plants." Molecular & General Genetics 236: 331-40.
Yamaguchi-Shinozaki, K. and K. Shinozaki (1994). "A novel cis-acting element in an Arabidopsis gene is involved in responsiveness to drought, low-temperature, or high-salt stress." The Plant Cell 6: 251-64.
Yang, F., L. G. Moss and G. N. Phillips (1996). "The molecular structure of the green fluorescent protein." Nature Biotechnology 14: 1246-51.
Zaccolo, M., F. De Giorgi, C. Y. Cho, L. Feng, T. Knapp, P. A. Negulescu, S. S. Taylor, R. Y. Tsien and T. Pozzan (2000). "A genetically encoded, fluorescent indicator for cyclic AMP in living cells." Nature Cell Biology 2(1): 25-9.
Zeevaart, J. A. D. and R. A. Creelman (1988). "Metabolism and physiology of abscisic acid." Annual Review of plant physiology and Plant Molecular Biology 39: 439-73.
Zuo, J. and N. H. Chua (2000). "Chemical-inducible systems for regulated gene expression of plant genes." Current Opinion in Biotechnology 11: 146-51.
Xu, X, A.L Gerard, B.C. Huang, D.C. Anderson, D.G. Payan, Y. Luo (1998). "Detection of programmed cell death using fluorescence energy transfer" Nucleic Acids Research 26: 2034-35

Samenvatting

Rhizobium bacteriën kunnen resulteren in de vorming van een nieuw plantorgaan: een wortelknol. Dit is het orgaan waarin de Rhizobium gehuisvest wordt. Dit samenleven van plant en bacterie in de knol is voor beide organismen voordelig. De bacterie haalt stikstof uit de lucht en zet deze om in ammonia voor de plant. De bacterie krijgt hiervoor voedsel in de vorm van bijvoorbeeld dicarbonzuren terug. Hierdoor kan de plant ook groeien op stikstofarme gronden en heeft ze geen behoefte aan stikstofhoudende meststoffen. De toelatingsprocedure van de plantenwortel voor de bacterie is zeer stringent. Eerst moet herkenning van de bacterie plaatsvinden, want de plant laat alleen gastheer-specifieke rhizobia toe. De plant herkent haar eigen *Rhizobium* door middel van lipo-oligosachariden genaamd Nod-factoren, die uitgescheiden worden door de rhizobia (Hoofdstuk 1, Figuur 6). Na herkenning kan de bacterie via de wortelhaar de wortel binnengaan. Hiervoor maakt de plant een naar binnen groeiende buisvormige structuur: de infectiedraad. Deze draad groeit van de wortelhaartop naar de cortex. Tijdens dit proces delen cellen in de wortelcortex zich en vormen een knol primordium. De infectiedraad groeit naar dit primordium , waar de bacteriën worden vrijgeven. Vervolgens ontwikkelt het primordium zich tot een knol en daar zijn de rhizobia in staat stikstofgas uit de atmosfeer om te zetten in ammonia.
In dit proefschrift worden technieken ontwikkeld om meer inzicht te krijgen in vroege processen die plaatsvinden als de wortelhaar geïnfecteerd wordt. Het gaat hierbij met name om het visualiseren van F-actine en calcium in levende wortelhaar cellen. Deze twee zijn van belang na herkenning van de Nod-factoren en het prepareren van de wortelharen voor infectie. Om deze visualisatie mogelijk te maken, moet eerst een verscheidenheid aan technieken ontwikkeld worden. Eerst is een optimalisatie van het maken van transgene plantenwortels gewenst. Voor transformatie wordt een *Agrobacterium rhizogenes* transformatie procedure gebruikt (Hoofdstuk 2). Hiermee worden transgene wortels aan een niet-transgene scheut gecreëerd. Een groot voordeel van deze procedure is dat transgene wortels binnen 6 tot 8 weken worden gevormd. Dit in tegenstelling tot het maken van stabiel getransformeerde planten door middel van *Agrobacterium tumefaciens*, waarmee na ongeveer 9 maanden een (geheel) transgene plant kan worden verkregen. Belangrijk voordeel van deze transgene planten is dat transgeen zaad verkregen kan worden en dat kruisingen met mutanten mogelijk zijn. In dit proefschrift wordt de *A.rhizogenes* procedure toegepast omdat deze het snelst is en daarmee het meest geschikt om DNA constructen te testen in wortelharen. De optimalisatie van de *A. rhizogenes* transformatie van *Medicago truncatula* (Medicago) zoals beschreven in hoofdstuk 2 geeft bij 80% van de planten tenminste 1 transgene wortel. Gemiddeld hebben deze planten 10 wortels waarvan er 6 transgeen zijn. Een ongeveer vergelijkbare transformatie efficiëntie is door ons gevonden voor *Lotus japonicus* (Lotus). Medicago en Lotus worden in dit proefschrift gebruikt en zijn de modelplanten voor vlinderbloemigen. Eigenschappen die deze planten tot modelsystemen gemaakt hebben, zijn onder andere hun naar verhouding kleine genoom, de eenvoud van het verkrijgen van transgene planten, het voorhanden zijn van mutanten en tevens worden de genomen van deze 2 vlinderbloemigen momenteel gesequenced.
Het beschikbaar hebben van een efficiënte transformatie procedure betekent dat F-actine- en calcium- verklikkergenen tot expressie gebracht kunnen worden. Zulke genen maken het mogelijk F-actine structuren en calcium concentraties in

wortelharen zichtbaar te maken. Dit gebeurt met behulp van fluorescentie-microscopie. De verklikkergenen (hierna reportergenen genoemd) moeten in de wortelhaar epidermis hoog genoeg tot expressie worden gebracht. Door tevens de expressie zoveel mogelijk epidermis-specifiek te maken, worden eventuele negatieve gevolgen voor de wortelgroei door reportergenen tot een minimum beperkt.
In hoofdstuk 2 zijn vier promotoren getest op hun wortelhaar specificiteit en hun niveau van expressie. Dit zijn *CaMV35S, PsLYK3*, *PsRH2* en *LeEXT1.* Alleen *PsRH2* en *LeEXT1* bleken in Medicago voornamelijk in de wortelepidermis tot expressie te komen en *LeEXT1* zelfs alleen in wortelharen. Hoewel deze twee promotoren in de wortel redelijk epidermis-specifiek zijn, kan niet worden uitgesloten dat ze tijdens wortelformatie van het door agrobacterium gevormde callus wel actief zijn. Om ongewilde activiteit van reportergenen nog verder te kunnen uitsluiten zijn ook induceerbare promotoren getest (Hoofdstuk 3,4 en 5).
Induceerbare promotoren kunnen op een zelf te bepalen moment tijdens de ontwikkeling aangezet worden door middel van stimuli. In hoofdstuk 3 is een alcohol induceerbare promotor (AlcR/AlcA) getest en wortelhaar specifiek gemaakt met behulp van de *PsRH2* promotor. Dit systeem bestaat uit een gedeelte dat de inductie alcohol-specifiek maakt en een gedeelte dat de plaats van inductie kan regelen. Dit alcohol induceerbare systeem als geheel heeft echter de bijkomende moeilijkheid van auto-inductie, wat wil zeggen dat de plant zelf alcohol kan produceren als deze opgroeit in een afgesloten ruimte. Bij het maken van transgene planten is zo'n afgesloten ruimte over het algemeen in het begin van de transformatie procedure noodzakelijk. Om dit te omzeilen is de standaard groeimethode aangepast. Hierdoor is geen gen activiteit detecteerbaar aan het begin van de daadwerkelijke inductie. Door nu vervolgens de wortels te drenken in een 2% alcohol oplossing vindt in 50-75% van de planten inductie plaats. Deze inductie is ook epidermis-specifiek omdat de plaats van inductie geregeld wordt door middel van een ingebouwde *PsRH2* promotor.
In hoofdstuk 4 is een door kou te induceren promotor, *AtRD29A(-694,1)* en een afgeleide hiervan *AtRD29A*/71bpX3(DREX3) gemaakt en getest. Deze promotoren kunnen in *Arabidopsis thaliana* geïnduceerd worden door onder andere een behandeling bij 4°C. De *AtRD29A*/71bpX3(DREX3) bleek echter in Medicago niet te induceren en de *AtRD29A(-694,1)* promotor had zowel voor als na inductie een hoge activiteit. Daarom zijn deze twee promotoren ongeschikt als induceerbare promotoren.
In hoofdstuk 5 is een door *Rhizobium* of Nod factoren te induceren promotor gemaakt en getest. Dit is een 0.8 kb fragment van de *MtENOD12* promotor die na inoculatie met *Sinorhizobium meliloti* geactiveerd wordt. Activering vindt plaats op de plek van infectiedraad groei, in de knol-primordia en in de infectiezone van de knol. Deze promotor heeft als nadeel dat deze ook continu actief is in de worteltop en daarmee zo mogelijk niet geschikt is als induceerbare promotor. Deze promotor heeft tevens als nadeel dat alleen tijdens een vrij late fase van wortelhaar-infectie de reportergenen worden aangezet. Van de drie induceerbare promotorsystemen hier getest lijkt de alcohol induceerbare promotor (AlcR/AlcA) het meest geschikt.
Na optimalisatie van de *A.rhizogenes* transformatie procedure en het vinden van mogelijk geschikte promotoren, is de toepasbaarheid van deze technieken getest met het calcium reportergen Yellow-cameleon (Ycam). Ycam is een reportergen gebaseerd op een quantum mechanisch fenomeen: Fluorescence Resonance Energy Transfer (FRET). FRET is een verschijnsel waarbij energie wordt overgedragen van de donor-fluorofoor naar de acceptor-fluorofoor, mits aan

bepaalde voorwaarden wordt voldaan, waaronder een kleine afstand tussen de twee fluoroforen. Ycam bestaat uit twee van zulke fluoroforen: een cyaankleurig fluorescerend donor-eiwit (CFP) en een geel fluorescerend acceptor-eiwit (YFP) (Hoofdstuk 1, Figuur 4). Beide fluoroforen zijn weer gescheiden door een calcium-bindend calmoduline eiwit en een M13 eiwitdomein. In afwezigheid van calcium liggen de beide fluoroforen te ver van elkaar af voor FRET waardoor CFP excitatie voornamelijk CFP emissie geeft. Maar na binding van calcium door het calmoduline domein krijgt deze affiniteit voor het M13 gedeelte. Hierdoor ondergaat Ycam een conformatie verandering met als gevolg dat de fluoroforen dicht bij elkaar getrokken worden. Doordat nu de fluoroforen dicht bij elkaar liggen kan FRET optreden van CFP naar YFP. Hierdoor verandert ook het fluorescentie emissie-spectrum van Ycam. De CFP fluorescentie intensiteit neemt namelijk af, terwijl YFP fluorescentie toeneemt. Dus met andere woorden het emissie-spectrum van Ycam is een graadmeter voor de mate van FRET, en daarmee voor de calcium concentratie in de cel. Door nu Ycam tot expressie te brengen in de epidermis van wortels met behulp van de *PsRH2* promotor, kan de calcium-concentratie in de wortelharen bepaald worden. Ycam laat een verhoogde calcium-concentratie in de top van een levende groeiende wortelhaar zien. Deze gradiënt is overeenkomstig met eerder gevonden resultaten. Hiermee is duidelijk dat het gebruik van deze op FRET gebaseerde reportergenen te gebruiken is in wortelharen. Echter het aantal transgene wortels met een voldoende hoog expressieniveau van Ycam is zeer laag. De efficiëntie is verre van die zoals gevonden in hoofdstuk 2. Ycam vangt calcium weg en zou zo de wortelvorming negatief kunnen beïnvloeden. Dit geeft aan dat *A.rhizogenes* transformatie bij voorkeur zou moeten worden gebruikt in combinatie met genen die onder controle staan van een induceerbare promotor. Het in hoofdstuk 3 geteste alcohol-induceerbare promotorsysteem zou hiervoor zeer geschikt kunnen zijn. Naast het visualiseren van intra-moleculair FRET, is ook inter-moleculair FRET mogelijk (Hoofdstuk 1, Figuur 4). Inter-FRET wil zeggen dat bijvoorbeeld twee eiwitten met ieder één van de fluoroforen van het donor-acceptorpaar na binding met elkaar ook FRET kunnen induceren. Mogelijk kan dan ook met inter-FRET interactie tussen twee van belang zijnde eiwitten in wortelharen worden gevisualiseerd.

Na het visualiseren van calcium in de wortelhaar is ook gezocht naar een reportergen om F-actine te visualiseren. Hiervoor zijn eiwitfusies gemaakt tussen verschillende actines (Hsßact, DdAct15 en PsAct1) en een fluorescent eiwit of tussen een actine bindend eiwit (gedeelte) (DdCortN$_{1-233}$, DdTalin$_{2302-2491}$ en ZmADF3) en een fluorescent eiwit. Deze fusies zijn vervolgens getest op hun F-actine visualiserende capaciteit in Cowpea (*Vigna unguiculata L.)* protoplasten. Van al deze fusies bleek alleen DdTalin$_{2302-2491}$ een redelijk reportergen voor het F-actine in protoplasten. Ook deze fusie is onder controle van de *PsRH2* promotor geplaatst en tot expressie gebracht in wortelharen, echter zonder te resulteren in fluorescente wortelharen. Dit fusie gen heeft dus waarschijnlijk ook een negatief effect op de groei door de interactie met F-actine. Ook hier zou dus een induceerbaar systeem een bijdrage kunnen leveren aan het verkrijgen van transgene wortels. Hierbij moet echter opgemerkt worden dat recent verschenen publicaties aannemelijk maken dat DdTalin$_{2302-2491}$ ook na inductie de normale processen in de wortel sterk verstoort. Hiermee zou het dus ook geen goede reporter zijn om F-actine te visualiseren in levende wortelharen van vlinderbloemige planten.